THE UNIVERSITY OF MICHIGAN

# STUDIES IN RADAR CROSS-SECTIONS XXII

## ELEMENTARY SLOT RADIATORS

R. F. Goodrich, A. L. Maffett, N. Reitlinger
C. E. Schensted, and K. M. Siegel

Contract AF 33(038)-28634
HAC-PO L-265165-F31

15 November 1956

2472-13-T

**2472-13-T = RL-2052**

THE UNIVERSITY OF MICHIGAN
ENGINEERING RESEARCH INSTITUTE
ANN ARBOR, MICHIGAN

STUDIES IN RADAR CROSS-SECTIONS

I Scattering by a Prolate Spheroid, by F. V. Schultz (UMM-42, March 1950), W-33(038)-ac-14222, UNCLASSIFIED.

II The Zeros of the Associated Legendre Functions $P^m_n(\mu')$ of Non-Integral Degree, by K. M. Siegel, D. M. Brown, H. E. Hunter, H. A. Alperin, and C. W. Quillen (UMM-82, April 1951), W-33(038) -ac-14222, UNCLASSIFIED.

III Scattering by a Cone, by K. M. Siegel and H. A. Alperin (UMM-87, January 1952), AF-30(602)-9, UNCLASSIFIED.

IV Comparison Between Theory and Experiment of the Cross-Section of a Cone, by K. M. Siegel, H. A. Alperin, J. W. Crispin, Jr., H. E. Hunter, R. E. Kleinman, W. C. Orthwein, and C. E. Schensted (UMM-92, February 1953), AF-30(602)-9, UNCLASSIFIED.

V An Examination of Bistatic Early Warning Radars, by K. M. Siegel (UMM-98, August 1952), W-33(038)-ac-14222, SECRET.

VI Cross-Sections of Corner Reflectors and Other Multiple Scatterers at Microwave Frequencies, by R. R. Bonkowski, C. R. Lubitz, and C. E. Schensted (UMM-106, October 1953), AF-30(602)-9, SECRET - UNCLASSIFIED when Appendix is removed.

VII Summary of Radar Cross-Section Studies Under Project Wizard, by K. M. Siegel, J. W. Crispin, Jr., and R. E. Kleinman (UMM-108, November 1952), W-33(038)-ac-14222, SECRET.

VIII Theoretical Cross-Section as a Function of Separation Angle Between Transmitter and Receiver at Small Wavelengths, by K. M. Siegel, H. A. Alperin, R. R. Bonkowski, J. W. Crispin, Jr., A. L. Maffett, C. E. Schensted, and I. V. Schensted (UMM-115, October 1953), W-33(038)-ac-14222, UNCLASSIFIED.

IX Electromagnetic Scattering by an Oblate Spheroid, by L. M. Rauch (UMM-116, October 1953), AF-30(602)-9, UNCLASSIFIED.

X Scattering of Electromagnetic Waves by Spheres, by H. Weil, M. L. Barasch, and T. A. Kaplan (2255-20-T, July 1956), AF-30(602)-1070, UNCLASSIFIED.

XI The Numerical Determination of the Radar Cross-Section of a Prolate Spheroid, by K. M. Siegel, B. H. Gere, I. Marx, and F. B. Sleator (UMM-126, December 1953), AF-30(602)-9, UNCLASSIFIED.

XII Summary of Radar Cross-Section Studies Under Project MIRO, by K. M. Siegel, M. E. Anderson, R. R. Bonkowski, and W. C. Orthwein (UMM-127, December 1953), AF-30(602)-9, SECRET.

XIII Description of a Dynamic Measurement Program, by K. M. Siegel and J. M. Wolf (UMM-128, May 1954), W-33(038)-ac-14222, CONFIDENTIAL.

XIV Radar Cross-Section of a Ballistic Missile, by K. M. Siegel, M. L. Barasch, J. W. Crispin, Jr., W. C. Orthwein, I. V. Schensted, and H. Weil (UMM-134, September 1954), W-33(038)-ac-14222, SECRET.

XV Radar Cross-Sections of B-47 and B-52 Aircraft, by C. E. Schensted, J. W. Crispin, Jr., and K. M. Siegel (2260-1-T, August 1954), AF-33(616)-2531, CONFIDENTIAL.

XVI Microwave Reflection Characteristics of Buildings, by H. Weil, R. R. Bonkowski, T. A. Kaplan, and M. Leichter (2255-12-T, May 1955), AF-30(602)-1070, SECRET.

XVII Complete Scattering Matrices and Circular Polarization Cross-Sections for the B-47 Aircraft at S-band, by A. L. Maffett, M. L. Barasch, W. E. Burdick, R. F. Goodrich, W. C. Orthwein, C. E. Schensted, and K. M. Siegel (2260-6-T, June 1955), AF-33(616)-2531, CONFIDENTIAL.

XVIII Airborne Passive Measures and Countermeasures, by K. M. Siegel, M. L. Barasch, J. W. Crispin, Jr., R. F. Goodrich, A. H. Halpin, A. L. Maffett, W. C. Orthwein, C. E. Schensted, and C. J. Titus (2260-29-F, January 1956), AF-33(616)-2531, SECRET.

XIX Radar Cross-Section of a Ballistic Missile - II, by K. M. Siegel, M. L. Barasch, H. Brysk, J. W. Crispin, Jr., T. B. Curtz, and T. A. Kaplan (2428-3-T, January 1956), AF-04(645)-33, SECRET.

XX Radar Cross-Section of Aircraft and Missiles, by K. M. Siegel, W. E. Burdick, J. W. Crispin, Jr., and S. Chapman (WR-31-J, 1 March 1956), SECRET.

XXI Radar Cross-Section of a Ballistic Missile - III, by K. M. Siegel, H. Brysk, J. W. Crispin, Jr., and R. E. Kleinman (2428-19-T, October 1956) AF-04(645)-33, SECRET.

XXII Elementary Slot Radiators, R.F.Goodrich, A.L.Maffett, N.Reitlinger, C.E.Schensted, and K.M.Siegel, (2472-13-T, November 1956), AF 33(038)-28634; HAC-PO L-265165-F31. UNCLASSIFIED.

TABLE OF CONTENTS

## PREFACE

This paper is the twenty-second in a series growing out of studies of radar cross-sections at the Engineering Research Institute of The University of Michigan. The primary aims of this program are:

1. To show that radar cross-sections can be determined analytically.

2. A. To determine means for computing the radiation patterns from antennas by approximate techniques which determine the pattern to the accuracy required in military problems but which do not require the unique determination of exact solutions.

   B. To determine means for computing the radar cross-sections of various objects of military interest.

   (Since 2A and 2B are inter-related by the reciprocity theorem it is necessary to solve only one of these problems)

3. To demonstrate that these theoretical cross-sections and theoretically determined radiation patterns are in agreement with experimentally determined ones.

Intermediate objectives are:

1. A. To compute the exact theoretical cross-sections of various simple bodies by solution of the approximate boundary-value problems arising from electromagnetic theory.

B. Compute the exact radiation patterns from infinitesimal solutions on the surface of simple shapes by the solution of appropriate boundary-value problems arising from electromagnetic theory.

(Since 1A and 1B are inter-related by the reciprocity theorem it is necessary to solve only one of these problems)

2. To examine the various approximations possible in this problem and to determine the limits of their validity and utility.

3. To find means of combining the simple-body solutions in order to determine the cross-sections of composite bodies.

4. To tabulate various formulas and functions necessary to enable such computations to be done quickly for arbitrary objects.

5. To collect, summarize, and evaluate existing experimental data.

Titles of the papers already published or presently in process of publication are listed on the preceding page.

The major portion of the effort in this report was performed for the Hughes Aircraft Company under purchase order L-265165-F31 under Air Force Contract AF33(038)-28634.

K. M. Siegel

# CHAPTER I

## INTRODUCTION AND STATEMENT OF PROBLEM

This report concerns methods of readily computing radiation patterns, to the accuracy required in practical problems, from slot sources on various perfectly conducting shapes, with particular emphasis on the semi-infinite cone. The methods used are based on the equivalence between a slot source (voltage impressed across a slot) and a magnetic dipole source. The approximations of significance in the applications with which we are concerned are those used for a wavelength limit which is small in comparison to all dimensions of the body in question.

The purpose of this study is to determine the behavior of the elementary slot radiators. Such a study is a necessary prelude to the development of arrays of such elements, arrays which will serve as useful flush-mounted antennas.

In Chapter 2 radiation problems are discussed from the point of view of known solutions of the reciprocal scattering problems. Chapter 3 then lays the foundation for the calculation of radiation patterns arising from various excitations of a circumferential slot on a perfectly conducting semi-infinite cone. A representative set of patterns, computed on the basis of this chapter, is presented in Appendix C. In Chapter 4 a particular pattern optimization technique, with application to a circumferential slot on a cone, is given. The

material of Chapters 3 and 4 is based on optical techniques; more precise treatments for wedges and cones are given in Appendices A and B, respectively.

An alternative approach to electromagnetic boundary value problems is suggested in Chapter 5 by a discussion of Wiener integral methods.

Finally, Chapter 6 presents the conclusions we have drawn to date and offers a prospectus for future endeavor.

# CHAPTER 2

# GENERAL DISCUSSION OF RADIATION AND SCATTERING PROBLEMS

## 2.1. Reciprocity

In order to be able to draw on the large body of knowledge of scattering problems in electromagnetic theory we make use of the reciprocity properties of the electromagnetic field. For our purpose we state the Lorentz reciprocity theorem in the form

$$\int \vec{H}_1 \cdot \vec{M}_2 \, dv = \int \vec{H}_2 \cdot \vec{M}_1 \, dv \tag{2.1}$$

where $\vec{H}_1(\vec{H}_2)$ is the field due to the magnetization $\vec{M}_1(\vec{M}_2)$ and the integration is over all space. If $\vec{M}_{1,2}$ are of the form $\hat{m}_{1,2}\delta(\vec{r}-\vec{r}_{1,2})$, i.e., point sources, then we find

$$\vec{H}_1(\vec{r}_2) \cdot \hat{m}_2 = \vec{H}_2(\vec{r}_1) \cdot \hat{m}_1 \quad . \tag{2.2}$$

Consider now a magnetic dipole on the surface of a perfect conductor S having a position vector $\vec{r}_2$ and a magnetic dipole of the same strength located at some position $\vec{r}_1$ in space (see the following figure). Under these conditions it follows that by varying the orientation of $\hat{m}_1$, the field induced at $\vec{r}_2$ on the surface of S by the source at $\vec{r}_1$ determines the field at $\vec{r}_1$ due to the source on the surface S at $\vec{r}_2$.

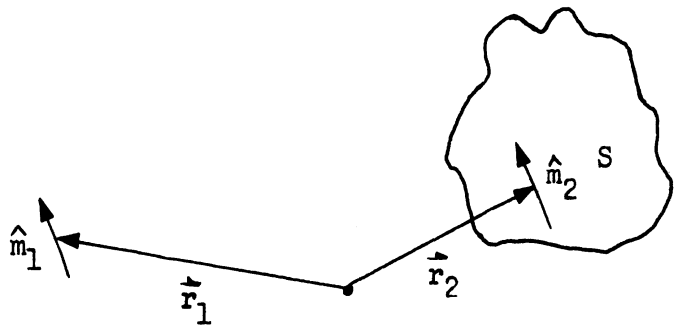


If we let $|\vec{r}_1|$ increase without limit, we see that the field induced on S at $\vec{r}_2$ due to the incoming plane waves determines the radiation pattern due to a source at $\vec{r}_2$ in the direction of the incoming plane wave.

The exact solution of the scattering problem is no simpler to obtain than the exact solution of the reciprocal radiation problem. In contrast, we have readily available a large number of approximate solutions of various scattering problems. We now propose to consider a number of these approximate solutions, most of which are based on some assumption about the field induced on the scatterer, i.e., the radiation field of the reciprocal problem.

## 2.2. Geometric Optics

All of the approximations we will examine are for short wavelengths. We start with the simplest, gometric optics, the exact limit of vanishingly small wavelength. For a finite wavelength the geometric optics approximation is equivalent to replacing the body S on which the source is located at $\vec{r}_2$ by an infinite perfectly conducting plane tangent to S at $\vec{r}_2$ with the source at the point of tangency. It is apparent that the pertinent parameters are the radii of curvature at $\vec{r}_2$ in wavelengths.

With these assumptions, the electric field $\vec{E}$ produced by a radiating slot on a body with voltage $V_o$ across the slot takes the form

$$\vec{E} \approx \frac{V_o}{2\pi} \text{ curl } \int_{\substack{\text{visible} \\ \text{portion} \\ \text{of slot}}} \frac{e^{ikR}}{R} \vec{dl} \qquad (2.3)$$

where R is the distance between field point and integration point along the slot and $\vec{dl}$ is an infinitesimal of length in the direction of the magnetic dipole. In particular, when the body containing the slot becomes an infinite perfectly conducting plane, the expression (2.3) becomes the exact solution for the boundary value problem of a radiating slot on such a body.

The expression (2.3) for the electric field $\vec{E}$ will depend on the body under consideration only in the sense that it will depend on the position and orientation of the slot on that body; that is, the optics method typified by Equation 2.3 will not yield any information concerning possible diffraction effects due to the body itself. Thus the form of Equation 2.3 will be similar for all bodies whose shapes are in a certain sense similar, indeed, when an approximation of the form (2.3) is applied to an arbitrary convex body of revolution having a circumferential slot in a plane normal to the axis of revolution, the problem reduces to that for a cone, tangent to the body of revolution at the slot, with a slot at the circle of tangency.

Schensted (Ref. 1) has shown that the geometric optics answer is the exact scattering answer for a plane wave incident along the axis of a paraboloid. Thus, applying the reciprocity theorem, the far field produced by a magnetic dipole located arbitrarily on the surface of a paraboloid is given exactly in the direction of the axis of the paraboloid by the geometric optics field. The expression for the magnetic far field in the direction of the axis of the paraboloid is just twice the free space expression for the magnetic dipole (i.e., $\vec{H} \sim \frac{2\, e^{ik(z-z_o)}}{z-z_o} \hat{i}$ for a magnetic dipole oriented in the $\hat{i}$ - direction, where z is the distance to field point parallel to the axis of the paraboloid, and $z_o$ is the corresponding distance to the dipole.)

In this same vein, it is worth noting that similar reasoning can be applied to the cone. We recall that the bistatic radar cross-section is very closely approximated by the physical optics formulation for illumination along the axis of the cone. This suggests that the use of the physical optics field in the reciprocity theorem will give a higher order approximation for the field in the direction of the cone axis due to a slot excitation of the cone.

In the case of a circumferential slot on either the paraboloid or the cone we note that, of cos $n\phi$ excitations, only the cos $\phi$ excitation will produce a non-vanishing contribution along the axis of symmetry. Using the above method for the paraboloid will, as indicated, give the

exact field along the axis of symmetry for the cosine excited circumferential slot. Although the reciprocity theorem is not obeyed by the physical optics field, Felsen (Ref. 6) has demonstrated that for plane wave illumination along the cone axis the physical optics field agrees with the first order small cone angle approximation to the exact scattered field outside the region of specular reflection $\theta < (2\theta_0 - \pi)$. Recently Felsen (Ref. 2) has indicated that this result can be continued past the specular reflection region, and hence, to the surface of the cone, where the agreement with physical optics also obtains. Thus we may use the physical optics field on the surface of the cone. We expect to have reciprocity obeyed by physical optics to first order in the small cone angle approximation and to first order in $(ka)^{-1}$ where a is the distance from the slot to the tip and $k = 2\pi/\lambda$. In this way we obtain the field on the axis of symmetry produced by the slot on the cone to the same order of approximation.

## 2.3 Refinements of Geometric Optics.

In looking for refinements of geometric optics we turn to the reciprocal scattering problems - in particular to the method of Fock based on an approximate formulation of the scattering problem and to the use of approximations of the exact solution for separable surfaces.

The first approach, that of Fock (Ref. 3), is based on an approximation to Maxwell's equations depending upon the physical assumption of a

sufficiently short wavelength. This formulation we can consider as a modification of geometric optics based on a local analysis of the field in the region of the shadow boundary. In particular, Fock defines two universal scalar functions whose argument is a reduced distance measured from the shadow boundary. Depending upon the polarization of the incident radiation with respect to the tangent to the shadow boundary, one of the Fock functions is approximately proportional to the field induced on the scatterer.

Following is an account of the general procedure. Let a convex closed surface S, $f(x,y,z) = 0$, be illuminated by a plane wave incident in the direction of the x-axis. The geometrical shadow is then given by the two equations $f(x,y,z) = 0$, $\frac{\partial f}{\partial x} = 0$. Let the origin be located at a point on the shadow boundary with the z-axis the outward directed normal to S and the y-axis chosen to form a right-handed system. Using the geometric assumption that the surface can be approximated by a paraboloid at any point, i.e.

$$z + 1/2\ (ax^2 + 2bxy + cy^2) = 0,$$

so that $\frac{\partial f}{\partial x} = ax + by$ and the physical assumption that the variation of this field in the z-direction is much smaller than that in either the x- or y-direction for sufficiently small $\lambda$, Fock obtains an approximation to Maxwell's equations which lead to the solutions:

$$H_y = H_y^o \, G(\xi)$$

$$H_x = \left(\frac{2a}{k}\right)^{1/3} i \, H_z^o \, e^{ikx} \, F(\xi)$$

$$H_z = 0$$

on the surface. The incident field is given by

$$\vec{H}_o = (0, H_y^o, H_z^o)$$

while the functions G and F have the asymptotic behavior

$$\lim_{\xi \to \mp\infty} |G(\xi)| = \begin{cases} 2 \\ 0 \end{cases}$$

$$\lim_{\xi \to \mp\infty} |F(\xi)| = \begin{cases} 2\xi \\ 0 \end{cases}$$

where $\xi$ is a reduced distance from the shadow boundary given by

$$\xi = \left(\frac{k}{2a}\right)^{1/3} (ax + by).$$

We have a modification of geometric optics field induced on S which gives a smooth transition through the shadow boundary. Hence, we have an approximate solution to the reciprocal radiation problems as noted above.

By way of illustration, the application of Fock's method to the radiation pattern from an axial slot in an infinite perfectly conducting cylinder has been compared with Bailin's evaluation of the exact series (Ref. 4) for this problem. If a is the radius of the cylinder, and $k = 2\pi/\lambda$ ($\lambda$ the wavelength), ka = 12, so that $\xi = \left(\frac{ka}{2}\right)^{1/3} \frac{x}{a}$. The comparison along with the geometric optics result appears in Fig. 2-1. Following the method of N. Logan (Ref. 18) the oscillations in the Fock expression were found by including the contribution going around the rear of the cylinder. Logan has made the same comparison for ka = 8.

In detail we substitute for x, which is the correct variable near its shadow boundary, the path length S along the surface of the cylinder. The magnitude of the field is then proportional to

$$|\vec{E}| \sim |G(\xi) + G(\xi')|$$

where

$$\xi = \left(\frac{ka}{2}\right)^{1/3} \frac{S}{a}$$

$$\xi' = \left(\frac{ka}{2}\right)^{1/3} \frac{S'}{a}$$

where S is the path length from one shadow boundary, S' that from the other.

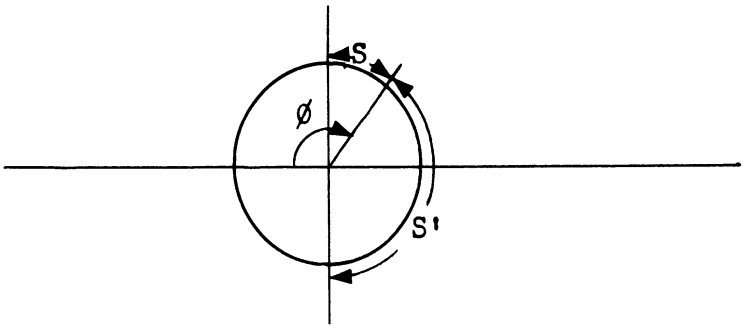

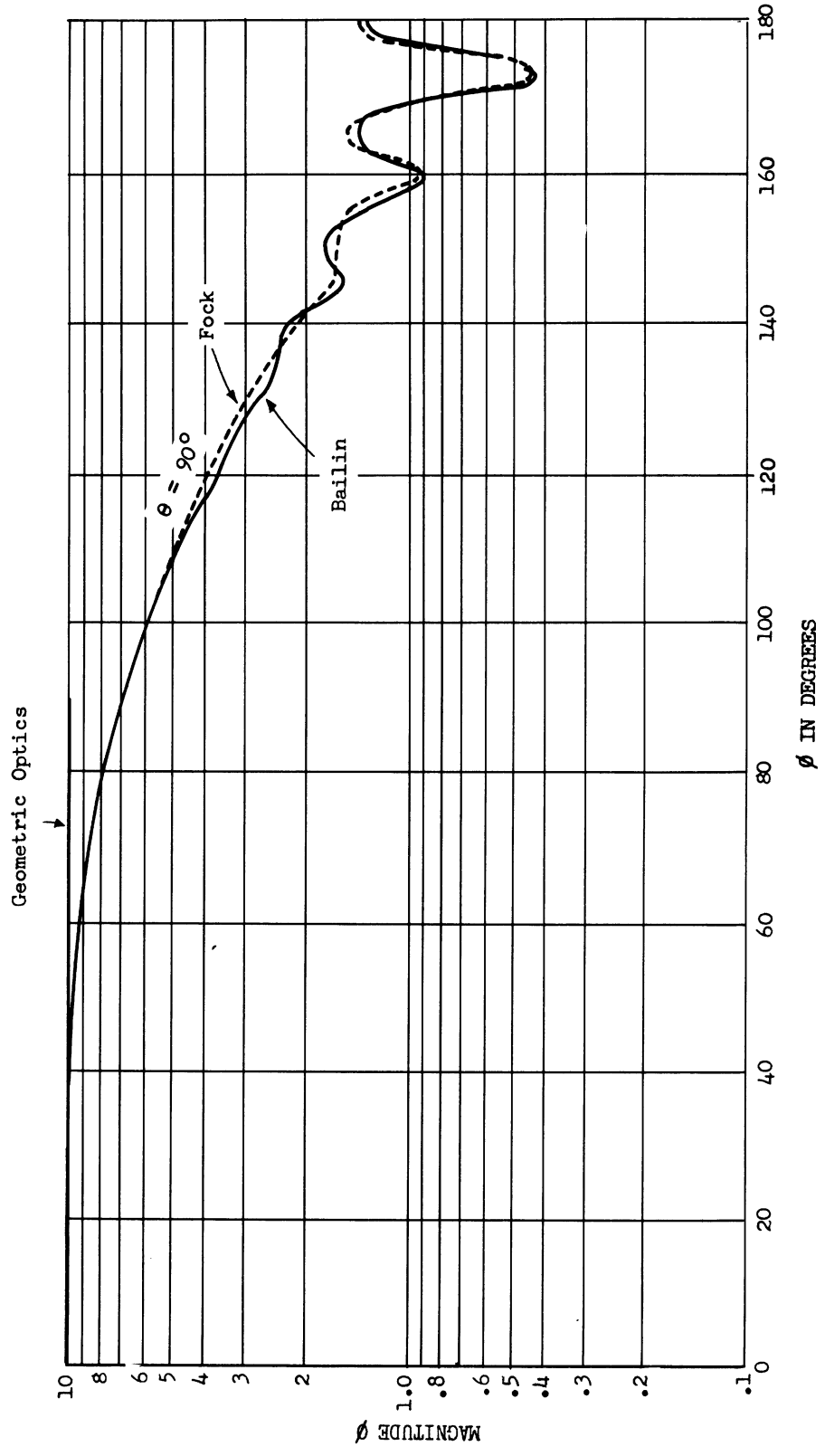


FIG. 2.1 COMPARISON OF SCATTERING AMPLITUDES FROM THE EXACT SERIES, FOCK'S CURRENT DISTRIBUTION, AND THE GEOMETRICAL OPTICS APPROXIMATION FOR AN AXIAL HALF-WAVELENGTH SLOT ON AN INFINITE CYLINDER WITH ka = 12

In terms of polar coordinates

$$S = a(\phi - \frac{\pi}{2})$$

$$S' = a(\frac{3\pi}{2} - \phi)$$

hence,

$$|\vec{E}| \sim \left| G\left(\left(\frac{ka}{2}\right)^{1/3} (\phi - \frac{\pi}{2})\right) + G\left(\left(\frac{ka}{2}\right)^{1/3} (\frac{3\pi}{2} - \phi)\right)\right|$$

In applying Fock's method to general shapes we must exercise some caution. First, since the method is in fact a modification of geometric optics and therefore a short wavelength approximation, all dimensions of the surface must be large with respect to a wavelength. Second, the radii of curvature must be continuous. To illustrate this, consider a modified spindle shape.

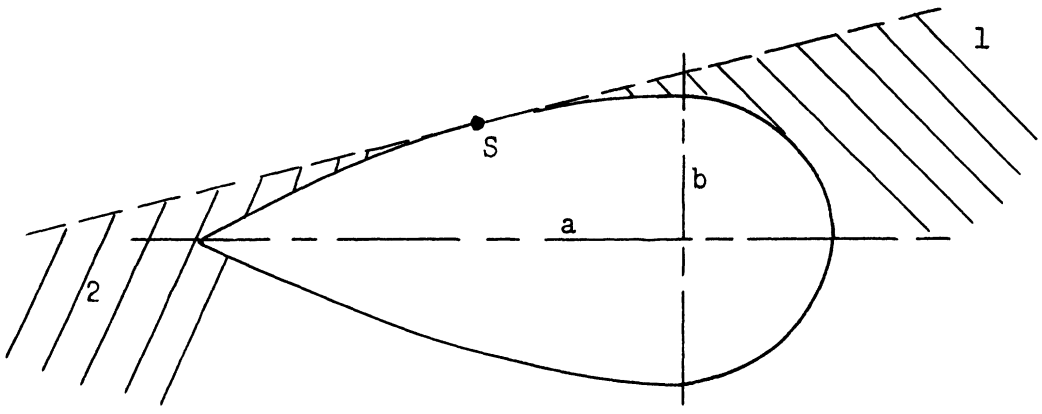

Let a source be located at S. Then, so long as the dimensions a and b are large with respect to the wavelength, the Fock approach is useful in determining the radiation pattern in region 1 but must not be used in region 2 since the radius of curvature is discontinuous at the tip.

The second approach depends upon the decomposition of the exact solution into the geometric optics contribution plus the remainder which we will call the diffraction term. This method has been applied in various separable cases for which the exact solution is available. The use of this method to refine the geometric optics contribution depends upon a ready approximation of the diffracted term. This has been achieved by Franz et al. (Ref. 5) for the infinite circular cylinder and the sphere and by Oberhettinger (Ref. 16) and others for the infinite wedge. The diffraction term appearing in the exact solution of the infinite right circular cone, however, is not so easily approximated except in the limits of a large and small cone angle (Ref. 6).

Because of our particular interest we consider the cone and its two-dimensional counterpart, the wedge, at length. The details of the decomposition into the geometrical optics and diffraction terms appear in Appendices A and B for the wedge and cone, respectively. Except as noted above we do not have much of a hold on the diffracted term for the cone but since we can form an estimate of its size we can discover the range of usefulness of the optics result for sources located at various places on the cone. We find that if the source is a radial distance a from the

tip of the cone, the diffracted term is of order 1/ka as compared with the optics term as long as the source is in view. As we move the observer out of view of the source on the cone, the optics solution is discontinuous, and we must make use of a more sensitive technique. Since we eventually intend to discuss a cylindrically symmetric distribution of sources about the cone axis, we make the point that the effect of the discontinuity in the optics result becomes negligible for a sufficiently dense distribution of sources.

In the following chapter a method of using the optics solution in obtaining the entire radiation pattern from variously excited circumferential slots on a cone will be given.

# CHAPTER 3

## CONE RADIATION PATTERNS BY OPTICAL TECHNIQUES

In determining the radiation from slots in a perfectly conducting semi-infinite cone by means of the geometric optics approximation we note that the case of radial slots can be subsumed under the general theory of linear slots in an infinite plane and hence presents no new difficulty. Contrariwise, the case of the circumferential slot introduces a more difficult problem of characterizing the radiation pattern arising from an arbitrary excitation. The case of a cone, $\theta = \theta_0$, where $\theta$ is the usual spherical polar variable, with an arbitrarily excited circumferential slot at a distance "a" from its tip will be illustrated in some detail.

Let $(r, \theta, \phi)$ and $(a, \theta_0, \beta)$ designate field and integration points (spherical coordinate system), respectively. Then Equation 2.3 takes the form

$$\vec{E} \approx \frac{V_0}{2\pi} \operatorname{curl} \int_{\substack{\text{visible} \\ \text{portion} \\ \text{of slot}}} \frac{e^{ikR}}{R} \left(\hat{j} \cos\beta - \hat{i} \sin\beta\right) a \sin\theta_0 \, f(\beta) \, d\beta \qquad (3.1)$$

where $\hat{i}$ and $\hat{j}$ are unit vectors in the x and y directions, respectively, $V_0$ is a voltage across the slot, and

$$R^2 = r^2 + a^2 - 2ar \left[\cos\theta \cos\theta_0 + \sin\theta \sin\theta_0 \cos(\phi - \beta)\right].$$

The function $f(\beta)$ is an excitation, arbitrary to the extent that it is representable by a Fourier decomposition

$$f(\beta) = \sum_{n=-\infty}^{\infty} C_n \, e^{in\beta} \quad , \; -\pi < \beta < \pi ,$$

where

$$C_m = \frac{1}{2\pi} \int_{-\pi}^{\pi} f(\beta) \, e^{-im\beta} \, d\beta$$

Then for $|\theta| < \pi - \theta_o$, the region where the entire slot can be seen, and for $r \gg a$, Equation 3.1 becomes

$$\vec{E} \approx \frac{ik \, V_o}{2\pi} \, \frac{e^{ikr}}{r} \, a \sin\theta_o \, e^{-ika \cos\theta \cos\theta_o} \sum_{n=-\infty}^{\infty} C_n \, e^{in\phi} \cdot \left[ S_n' \, \hat{\theta} + iT_n' \cos\theta \, \hat{\phi} \right] \qquad (3.2)$$

where $\hat{\theta}$ and $\hat{\phi}$ are unit vectors in the usual spherical coordinate system and

$$S_n' = \frac{\pi}{i^{n-1}} \left[ J_{n-1} (ka \sin\theta \sin\theta_o) - J_{n+1} (ka \sin\theta \sin\theta_o) \right]$$

$$T_n' = \frac{\pi}{i^{n-1}} \left[ J_{n-1} (ka \sin\theta \sin\theta_o) + J_{n+1} (ka \sin\theta \sin\theta_o) \right]. \qquad (3.3)$$

When $\theta > \pi - \theta_o$, the integration of (3.1) is accomplished by the method of stationary phase; the error thus incurred is comparable to the error of the

integral itself. Then for large ka, since there is just one stationary phase point at $\beta = 0$,

$$\vec{E} \approx V_o \frac{e^{ikr}}{r} \sqrt{\frac{ka \sin \theta_o}{2\pi \sin \theta}}\ e^{-ika \cos(\theta_o - \theta) - (\frac{\pi i}{4})} f(0)\ \hat{\theta},\ \pi - \theta_o < \theta \ . \quad (3.4)$$

Using the excitation $f(\beta) \equiv 1$, Bailin and Silver (Ref. 7) have calculated from an exact series the expression

$$\left( ika\ V_o \sqrt{\frac{\pi}{2ka}}\ \frac{e^{ikr}}{r} \right)^{-1} E_\theta \equiv BE_\theta \quad (3.5)$$

for four points, when $\theta_o = 165^\circ$ and $ka = 50\pi$. A comparison between their results and the results from Equation 3.4 is given in Table 3.1.

TABLE 3.1

$\theta_o = 165^\circ$, $ka = 50\pi$

| $\theta$ | $60^\circ$ | $75^\circ$ | $90^\circ$ | $105^\circ$ |
|---|---|---|---|---|
| $BE_\theta$ from Ref.7 | .182 + .087i | -.102 - .110i | .088 + .141i | .108 + .171i |
| $BE_\theta$ from Eq.3.5 | .144 + .098i | -.117 - .117i | .092 + .134i | .117 + .117i |

Figure 3.1 gives a graphical picture, $|BE_\theta|$ versus $\theta$, of Table 3.1.

We felt that it would be valuable to present additional patterns for various excitations and several different cones with circumferential slots at various locations on the cone. In particular, patterns have been computed for $\cos\beta$ (Fig. 3-2) and $\cos 2\beta$ (Fig. 3-3) excitations with the values of $\theta_o$ and ka used above. These are presented on the succeeding pages.

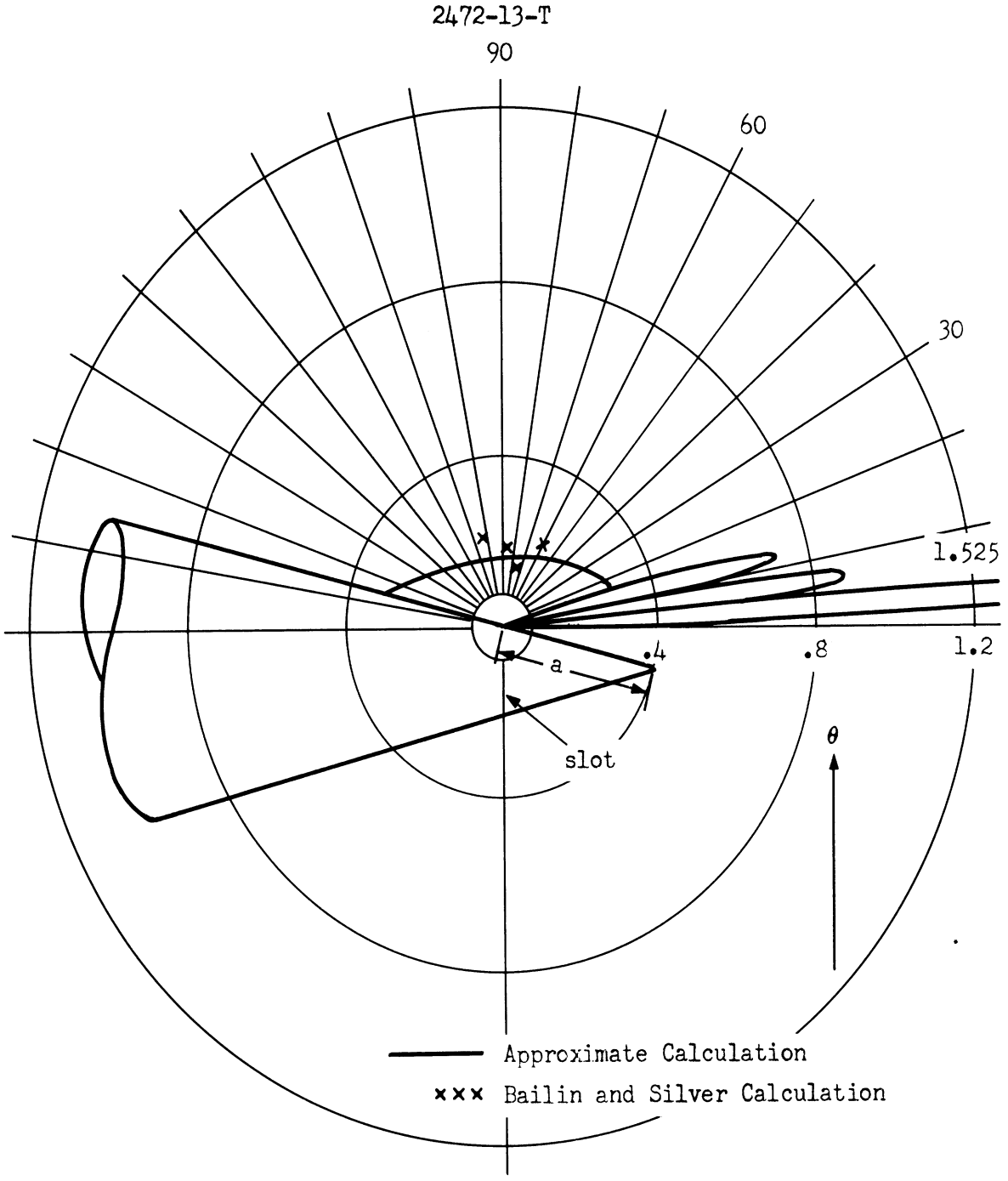


FIG 3.1 NORMALIZED FIELD INTENSITY, $|BE_{\phi}|$, VS $\theta$ FOR A UNIFORMLY EXCITED CIRCUMFERENTIAL SLOT ON A $30^{\circ}$ CONE WITH $ka = 50\pi$

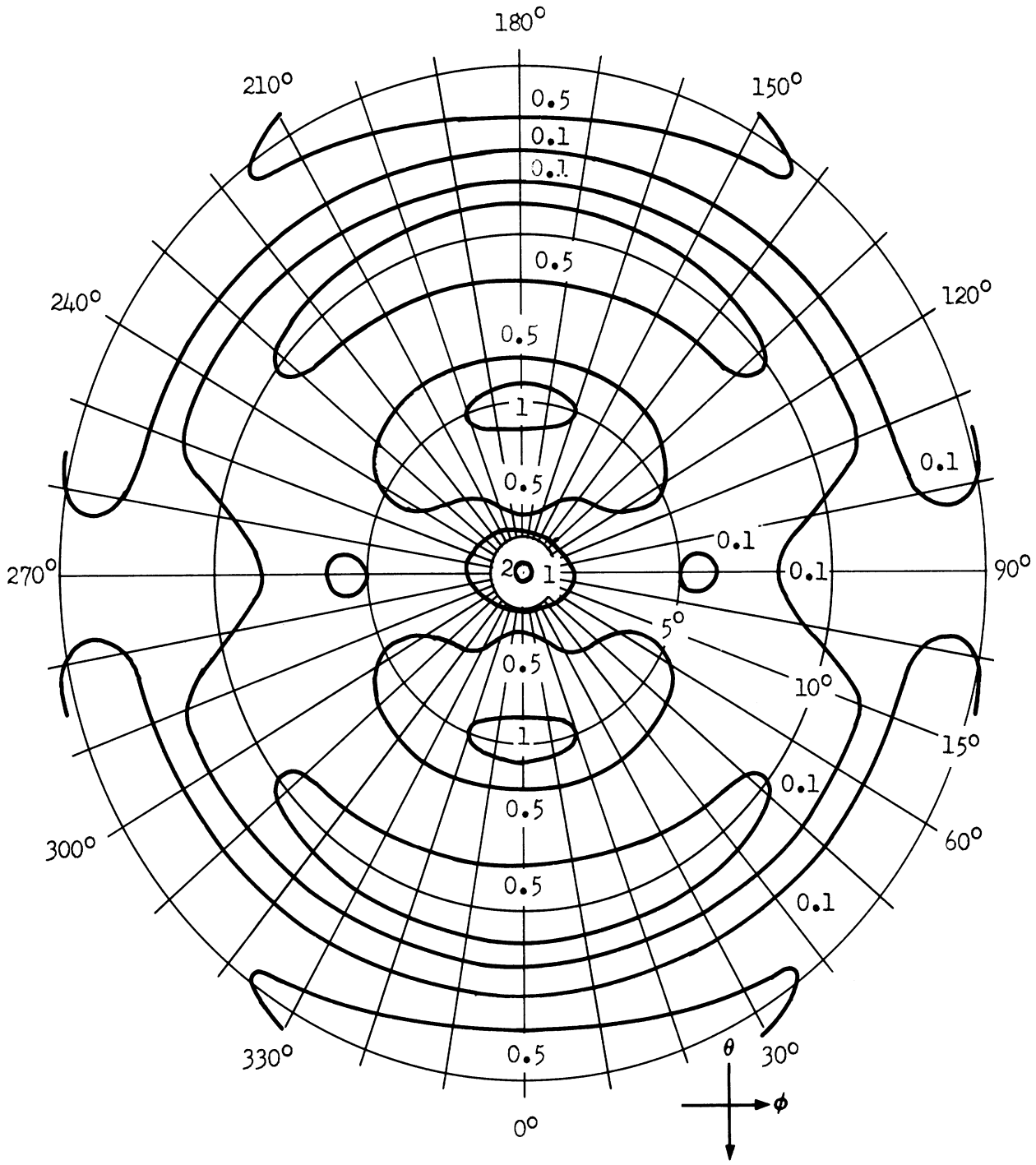


FIG. 3.2 CONTOUR PLOT OF RADIATION PATTERN FROM A 30° CONE WITH CIRCUMFERENTIAL SLOT HAVING COS Ø EXCITATION

(ka = 50π)

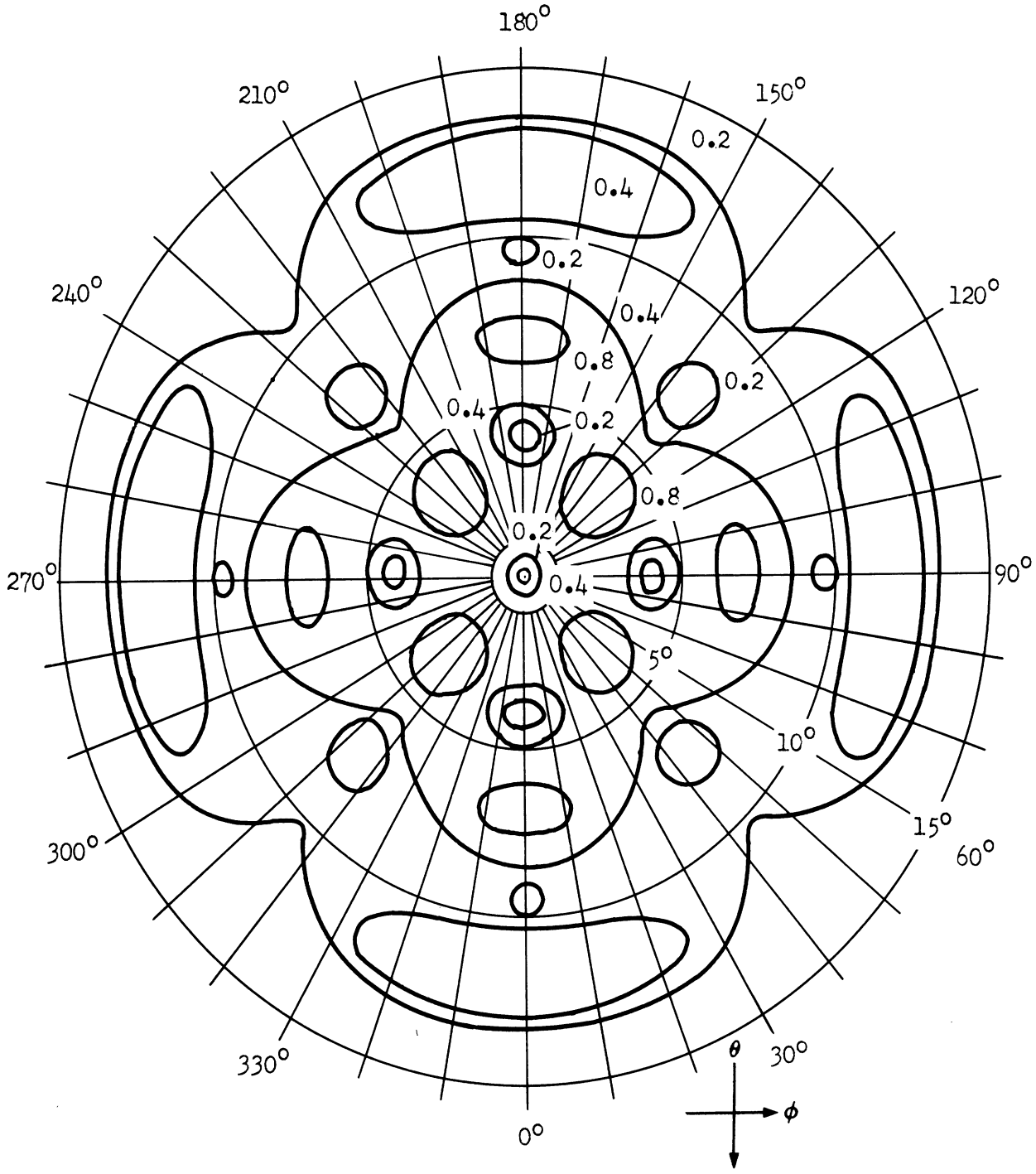


FIG. 3.3 CONTOUR PLOT OF RADIATION PATTERN FROM A 30° CONE WITH CIRCUMFERENTIAL SLOT HAVING COS 2$\phi$ EXCITATION

(ka = 50$\pi$)

In addition, patterns have been computed for all combinations of these parameters: cone angle $\theta_o = 160^o, 165^o, 170^o$; ka = $50\pi, 75\pi$; and excitations $e^{in\beta}$, n = 1, 2, 3. These patterns are presented in Appendix C.

In the following chapter we present a beam optimumization technique using the above results.

# CHAPTER 4

## AN OPTIMIZATION TECHNIQUE

One method of designing an array of radiators to produce a narrow beam is to fix the power radiated in some particular direction and then to minimize the total power radiated in all other directions. As an example, the case of a single circumferential slot, which is especially simple due to the orthogonality of $e^{in\phi}$, is studied below.

Here the excitation coefficients are obtained directly in terms of the Lagrange multipliers (Equations 4.18). In the case of M circumferential slots we would have to solve M simultaneous equations for the magnitudes of the $e^{in\phi}$ excitation in the M slots.

We will concern ourselves here only with the forward directions contained in the extension of the cone. In this case, the field produced by a circumferential slot with an $e^{+in\phi}$ excitation has, to a good approximation, the following simple form (see Equations 3.2, 3.3):

$$\vec{E}_n \approx \frac{ikV_o}{2\pi} \frac{e^{ikr}}{r} a \sin\theta_o \, e^{-ika \cos\theta \cos\theta_o} \, e^{+in\phi} \left[ S'_n \hat{\theta} + iT'_n \cos\theta \, \hat{\phi} \right] \tag{4.1}$$

where

$$S'_n \equiv \frac{\pi}{i^{n-1}} \left[ J_{n-1}(ka \sin\theta \sin\theta_o) + J_{n+1}(ka \sin\theta \sin\theta_o) \right]$$

and

$$T'_n \equiv \frac{\pi}{i^{n-1}} \left[ J_{n-1}(ka \sin\theta \sin\theta_o) + J_{n+1}(ka \sin\theta \sin\theta_o) \right].$$

Here the symbols have the same meaning they have had in Chapter 3. What we want to do is to find an excitation

$$\sum_{n=-N}^{N} (A_n + iB_n)\, i^{n-1}\, e^{in\phi}$$

which will give a pencil beam in the direction $\theta = \alpha$, $\phi = 0$. We proceed by first specifying the field in the direction $\theta = \alpha$, $\phi = 0$, to be

$$\vec{E}(\alpha,0) \approx \frac{ikV_o}{2\pi} \frac{e^{ikr}}{r}\, a \sin\theta_o\, e^{-ika\cos\alpha\cos\theta_o}\, (\hat{\theta} + i\hat{\phi}) \quad . \tag{4.2}$$

This done, we minimize the energy radiated in the forward cone. In order to minimize the radiated energy while simultaneously keeping the field fixed in the specified direction, it is necessary to have a narrow beam pointed in the specified direction.

We now proceed to evaluate the excitation coefficients $A_n$ and $B_n$ in accord with the above program. We let $S_n = S_n'\, i^{n-1}$ and $T_n = T_n'\, i^{n-1}\cos\theta$ so as to be able to deal with real quantities. Now (4.2) gives us the following requirements

$$\sum_{n=-N}^{N} (A_n + iB_n)\, S_n(\alpha) = 1,$$

$$\sum_{n=-N}^{N} (A_n + iB_n)\, T_n(\alpha) = 1 \quad . \tag{4.3}$$

The minimum radiated energy requirement means that we minimize

$$\int_0^{\pi-\theta_o} \int_0^{2\pi} \sin\theta \left\{ \left| \sum_{n=-N}^{N} (A_n + iB_n)\, S_n(\theta)\, e^{in\phi} \right|^2 + \left| \sum_{n=-N}^{N} (A_n + iB_n)\, T_n(\theta)\, e^{in\phi} \right|^2 \right\} d\phi\, d\theta \quad , \tag{4.4}$$

subject, of course, to (4.3). If we let

$$C_n^2 \equiv \int_0^{\pi-\theta_o} \sin\theta \left[ S_n^2(\theta) + T_n^2(\theta) \right] d\theta \tag{4.5}$$

and use Lagrange multipliers to take account of the constraints (4.3), we find that we must minimize

$$\sum_{n=-N}^{N} C_n^2 (A_n^2 + B_n^2) - 2\lambda \sum_{n=-N}^{N} A_n S_n(\gamma) - 2\mu \sum_{n=-N}^{N} A_n T_n(\gamma) - 2\rho \sum_{n=-N}^{N} B_n S_n(\gamma) - 2\nu \sum_{n=-N}^{N} B_n T_n(\gamma) \quad . \tag{4.6}$$

The minimum is obtained by taking

$$A_n = \frac{\lambda S_n(\gamma) + \mu T_n(\gamma)}{C_n^2} \tag{4.7}$$

$$B_n = \frac{\rho S_n(\gamma) + \nu T_n(\gamma)}{C_n^2}$$

The Lagrange multipliers $\lambda, \mu, \rho, \nu$ are determined by substituting (4.7) into (4.3). We find $\rho = \nu = 0$ and

$$\lambda \sum_{n=-N}^{N} \frac{S_n^2(\gamma)}{C_n^2} + \mu \sum_{n=-N}^{N} \frac{S_n(\gamma)\, T_n(\gamma)}{C_n^2} = 1$$

$$\lambda \sum_{n=-N}^{N} \frac{S_n(\gamma)\, T_n(\gamma)}{C_n^2} + \mu \sum_{n=-N}^{N} \frac{T_n^2(\gamma)}{C_n^2} = 1 \qquad (4.8)$$

or

$$A_n = \frac{\begin{vmatrix} 0 & -\dfrac{S_n(\gamma)}{C_n^2} & -\dfrac{T_n(\gamma)}{C_n^2} \\ 1 & \displaystyle\sum_{k=-N}^{N} \frac{S_k^2(\gamma)}{C_k^2} & \displaystyle\sum_{k=-N}^{N} \frac{S_k(\gamma)\, T_k(\gamma)}{C_k^2} \\ 1 & \displaystyle\sum_{k=-N}^{N} \frac{S_k(\gamma)\, T_k(\gamma)}{C_k^2} & \displaystyle\sum_{k=-N}^{N} \frac{T_k^2(\gamma)}{C_k^2} \end{vmatrix}}{\begin{vmatrix} \displaystyle\sum_{k=-N}^{N} \frac{S_k^2(\gamma)}{C_k^2} & \displaystyle\sum_{k=-N}^{N} \frac{S_k(\gamma)\, T_k(\gamma)}{C_k^2} \\ \displaystyle\sum_{k=-N}^{N} \frac{S_k(\gamma)\, T_k(\gamma)}{C_k^2} & \displaystyle\sum_{k=-N}^{N} \frac{T_k^2(\gamma)}{C_k^2} \end{vmatrix}} \qquad (4.9)$$

The derivation given above was for the case where circular polarization is desired in the beam direction (see Equation 4.2). A similar derivation could be just as readily carried out for any other polarization.

We have presented above a method for determining the excitation of a circumferential slot so as to obtain a narrow beam. The presentation of the method was based on a particular approximate formula for the field which holds only in the forward regions. In the remainder of the chapter we show that the method holds in general and give general formulas which can use more exact representations of the field (either theoretical or experimental).

First of all we need to observe that if the slot has an $e^{in\phi}$ excitation then the only $\phi$ dependence of the $\theta$ and $\phi$ components of the electric field will be a factor $e^{in\phi}$. We can prove this as follows: Suppose the excitation $e^{in\phi}$ gives the following field for $\phi = 0$:

$$e^{in\phi} \rightarrow \vec{E}_n(\theta, 0) \approx \left\{ \left[ f_n(\theta) + ig_n(\theta) \right] \hat{\theta} + \left[ h_n(\theta) + ij_n(\theta) \right] \hat{\phi} \right\} \frac{e^{ikr}}{r} \quad . \qquad (4.10)$$

Then the excitation $e^{in(\phi - \alpha)}$ will give the same field for $\phi = \alpha$ since the problems are identical:

$$e^{in(\phi - \alpha)} \rightarrow \vec{E}_n(\theta, \alpha) \approx \left\{ \left[ f_n(\theta) + ig_n(\theta) \right] \hat{\theta} + \left[ h_n(\theta) + ij_n(\theta) \right] \hat{\phi} \right\} \frac{e^{ikr}}{r} \quad . \qquad (4.11)$$

The field for the excitation $e^{in\phi}$ can be obtained from that for the excitation $e^{in(\phi - \alpha)}$ simply by multiplying by $e^{in\alpha}$. Then replacing $\alpha$ by $\phi$ we get the desired relation

$$e^{in\phi} \rightarrow \vec{E}_n(\theta, \phi) \approx \left\{ \left[ f_n(\theta) + ig_n(\theta) \right] \hat{\theta} + \left[ h_n(\theta) + ij_n(\theta) \right] \hat{\phi} \right\} e^{in\phi} \frac{e^{ikr}}{r} \quad . \tag{4.12}$$

Now let us suppose that we require that the field in the direction $(\gamma, 0)$ be

$$\vec{E}(\gamma, 0) \approx (\hat{\theta} + i\hat{\phi}) \frac{e^{ikr}}{r} \tag{4.13}$$

where the excitation is

$$\sum_{n=-N}^{N} (A_n + iB_n) e^{in\phi} \quad .$$

We now require that the quantity

$$\int_0^{\theta_0} \int_0^{2\pi} \sin\theta \left| \vec{E}(\theta, \phi) \right|^2 d\phi \, d\theta$$

be minimized. This gives us the condition that

$$\int_0^{\theta_0} \int_0^{2\pi} \sin\theta \left| \sum_{n=-N}^{N} (A_n + iB_n) \left[ f_n(\theta) + ig_n(\theta) \right] e^{in\phi} \right|^2 d\phi \, d\theta \tag{4.14}$$

$$+ \int_0^{\theta_0} \int_0^{2\pi} \sin\theta \left| \sum_{n=-N}^{N} (A_n + iB_n) \left[ h_n(\theta) + ij_n(\theta) \right] e^{in\phi} \right|^2 d\phi \, d\theta$$

be minimized subject to the constraints

$$\sum_{n=-N}^{N} (A_n + iB_n) \left[ f_n(\gamma) + ig_n(\gamma) \right] = 1 \ ,$$

$$\sum_{n=-N}^{N} (A_n + iB_n) \left[ h_n(\gamma) + ij_n(\gamma) \right] = i \ . \tag{4.15}$$

Now we let

$$C_n^2 \equiv \int_0^{\theta_o} \sin\theta \left[ f_n^2(\theta) + g_n^2(\theta) + h_n^2(\theta) + j_n^2(\theta) \right] d\theta \tag{4.16}$$

Using Lagrange multipliers $\lambda, \mu, \rho, \upsilon$ we minimize

$$\sum_{n=-N}^{N} \Big\{ C_n^2 (A_n^2 + B_n^2) - 2\lambda \left[ A_n f_n(\gamma) - B_n g_n(\gamma) \right] - 2\mu \left[ A_n g_n(\gamma) + B_n f_n(\gamma) \right]$$

$$- 2\rho \left[ A_n h_n(\gamma) - B_n j_n(\gamma) \right] - 2\upsilon \left[ A_n j_n(\gamma) + B_n h_n(\gamma) \right] \Big\} . \tag{4.17}$$

The result is

$$A_n = \frac{\lambda f_n(\gamma) + \mu g_n(\gamma) + \rho h_n(\gamma) + \upsilon j_n(\gamma)}{C_n^2}$$

$$B_n = \frac{\mu f_n(\gamma) - \lambda g_n(\gamma) + \upsilon h_n(\gamma) - \rho j_n(\gamma)}{C_n^2} \tag{4.18}$$

or

$$A_n + iB_n = \frac{(\lambda + i\mu)\left[f_n(\gamma) - ig_n(\gamma)\right] + (\rho + i\nu)\left[h_n(\gamma) - ij_n(\gamma)\right]}{C_n^2} \tag{4.19}$$

It is convenient to deal with the following complex numbers

$$\begin{aligned} D_n &\equiv A_n + iB_n \\ L &\equiv \lambda + i\mu \\ P &\equiv \rho + i\nu \\ F_n(\theta) &\equiv f_n(\theta) + ig_n(\theta) \\ H_n(\theta) &\equiv h_n(\theta) + ij_n(\theta) \quad . \end{aligned} \tag{4.20}$$

Then (4.19) becomes

$$D_n = \frac{LF_n^*(\gamma) + PH_n^*(\gamma)}{C_n^2} \tag{4.21}$$

while (4.15) takes the form

$$\sum_{n=-N}^{N} \frac{L\left|F_n(\gamma)\right|^2 + PF_n(\gamma)\, H_n^*(\gamma)}{C_n^2} = 1$$

$$\sum_{n=-N}^{N} \frac{LF_n^*(\gamma)\, H_n(\gamma) + P\left|H_n(\gamma)\right|^2}{C_n^2} = i \quad . \tag{4.22}$$

Solving (4.21) and (4.22) for $D_n$ we find

$$D_n = \frac{\begin{vmatrix} 0 & -\frac{F_n^*(\gamma)}{C_n^2} & -\frac{H_n^*(\gamma)}{C_n^2} \\ 1 & \sum_{n=-N}^{N} \frac{|F_n(\gamma)|^2}{C_n^2} & \sum_{n=-N}^{N} \frac{F_n(\gamma)\, H_n^*(\gamma)}{C_n^2} \\ i & \sum_{n=-N}^{N} \frac{F_n^*(\gamma)\, H_n(\gamma)}{C_n^2} & \sum_{n=-N}^{N} \frac{|H_n(\gamma)|^2}{C_n^2} \end{vmatrix}}{\begin{vmatrix} \sum_{n=-N}^{N} \frac{|F_n(\gamma)|^2}{C_n^2} & \sum_{n=-N}^{N} \frac{F_n(\gamma)\, H_n^*(\gamma)}{C_n^2} \\ \sum_{n=-N}^{N} \frac{F_n^*(\gamma)\, H_n(\gamma)}{C_n^2} & \sum_{n=-N}^{N} \frac{|H_n(\gamma)|^2}{C_n^2} \end{vmatrix}} \quad . \tag{4.23}$$

This gives the required excitation when circular polarization is desired in the beam direction. If it is desired that the field in the direction $(\gamma, 0)$ have the form

$$\vec{E}(\gamma, 0) \approx (\alpha \hat{\theta} + \beta \hat{\phi}) \frac{e^{ikr}}{r} \quad , \tag{4.24}$$

where $\alpha$ and $\beta$ are arbitrary complex numbers, then the only change in (4.23) is to replace the column

$$\begin{pmatrix} 0 \\ 1 \\ i \end{pmatrix} \quad \text{by} \quad \begin{pmatrix} 0 \\ \alpha \\ \beta \end{pmatrix}$$

in the upper determinant.

One of the interesting conclusions is that for a beam in the forward direction ($\gamma = 0$) it is not possible to reduce the total radiated power to an arbitrarily small value (while keeping the radiated power in the forward direction fixed) when using a single circumferential slot, since for $\gamma = 0$ we have $D_n = 0$ unless $n = \pm 1$.

# CHAPTER 5

## WIENER INTEGRAL METHODS

Because standard techniques of solving scattering and radiation problems have proved inadequate for some problems of interest, there has been a certain amount of interest in developing new approaches. One such new method, the Wiener integral method, is discussed here. It is not yet clear whether or not this method will prove practicable; but the possibility that it might, may justify this discussion.

The Wiener integral method actually is a method of attack for boundary value problems involving the diffusion equation. Since our interest centers in the wave equation rather than the diffusion equation, we will start the discussion by pointing out a connection between the two problems. Such a connection is mentioned, among other places, in Reference 8.

Let $\mathcal{G}(x,y,z,t)$ be the solution of the equation

$$\nabla^2 \mathcal{G} - 4 \frac{\partial \mathcal{G}}{\partial t} = -4f(x,y,z)\, \delta(t) \tag{5.1}$$

which is zero for $t < 0$ and which satisfies a linear, time-independent boundary condition on some surface. Here $\delta(t)$ is the Dirac delta function. Now consider the function

$$G(x,y,z,p) = \int_{-\infty}^{\infty} e^{-\frac{1}{4} p^2 t}\, \mathcal{G}(x,y,z,t)\, dt \quad . \tag{5.2}$$

If we differentiate under the integral sign we find that

$$\nabla^2 G - p^2 G = -4f(x,y,z) \quad , \tag{5.3}$$

and that G satisfies the same boundary condition as $\mathcal{G}$. The equation for which we would actually like a solution is

$$\nabla^2 G + k^2 G = -4f(x,y,z) \ . \tag{5.4}$$

If we assume that $G(x,y,z,p)$ is an analytic function of p, then we can replace p by ik or -ik to get solutions of (5.3). In order to proceed in this way it will be very desirable to obtain G as a function of p rather than obtaining G numerically for various values of p. The reason that we do not take $p = \pm ik$ directly in (5.2) is that then the integral would not, in general, converge.

Although we have mentioned only a scalar problem, it is evident that the above reasoning applies equally well to vector problems.

Having made the connection, we will now restrict our attention to diffusion problems. In order to see the relationship between Wiener integrals and diffusion problems it is simplest to start with the free-space problem. In this case it is well-known (and easily verified) that the solution of (5.1) is

$$\mathcal{G}(x,y,z,t) = \frac{1}{(\pi t)^{3/2}} \int_{-\infty}^{\infty}\int_{-\infty}^{\infty}\int_{-\infty}^{\infty} e^{-\frac{\xi^2+\eta^2+\zeta^2}{t}} f(x-\xi, y-\eta, z-\zeta)\, d\xi\, d\eta\, d\zeta \ . \tag{5.5}$$

We can write this concisely in terms of Wiener integrals by using the following relationship

$$\int_c^w \Phi\left[x(t)\right] \, d_w x = \int_{-\infty}^{\infty} \frac{e^{-\frac{x^2}{t}}}{\sqrt{\pi t}} \, \Phi(x) \, dx \quad . \tag{5.6}$$

This equation, as well as a brief discussion of what a Wiener integral is, will be found in Reference 9. The result of using (5.6) in (5.5) is that we can write

$$\psi(x,y,z,t) = \int_c^w \int_c^w \int_c^w f\left[x-\xi(t),\ y-\eta(t),\ z-\zeta(t)\right] \, d_w\xi \, d_w\eta \, d_w\zeta \quad . \tag{5.7}$$

In order to see how to proceed in the case when a scattering surface is present it is convenient to give a physical interpretation to (5.7). The interpretation we use is the following. At time t = 0 we release particles with a density f(x,y,z). A typical particle follows a path which at time s has coordinates $x-\xi(t-s)$, $y-\eta(t-s)$, $z-\zeta(t-s)$. The probability of this particular path is $d_w\xi \, d_w\eta \, d_w\zeta$. Then $\psi(x,y,z,t)$ is the density of particles at time t.

Using this type of interpretation, we can conceive problems whose solutions in terms of Wiener integrals are obvious, but which are at the same time solutions of (5.1) subject to certain boundary conditions. For

example, suppose we want $\psi(x,y,z,t)$ to vanish on some given surface. We can accomplish this in the following way. We again let $\psi$ be a density of particles. We again start the particles out at a density $f(x,y,z)$ and let them follow paths $x-\xi(t-s), \ldots$ . However, now whenever a particle hits the given surface we assume that it is absorbed. The density of particles will satisfy (5.1). On the surface the density of particles will be zero since all particles on the surface are absorbed. Thus the particle density is a solution of the desired problem. But, from the description of what happens to the particles, we see that the density of particles can be written as

$$\psi(x,y,z,t) = \int_{C_w}\int_{C_w}\int_{C_w} \chi(\xi,\eta,\zeta)\, f\left[x-\xi(t),\ y-\eta(t),\ z-\zeta(t)\right] d_w\xi\, d_w\eta\, d_w\zeta \tag{5.8}$$

where $\chi$ is zero if the path $x-\xi(t-s), \ldots$ touches the given surface and is one otherwise. This is a well known way of satisfying this problem and is mentioned, for example, in Reference 8.

The above model is not the only one which will enable us to solve this problem in terms of Wiener integrals. The following is another of the possible models. We have two kinds of particles which we call positive particles and negative particles. We start with positive particles having a density $f(x,y,z)$. Now whenever a particle hits the given surface it is reflected off specularly and simultaneously is changed into a particle of the other kind. If we look at the particles near the surface we find that

half of the particles have just hit the surface and thus changed sign so that the numbers of positive and negative particles are equal. If we take $\mathcal{Y}$ to be the difference in the density of the positive and negative particles we see that $\mathcal{Y}$ is the solution to the desired problem. In terms of Wiener integrals the solution to this problem can be written immediately in the form

$$\mathcal{Y}(x,y,z,t) = \int_c^w \int_c^w \int_c^w (-)^n f(x^*,y^*,z^*) \; d_w\xi \; d_w\eta \; d_w\zeta \quad . \tag{5.9}$$

Here the path $x-\xi(t-s)$, ... is modified by reflection as indicated above (see Figure 5-1), n is the number of reflections the path undergoes and $x^*$, $y^*$ , $z^*$ are the points from which the modified path starts. We see

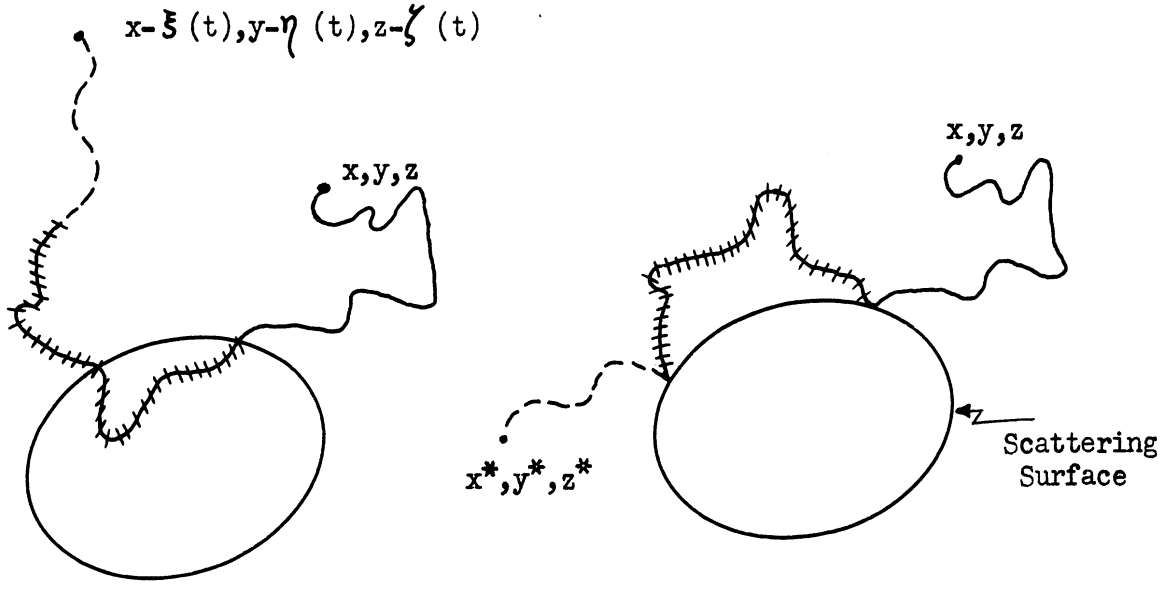


Unmodified Path Modified Path

FIG 5-1 PATH OF A PARTICLE IN FREE SPACE (UNMODIFIED PATH) AND IN THE PRESENCE OF A BODY (MODIFIED PATH)

that (5.8) and (5.9) give us two quite different expressions for the same thing. We could also construct other models which would give us still more expressions. For example we could think of a surface which absorbs some particles while reflecting and changing the sign of others. Also the reflection would not have to be specular. Other models might involve the creation of a number of particles whenever a particle hits the surface. All of these different models give us many Wiener integrals all having the same value. Now only in very rare cases will we be able to evaluate the integrals in a simple closed form. Generally we will have to resort to a series expansion or something similar. Thus the many different models give us some freedom in trying to choose a model for which the expansion will be rapidly convergent. Also it is possible to use the results for a second model as a check on the results of the first model.

Equations 5.8 and 5.9 have been applied to scattering by an infinite plane. A sequence of approximate evaluations of the Wiener integrals was used. (Cf. Equation 5.13). The approximate evaluations of (5.9) could all be carried out in closed form and all agree with the exact answer. The first two approximations to (5.8) were obtained. Figure 5-2 illustrates the relation between the approximations and the exact answer as a function of distance from the plane at a particular instant of time.

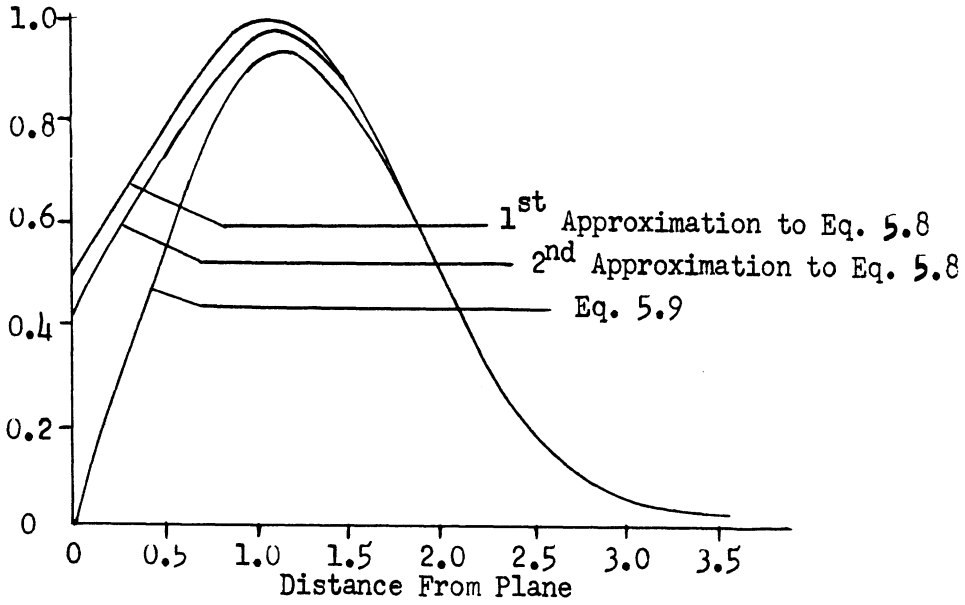


FIG 5-2 COMPARISON OF EXACT AND APPROXIMATE INFINITE PLANE SOLUTIONS

The above discussion has been for a scalar problem. We will now mention a model which may be used for electromagnetic problems where the bodies are perfect conductors. As a preliminary let us reconsider the model discussed above which involved two kinds of particles, positive and negative. A slightly different language to describe the situation is found to be convenient. We now assume that we have only one kind of particle, but that the particle carries along a label which can be either positive or negative. Whenever the particle hits a scatterer it is specularly reflected and its label changes sign. Now to compute $\mathcal{G}$ at a point we take a small volume, v, about the point and let

$$\mathcal{G} = \frac{1}{v} \sum L_n \,, \tag{5.10}$$

where $L_n$ is the label ( +1 or -1) of the $n^{th}$ particle in the volume.

In the vector case we proceed similarly, except that now the label is a unit vector. If we are trying to compute the electric field, we require that on reflection of a particle the tangential component of its label change sign while the normal component remains unchanged. The formula for $\vec{\mathcal{G}}$ is now

$$\vec{\mathcal{G}} = \frac{1}{v} \sum \vec{L}_n \quad . \tag{5.11}$$

We could equivalently use a model involving six kinds of particles corresponding to positive and negative components in three directions.

The above considerations allow us to write down (Wiener) integral representations for the solutions to scattering and radiation problems involving arbitrarily shaped bodies. However, in order for these representations to be useful we must have practical methods for evaluating the Wiener integrals involved. This is the problem which still awaits a completely satisfactory solution. We will discuss below an approach which can be used but which is quite laborious.

When one is faced with a Riemann integral which he cannot evaluate in a simple closed form, one frequently resorts to numerical integration. Certain general formulas have been developed for this purpose such as the

trapezoidal rule and Simpson's rule. For Wiener integrals Cameron (Ref. 10) has given some analogous approximation formulae. The simplest formula he gives is

$$\int_C^w F\left[x(\cdot)\right] d_w x \sim \int_{-\infty}^{\infty} \cdots \int_{-\infty}^{\infty} \frac{e^{-\xi_1^2 - \cdots \xi_n^2}}{\pi^{n/2}} F\left[\frac{2}{\pi} \sum_{j=1}^{n} \frac{\sqrt{2}\, \xi_j \sin\left\{(j-1)\pi(\cdot)\right\}}{2j-1}\right] d\xi_1 \cdots d\xi_n \tag{5.12}$$

Thus the Wiener integral is approximated by an n-fold Riemann integral. Cameron has shown under certain conditions that the right side of (5.12) approaches the left side of (5.12) when $n \to \infty$ .

Let us take a look at the application of (5.12) to (5.8). In order to use (5.12) we find that we must evaluate the functional for a path which is given by a trigonometric series with arbitrary coefficients (we integrate with respect to the coefficients from $-\infty$ to $\infty$). This means that, for (5.8), we must take a path whose x, y, and z components are trigonometric series in time with arbitrary coefficients, and find out if the path hits the body or not. We then integrate the coefficients over the region in which the path does not hit the body. Determining whether the path hits the body involves the solution of a complicated transcendental equation. The situation would be much simpler if the paths we had to consider were of some simpler form such as broken line segments. We can readily obtain a modification of (5.12)

in which the paths considered are broken line segments. We quote the formula without proof:

$$\int_c^w F[x(\cdot)]\, d_w x \sim \int_{-\infty}^{\infty}\cdots\int_{-\infty}^{\infty} F\left[\frac{1}{\sqrt{n}}\sum_{j=1}^{n}\zeta_j\,\alpha_j(\cdot)\right]\frac{e^{-\zeta_1^2-(\zeta_2-\zeta_1)^2-\cdots-(\zeta_n-\zeta_{n-1})^2}}{\pi^{n/2}}\, d\zeta_1\cdots d\zeta_n \qquad (5.13)$$

where $\sum_{j=1}^{n}\zeta_j\,\alpha_j(t)$ is the function shown in Figure 5-3.

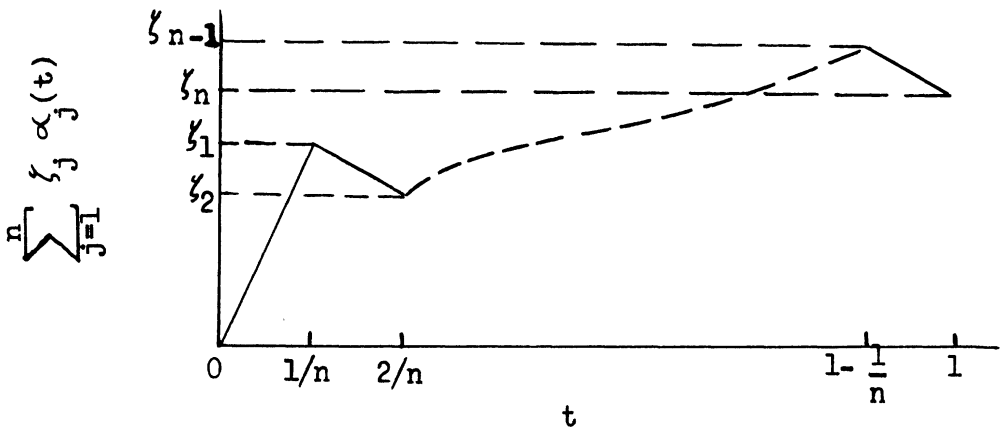


FIG 5-3 TYPICAL PATH

When we use (5.13) in conjunction with the model for the vector problem discussed in connection with (5.11), we find that for n = 1 we get just geometric optics. For larger n we get corrections to geometric optics including contributions from the shadow regions.

The sequence of approximations obtained is not an asympototic sequence although the greatest accuracy is probably obtained (for a given n) for short wavelengths.

If n is taken sufficiently large, we can get as accurate an answer as desired, but the amount of labor involved in evaluating the multiple integrals is very large. Thus it would be desirable to get improved integration formulas.

# CHAPTER 6

## CONCLUSIONS AND PROSPECTUS

In conclusion we find, on the basis of the above analysis (see Chapters 2,3,4), that radiation patterns of single circumferential or radial slots with arbitrary excitation can be given by optics techniques with sufficient accuracy that we may now turn to the problem of using such elements to produce a useful antenna. The solution of this problem requires that we determine for a given surface the distribution and excitation of such elements necessary to produce a radiation pattern of given beamwidth, side-lobe level, gain, and scan capabilities.

Hence, during the coming year, The University of Michigan plans to investigate the following problems:

(1) the problem of determining pattern features, corresponding to scan angles $0^\circ$ - $80^\circ$, resulting from (a) a linear array along a cone generator, and (b) a system of such linear arrays spaced at certain azimuthal intervals and excited with a constant, or cosine, azimuthal distribution. In connection with this problem an attempt will be made to ascertain the degree to which the control of beam shape can be specified in terms of phase distributions (possibly non-linear) along an array.

(2) the problem similar to 1 and for (a) an annular array, and (b) a set of such arrays.

Problems 1 and 2 will undoubtedly necessitate refinement and extension of the approximation methods of this report so as to obtain beam scan information to within prescribed limits of beam deterioration and cross-polarization effects.

A study will be made of

(3) the problem of determining what alterations in pattern features and scanning capabilities of a dipole-activated prolate spheroid result from alterations of the surface of the spheroid. Surface alteration would be defined to mean placement of dipoles on the surface in various ways in possible conjunction with bumps and indentations of the surface itself.

The Polytechnic Institute of Brooklyn and The University of Illinois are engaged in efforts complementary to those of The University of Michigan. These efforts are described below.

The Electrophysics group of the Microwave Research Institute, Polytechnic Institute of Brooklyn will continue to investigate the problems of scattering by and radiation from infinite and finite cones. In particular they will continue their study of the vector field problem of radiation from circumferential and infinitesimal slots on a cone via Green's function and modal techniques; in this consideration they will give particular attention to alternative representations which would permit casting the results into a rapidly convergent form applicable to the numerical description of fields in illuminated, shadow,

and transition regions surrounding various conical geometries. This group will investigate fields set up on coupled radiating slots and slot arrays on cones via integral equation and variational techniques; from this information they hope to apply the Green's function results alluded to above and thereby obtain radiation patterns from slot arrays of arbitrary elements. In connection with arrays of slots, they will investigate the "surface" and "leaky" waves whose propagation along the surface of a cone, in consequence of slot arrays thereon, and whose reflections by the cone boundaries, can modify the radiation pattern. The Electrophysics group will attempt to apply the above results to numerical calculation of radiation patterns for specific array geometries.

The University of Illinois will analyze a method of replacing an antenna system which can be enclosed by a given surface in space, by an array of slots in a conductor which coincides with the surface. In particular, they will attempt to determine the minimum density of slots on the surface of a sphere (and ultimately on a finite cone) necessary to reproduce the pattern arising from a continuous tangential field distribution (or a dish in free space) according to variously prescribed criteria.

# APPENDIX A

## WEDGE

The radiation from two slots parallel to and equidistant from the edge of an infinite perfectly conducting wedge is treated below: the exact boundary value problem is solved, and then, since the solution is not amenable to rapid computation, an asymptotic approximation as well as the geometrical optics solution is developed, and the results obtained from the exact and approximate methods are compared.

A more general solution for the radiation from a wedge, involving slots with various orientations relative to the edge, has been studied by Felsen and is given in Reference 11.

### A-1 Electromagnetic Field for an Infinite Perfectly Conducting Wedge with Uniformly Excited Slots Parallel to its Edge

Let $V_o$ = voltage across the slots

$a$ = distance of slots from the edge

$e^{-i\omega t}$ = time dependence of fields .

The electric field for the slotted wedge of Figure A-1 is given by TM modes, with the electric field perpendicular to the edge of the wedge.

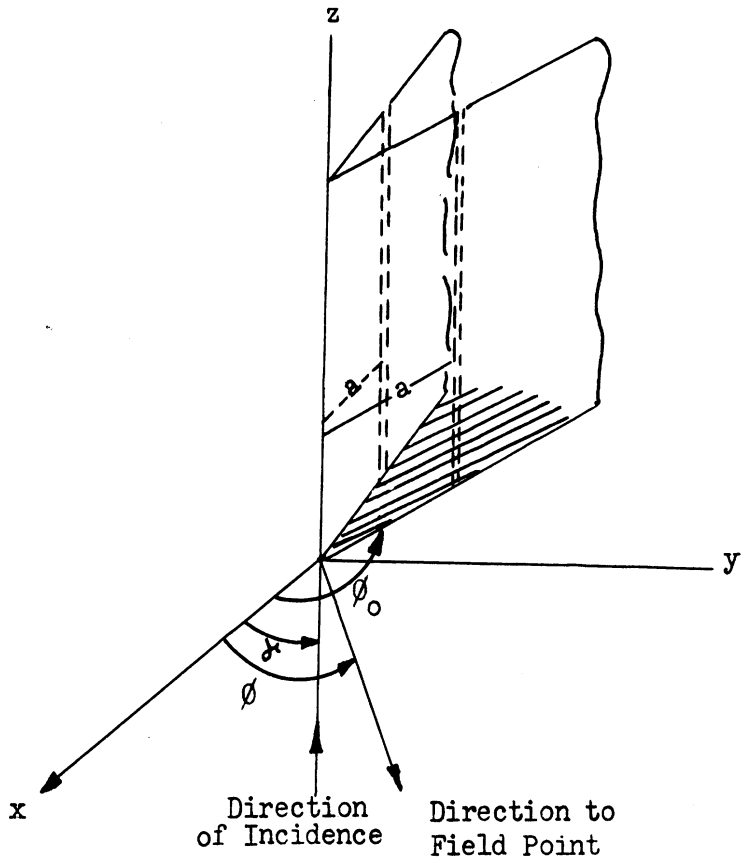


FIG A-1

A-1.1 Exact Solution

The exact solution is obtained from the boundary problem

$$(\nabla^2 + k^2)\psi = 0 \tag{A.1}$$

where

$$\vec{E} = -\frac{1}{ik}\nabla \times \hat{k}\psi = -\frac{1}{ik}\left[\frac{1}{r}\frac{\partial \psi}{\partial \phi}\hat{r} - \frac{\partial \psi}{\partial r}\hat{\phi}\right] \tag{A.2}$$

with boundary conditions

$$-\frac{1}{ik}\frac{1}{r}\frac{\partial \psi}{\partial \phi}\Bigg|_{\phi = \pm \phi_o} = V_o \delta(r-a) \tag{A.3}$$

since the tangential fields must vanish on the wedge, except at the slots. Solutions of Equation A.1 are:

$$\psi = J_\nu(kr)\left[A_\nu \cos\nu\phi + B_\nu \sin\nu\phi\right] \qquad (A.4)$$

for r small, so that the fields remain bounded near the edge, and

$$\psi = H^{(1)}_\nu(kr)\left[A_\nu \cos\nu\phi + B_\nu \sin\nu\phi\right] \qquad (A.5)$$

for r large; this corresponds to an outgoing wave.

From Equation A.3

$$\frac{\partial\psi}{\partial\phi} = 0 \text{ at } \phi = \pm\phi_o \quad \text{and} \quad \nu = \frac{n\pi}{2\phi_o}, \; B_n = 0 \text{ for n even.}$$

$A_n = 0$ for all n since the $\phi$ component of the electric fields as the edge is approached from above the $\phi = 0$ axis must be the negative of the $\phi$ component as the edge is approached from below the $\phi = 0$ axis.

Then

$$\psi = \sum_{n=1}^{\infty} B_{2n-1} H^{(1)}_{\frac{2n-1}{2\phi_o}\pi}(kr) \sin\frac{(2n-1)\pi\phi}{2\phi_o} \quad \text{for r large,} \qquad (A.6)$$

and

$$\psi = \sum_{n=1}^{\infty} B'_{2n-1} J_{\frac{2n-1}{2\phi_o}\pi}(kr) \sin\frac{(2n-1)\pi\phi}{2\phi_o} \quad \text{for r small .} \qquad (A.7)$$

The coefficients may be found by use of the Lorentz Reciprocity theorem in the form (Ref. 7):

$$0 = \int_S \left\{ \left[\vec{E} \times \vec{H}_M\right] \cdot \hat{n} - \left[\vec{E}_M \times \vec{H}\right] \cdot \hat{n} \right\} dS$$

where $\vec{E}$, $\vec{H}$ are the fields obtained from or given by Equation (A.6), and $\vec{E}_M$, $\vec{H}_M$, are the modal solutions corresponding to a given index n. S is the sum of $S_0$, $S_1$, $S_2$ and $S_\infty$ as shown in Figure A-2.

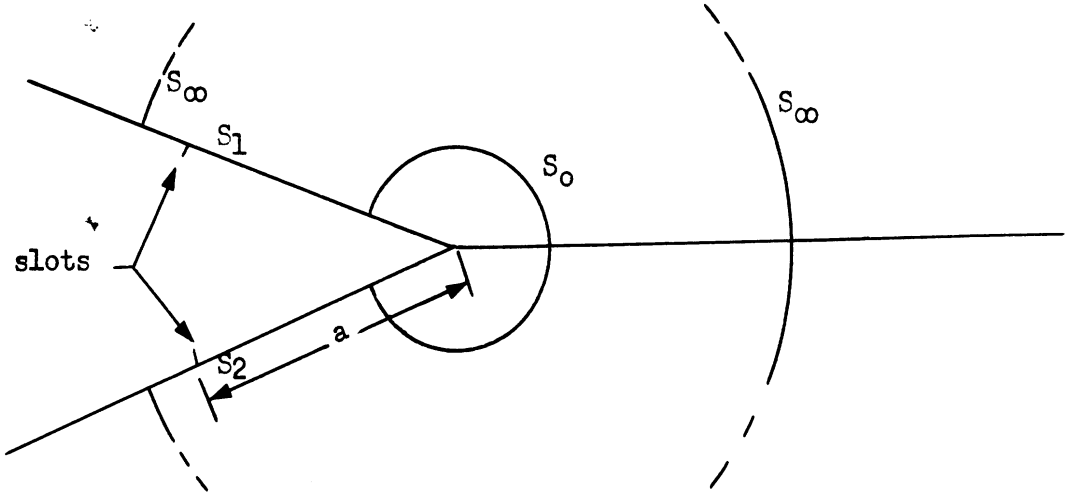


FIG A-2 REGIONS OF INTEGRATION FOR THE WEDGE

Integration over the surface yields:

$$\int_S = 0 = \frac{2\phi_o B_m}{\pi k} + 2\, V_o(-1)^n\, J_{\frac{m\pi}{2\phi_o}}(ka) \qquad m = 2n-1 \tag{A.8}$$

Using $B_m$ from Equation A.8 in Equation A.6 and applying Equation A.2 :

$$E_\phi = \frac{i\pi V_o}{\phi_o} \frac{\partial}{\partial r} \sum_{n=1}^{\infty} (-1)^n\, J_{\frac{2n-1}{2\phi_o}\pi}(ka)\; H^{(1)}_{\frac{2n-1}{2\phi_o}\pi}(kr) \sin \frac{2n-1}{2\phi_o}\pi\phi \tag{A.9}$$

for r large. For r small the Bessel and Hankel functions are reversed.

A-1.2 Asymptotic Solutions and Estimate of Error of Asymptotic Solutions

Approximate expressions for $E_\phi$ for $r \gg a$ and $ka \gg 1$ are obtained through three approaches. The first approximation may be obtained by considering a related scattering problem. The second method consists in expressing Equation A.9 in terms of integrals obtained by Oberhettinger (Ref. 12) and by obtaining asymptotic expansions of these integrals. A comparison between the exact solution (in terms of the integrals of Reference 12) and the approximations used provides an estimate of the error of the asymptotic approximation. A third method expresses the integrals encountered in the second method in terms of continued fractions at large distances. The same expression is obtained from the first and second methods; a different and more accurate one from the third method.

Method 1: Asymptotic Solution Obtained by Considering a Scattering Problem

a) Development of Asymptotic Solution

For $r \gg a$, Equation A.9 may be expressed as:

$$E_\phi = -\frac{iV_o}{2\pi} e^{ikr+\frac{\pi i}{4}} \sqrt{\frac{\pi k}{2r}} \left[ \frac{4\pi}{\phi_o} \sum_{n=0}^{\infty} e^{-i(n+\frac{1}{2})\frac{\pi^2}{2\phi_o}} J_{n+\frac{1}{2}}(ka) \sin\left[(n+\tfrac{1}{2})\frac{\pi\phi}{\phi_o}\right] \right] \quad \text{(A.10)}$$

The expression in brackets may be obtained from a two-dimensional scattering problem. For this purpose consider a perfectly conducting, non-slotted wedge in the polar coordinate system, a, $\phi$, as shown in Figure A-3:

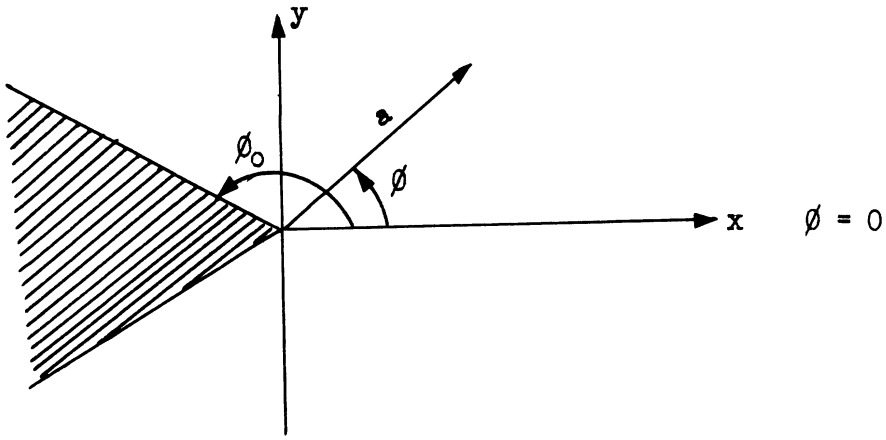


FIG A-3

For this wedge geometry the geometric optics fields are:

$$\psi_{G.O.}(\phi_o) = 2e^{-ika\cos(\phi-\phi_o)}\, u(\pi+\phi-\phi_o) \tag{A.11}$$

and

$$\psi_{G.O.}(-\phi_o) = 2e^{-ika\cos(\phi+\phi_o)}\, u(\pi-\phi-\phi_o) \tag{A.12}$$

where u is the Heaviside unit function. The scattered fields corresponding to the above geometric optics fields are (Ref. 13):

$$\frac{2\pi}{\phi_o}\sum_{n=0}^{\infty} e^{-in\frac{\pi^2}{4\phi_o}}\, J_{\frac{n\pi}{2\phi_o}}(ka)(1-\tfrac{1}{2}\delta_{no})\cos\frac{n\pi(\phi-\phi_o)}{2\phi_o} \tag{A.13}$$

and

$$\frac{2\pi}{\phi_o} \sum_{n=0}^{\infty} e^{-i\frac{n\pi^2}{4\phi_o}} J_{\frac{n\pi}{2\phi_o}}(ka)\,(-1)^n\left(1 - \tfrac{1}{2}\,\delta_{no}\right) \cos\frac{n\pi(\phi-\phi_o)}{2\phi_o} \quad . \qquad (A.14)$$

From this it appears that the bracketed expression in Equation A.10 is $\psi(\phi_o) - \psi(-\phi_o)$. The total geometrical optics solution $\psi_{G.O.}$, given by the sum of Equation A.11 and Equation A.12, may be expanded into the set of functions $\sin(n + \frac{1}{2})\frac{\pi\phi}{\phi_o}$ :

$$\psi_{G.O.} = \sum_{n=0}^{\infty} f_n(ka) \sin\left[\frac{(n + \frac{1}{2})}{\phi_o}\pi\phi\right] \qquad (A.15)$$

where, for ka large,

$$f_n(ka) \simeq (-1)^n \frac{2}{\phi_o}\sqrt{\frac{2\pi}{ka}}\left[e^{ika - \frac{\pi i}{4}} \cos(n + \tfrac{1}{2})\frac{\pi^2}{\phi_o} + e^{-ika + \frac{\pi i}{4}}\right]. \qquad (A.16)$$

By separating out the geometrical optics solution expressed in Equation A.15 and Equation A.16 from Equation A.10, and by using the asymptotic form of $f_n(ka)$ and $J_{(n + \frac{1}{2})\frac{\pi}{\phi_o}}(ka)$, and then summing the terms not involving $\psi_{G.O.}$ :

$$E_\phi \simeq -\frac{iV_o\, e^{ikr + \frac{\pi i}{4}}}{2\pi}\sqrt{\frac{\pi k}{2r}}\left[\psi_{G.O.} + \frac{e^{ika + \frac{\pi i}{4}}}{2\phi_o}\sqrt{\frac{2\pi}{ka}}\left\{\ \right\}\right] \qquad (A.17)$$

$$\left\{\right\} = \frac{1}{\cos\frac{\pi(\pi+\phi)}{2\phi_o}} - \frac{1}{\cos\frac{\pi(\pi-\phi)}{2\phi_o}} \quad .$$

This asymptotic expression may be obtained through other methods (see Section A-1.2, Method 2a). It is not applicable to the transition regions $\phi = \pm (\pi - \phi_o)$ for which an asymptotic formula must be derived separately.

b) Comparison of Scattering Problem with Results Obtained from the Pulse Solution of Keller and Blank

The bracketed expression in Equation A.17 may be obtained by considering the solution obtained by Keller and Blank (Ref. 14, pp. 75-94) for the two dimensional scattering problem of a plane pulse incident on a perfectly conducting infinite wedge. Again considering the polar coordinate system a, $\phi$ and letting $V(\alpha, \phi, t)$ be the pulse solution, the time harmonic solution is given by Duhamel's theorem (Ref. 14, p. 90):

$$\psi(\omega) = -i\omega \int_{-\infty}^{\infty} V(t)\, e^{i\omega t}\, dt \qquad (A.18)$$

and

$$V(t) = \frac{-1}{2\pi i} \int_{-\infty}^{\infty} \frac{\psi(\omega)}{\omega}\, e^{-i\omega t}\, dt \quad . \qquad (A.19)$$

The pulse solution corresponding to the geometric optics field

$$\psi_{G.O.} = 2\left[e^{-ika\cos(\phi-\phi_0)}\, u(\pi+\phi-\phi_0) - e^{-ika\cos(\phi+\phi_0)}\, u(\pi-\phi-\phi_0)\right] \tag{A.20}$$

$$V_{G.O.} = 2\left\{ u\left[t+\frac{a}{c}\cos(\phi-\phi_0)\right]u(\pi+\phi-\phi_0) - u\left[\left(t+\frac{a}{c}\cos(\phi+\phi_0)\right]u(\pi-\phi-\phi_0)\right\}\right. \tag{A.21}$$

The diffraction field obtained from Keller and Blank (Ref. 14, p.81) is:

$$V_D = \frac{2}{\pi}\left[\tan^{-1}\left\{\frac{(1-\rho^{2\lambda})\sin\lambda\pi}{(1+\rho^{2\lambda})\cos\lambda\pi - 2\rho^{\lambda}\sin\lambda\phi}\right\} - \tan^{-1}\left\{\frac{(1-\rho^{2\lambda})\sin\lambda\pi}{(1+\rho^{2\lambda})\cos\lambda\pi + 2\rho^{\lambda}\sin\lambda\phi}\right\}\right] u\left(t-\frac{a}{c}\right) \tag{A.22}$$

where $\rho = \dfrac{a}{ct+\sqrt{c^2t^2-a^2}}$ , $\lambda = \dfrac{\pi}{2\phi_0}$ and the $\tan^{-1}$ lies between 0 and $\pi$. The diffraction field may be obtained by applying Equation A.18 to Equation A.22

$$\psi_D = -i\omega\int_{\frac{a}{c}}^{\infty} e^{i\omega t}\,\frac{2}{\pi}\left[\tan^{-1}\left\{\frac{(1-\rho^{2\lambda})\sin\lambda\pi}{(1+\rho^{2\lambda})\cos\lambda\pi-2\rho^{\lambda}\sin\lambda\phi}\right\} - \tan^{-1}\left\{\frac{(1-\rho^{2\lambda})\sin\lambda\pi}{(1+\rho^{2\lambda})\cos\lambda\pi+2\rho^{\lambda}\sin\lambda\phi}\right\}\right] dt \ . \tag{A.23}$$

The integrals may be evaluated through rapidly convergent expansions (Ref. 15), of which only the first term is used here. By examining the value of the integrand for $t = \frac{a}{c} + \varepsilon$ ( $\varepsilon$ small,) it is observed that, except for $\phi = \pm(\pi - \phi_0)$, the integrand varies as $\sqrt{\varepsilon}$. Constant terms, however, are brought about by values of $\tan^{-1}$ close to $\pi$; hence, to avoid this, the $\tan^{-1}$ will be chosen between $-\frac{\pi}{2}$ and $\frac{\pi}{2}$. This will be indicated by $\tan^{-1}$. Equation A.23 is then in such a form that the rapidly convergent expansions mentioned above may be used.

$$\psi_D = 2e^{ika}\left[u(\phi-\phi_0+\pi) - u(\pi-\phi_0-\phi)\right]$$

$$-i\omega \int_{a/c}^{\infty} \frac{2}{\pi}\left[\tan^{-1}\left\{\frac{(1-\rho^{2\lambda})\sin\lambda\pi}{(1+\rho^{2\lambda})\cos\lambda\pi - 2\rho^{\lambda}\sin\lambda\phi}\right\}\right. \qquad \text{(A.24)}$$

$$\left. -\tan^{-1}\left\{\frac{(1-\rho^{2\lambda})\sin\lambda\pi}{(1+\rho^{2\lambda})\cos\lambda\pi + 2\rho^{\lambda}\sin\lambda\phi}\right\}\right] dt.$$

The field of Equation A.21 persists only until $t = \frac{a}{c}$; the terms introduced by the shutting off of Equation A.21 cancel the first term of Equation A.24 and the scattered field becomes (by using Equation 1 of Reference 15):

$$\psi = \psi_{G.O.} + \sqrt{\frac{2}{3\pi}}\, e^{ika}\left[ \tan^{-1}\left\{ \frac{(1-\rho^{2\lambda})\sin\lambda\pi}{(1+\rho^{2\lambda})\cos\lambda\pi - 2\rho^{\lambda}\sin\lambda\phi} \right\} \right. \qquad (A.25)$$

$$\left. - \tan^{-1}\left\{ \frac{(1-\rho^{2\lambda})\sin\lambda\pi}{(1+\rho^{2\lambda})\cos\lambda\pi + 2\rho^{\lambda}\sin\lambda\phi} \right\} \right] \Bigg|_{t=\frac{a}{c}+\frac{3i}{2}}$$

As $ka \to \infty$, this may be reduced to the expression between the brackets of Equation A.17.

Method 2: Asymptotic Expressions Obtained by Use of Oberhettinger's Formulas for Diffraction by a Wedge. Estimate of Error.

a) Asymptotic Expression Excluding the Transition Regions, and Estimate of Error.

Oberhettinger obtained the Dirichlet Green's function for the two dimensional case of an incident cylindrical wave with direction of incidence $\gamma$ and axis parallel to the edge.

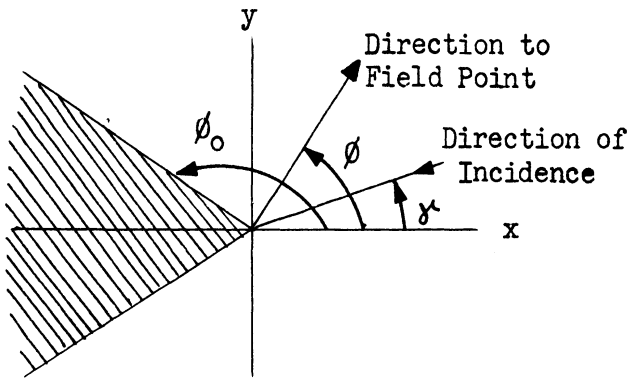


FIG A-4

The expression is:

$$G(\gamma') = \frac{\pi}{\phi_o}\left[J_o(ka)\, H_o^{(1)}(kr) + \sum_{n=1}^{\infty} \frac{J_{n\pi}}{2\phi_o}(ka)\, \frac{H_{n\pi}^{(1)}}{2\phi_o}(kr)\left\{\ \right\}\right] \qquad (A.26)$$

$$\left\{\ \right\} = \cos\frac{n\pi}{2\phi_o}(\phi - \gamma') + \cos\frac{n\pi}{2\phi_o}(\phi + \gamma' + 2\phi_o) \quad .$$

$\psi$, from expression (A.6) with the proper coefficients, may be expressed in terms of this Green function. Then

$$\psi = \frac{kV_o}{4}\left[G(\phi_o) - G(-\phi_o)\right] \quad . \qquad (A.27)$$

By use of Equations 29 - 35 of Reference 12, this may be written as:

$$\psi = \frac{kV_o}{4}\left\{2H_0^{(1)}\left[k(r^2 + a^2 - 2ar\cos(\phi - \phi_o))^{1/2}\right] u(\pi + \phi - \phi_o)\right.$$

$$\left. - 2H_0^{(1)}\left[k(r^2 + a^2 - 2ar\cos(\phi + \phi_o))^{1/2}\right] u(\pi - \phi - \phi_o)\right. \qquad (A.28)$$

$$+ \frac{1}{2\phi_o}\cos\frac{\pi}{2\phi_o}(\pi + \phi)\int_0^{\infty} \frac{H_0^{(1)}\left[k(r^2 + a^2 + 2ar\cosh x)^{1/2}\right] dx}{\cosh\frac{\pi x}{2\phi_o} - \sin\frac{\pi}{2\phi_o}(\pi + \phi)}$$

(This equation is continued on next page).

$$- \frac{1}{2\phi_o} \cos \frac{\pi}{2\phi_o} (\pi - \phi) \int_o^\infty \frac{H_o^{(1)} \left[k(r^2 + a^2 + 2ar \cosh x)^{1/2}\right] dx}{\cosh \frac{\pi x}{2\phi_o} + \sin \frac{\pi}{2\phi_o} (\pi - \phi)}$$

$$- \frac{1}{2\phi_o} \cos \frac{\pi}{2\phi_o} (\pi - \phi) \int_o^\infty \frac{H_o^{(1)} \left[k(r^2 + a^2 + 2ar \cosh x)^{1/2}\right] dx}{\cosh \frac{\pi x}{2\phi_o} - \sin \frac{\pi}{2\phi_o} (\pi - \phi)}$$

$$+ \frac{1}{2\phi_o} \cos \frac{\pi}{2\phi_o} (\pi + \phi) \int_o^\infty \frac{H_o^{(1)} \left[k(r^2 + a^2 + 2ar \cosh x)^{1/2}\right] dx}{\cosh \frac{\pi x}{2\phi_o} + \sin \frac{\pi}{2\phi_o} (\pi + \phi)}$$

Estimate of Error

An asymptotic expression as well as an estimate of the error was found for integrals of the type

$$\int_o^\infty \frac{H_o^{(1)} (kR)}{\cosh \frac{\pi x}{2\phi_o} \pm \sin \beta} dx \qquad (A.29)$$

where $\beta = \frac{\pi}{2\phi_o} (\pi \pm \phi_o)$ and $R^2 = r^2 + a^2 + 2ar \cosh x$. For $r >> a$ .

$$H_o^{(1)} (kR) \approx \sqrt{\frac{2}{\pi kR}} e^{ikR - \frac{\pi i}{4}} = A_o^{(1)} (kR) . \qquad (A.30)$$

Equation A.29 may be written as

$$\int_0^\infty \frac{A_0^{(1)}(kR)\,dx}{\cosh\frac{x\pi}{2\phi_0} \pm \sin\beta} + \int_0^\infty \frac{H_0^{(1)}(kR) - A_0^{(1)}(kR)}{\cosh\frac{\pi x}{2\phi_0} \pm \sin\beta}\,dx = I + D. \quad (A.31)$$

I may be evaluated by using a method which is elaborated in the following section:

$$I = \int_0^\infty \frac{A_0^{(1)}(kR)\,dx}{\cosh\frac{\pi x}{2\phi_0} \pm \sin\beta} = \sqrt{\frac{2}{\pi}}\, e^{-i\frac{\pi}{4}} \int_0^\infty \frac{e^{ikR}dx}{\sqrt{kR}\left[\cosh\frac{\pi x}{2\phi_0} \pm \sin\beta\right]}$$

$$= \sqrt{\frac{2}{\pi}}\, e^{-i\frac{\pi}{4}}\, \frac{1}{(1 \pm \sin\beta)\sqrt{2kar}} \int_{r+a}^\infty \frac{e^{ikR}dR}{\sqrt{R-r-a}} \quad (A.32)$$

$$-\frac{1}{ik}\int_0^\infty e^{ikR}\frac{\partial}{\partial x}\left[\frac{\sqrt{R}}{\sqrt{k}\,ar\sinh x(\cosh\frac{\pi x}{2\phi_0} \pm \sin\beta)} - \frac{1}{\sqrt{2kar(R-a-r)}(1 \pm \sin\beta)}\right]dx$$

$$= I_{sp} - \frac{1}{ik}\int_0^\infty e^{ikR}\frac{\partial B}{\partial x}\,dx$$

$$= I_{sp} - J.$$

Then $$\int_0^\infty \frac{H_o^{(1)}(kR)\,dx}{\cosh\frac{\pi x}{2\phi_o} \pm \sin\beta} = I_{sp} - J + D$$

$$I_{sp} = \frac{e^{ik(a+r)}}{k\sqrt{ar}\,(1 \pm \sin\beta)} \quad .$$

By using $$\int_0^\infty \frac{H_o^{(1)}(kR)\,dx}{\cosh\frac{\pi x}{2\phi} \pm \sin\beta} = I_{sp}$$ in Equation A.28, (A.33)

$$\Psi \approx \tfrac{1}{2} k V_o H_o^{(1)}\left[k\sqrt{r^2 + a^2 - 2ar\cos(\phi-\phi_o)}\right] u(\pi + \phi - \phi_o) \qquad (A.34)$$

$$- \tfrac{1}{2} k V_o H_o^{(1)}\left[k\sqrt{r^2 + a^2 - 2ar\cos(\phi+\phi_o)}\right] u(\pi - \phi - \phi_o)$$

$$+ \frac{V_o e^{ik(a+r)}}{4\phi_o\sqrt{ar}} \left\{ \frac{1}{\cos\frac{\pi}{2\phi_o}(\pi+\phi)} - \frac{1}{\cos\frac{\pi}{2\phi_o}(\pi-\phi)} \right\} .$$

The asymptotic form of $E_\phi$ obtained from Equation A.34 corresponds to Equation A.17.

In order to estimate the error of the approximation, bounds will be found for J and D. From the results of the following section

$$|J| \leq \frac{2(n+1)A}{k} \tag{A.35}$$

where n is the number of zeroes of $\frac{\partial B}{\partial x}$ and A is a bound of B.

It was found that

$$|B| \leq \frac{1}{4a\sqrt{k}\sqrt{r}\,(1 \pm \sin\beta)}\,, \tag{A.36}$$

which implies

$$|J| \leq \frac{1}{2k^{3/2}\,a\sqrt{r}\,(1 \pm \sin\beta)}\,. \tag{A.37}$$

Only one zero was used for $\frac{\partial B}{\partial x}$ in Equation A.35, since the other zeroes occur at the end points where B = 0.

A bound for D is obtained as follows:

$$\left|H_\nu^{(1)}(kR) - A_\nu^{(1)}(kR)\right| = \left|\sqrt{\frac{2}{\pi kR}}\,\frac{e^{i(kR - \frac{\nu\pi}{2} - \frac{\pi}{4})}}{\Gamma(\nu + \frac{1}{2})}\int_0^\infty e^{-u}\,u^{\nu-\frac{1}{2}}\left[\left(1+\frac{iu}{2kR}\right)^{\nu-\frac{1}{2}} - 1\right]du\right| \tag{A.38}$$

$$\leq \sqrt{\frac{2}{\pi kR}}\,\frac{\Gamma(\nu+3/2)}{\sqrt{2kR}\,\Gamma(\nu-\frac{1}{2})} \quad \text{for } \nu < 3/2$$

Then $$\left|H_o^{(1)}(kR) - A_o^{(1)}(kR)\right| \leq \frac{1}{8kR}\sqrt{\frac{2}{\pi kR}} \tag{A.39}$$

and using this in D gives a bound:

$$\left| \int_0^\infty \frac{H_0^{(1)}(kR) - A_0^{(1)}(kR)}{\cosh \frac{\pi x}{2\phi_0} \pm \sin\beta} \, dx \right| \leq \frac{\phi_0}{4\pi}\sqrt{\frac{2}{\pi}} \frac{1}{(kr + ka)^{3/2}} \left(\beta \pm \frac{\pi}{2}\right)\csc\left(\beta \pm \frac{\pi}{2}\right) \tag{A.40}$$

General Discussion of Error in the Stationary Phase Method

The object of our attention here will be the integral

$$I = \int_0^\infty g(t)\, e^{ikf(t)dt}$$

where $f'(t) > 0$ except for $t = 0$ and $f'(0) = 0$. By a change of variable the integral can be rewritten in the form

$$I = \int_{f(0)}^{f(\infty)} \frac{g(t)}{f'(t)}\, e^{ikf}\, df.$$

Near $t = 0$ we have

$$f(t) = f(0) + f''(0)\frac{t^2}{2} + f'''(0)\frac{t^3}{6} + \cdots$$

$$f'(t) = f''(0)t + \cdots = \sqrt{2f''(0)\left[f - f(0)\right]} + \cdots .$$

Making use of this behavior we split the integral into two parts, the first of which is the stationary phase contribution, as follows:

$$I = \int_{f(0)}^{f(\infty)} \frac{g(0)\, e^{ikf}\, df}{\sqrt{2f''(0)\,[f-f(0)]}} + \int_{f(0)}^{f(\infty)} \left[ \frac{g(t)}{f'(t)} - \frac{g(0)}{\sqrt{2f''(0)\,[f-f(0)]}} \right] e^{ikf} df.$$

On integrating the second integral by parts we get

$$I = I_{sp} + \left[ \frac{g(t)}{f'(t)} - \frac{g(0)}{\sqrt{2f''(0)\,[f(t)-f(0)]}} \right] \frac{e^{ikf(t)}}{ik} \Bigg|_0^\infty$$

$$- \frac{1}{ik} \int_0^\infty e^{ikf(t)} \frac{\partial}{\partial t} \left[ \frac{g(t)}{f'(t)} - \frac{g(0)}{\sqrt{2f''(0)\,[f(t)-f(0)]}} \right] dt$$

$$= I_{sp} + \left[ \frac{g(\infty)}{f'(\infty)} - \frac{g(0)}{\sqrt{2f''(0)\,[f(\infty)-f(0)]}} \right] \frac{e^{ikf(\infty)}}{ik}$$

$$- \frac{g(0)}{f''(0)} \left[ \frac{g'(0)}{g(0)} - \frac{f'''(0)}{3f''(0)} \right] \frac{e^{ikf(0)}}{ik}$$

$$- \frac{1}{ik} \int_0^\infty e^{ikf(t)} \frac{\partial}{\partial t} \left[ \frac{g(t)}{f'(t)} - \frac{g(0)}{\sqrt{2f''(0)\,[f(t)-f(0)]}} \right] dt.$$

Now by obtaining a bound for the last integral, J, in the above equation we can obtain a bound for the error incurred by using stationary phase. Such a bound is

$$|J| \leq \frac{1}{k} \int_0^\infty \left| \frac{d}{dt}\left[ \frac{g(t)}{f'(t)} - \frac{g(0)}{\sqrt{2f''(0)\ [f(t)-f(0)]}} \right] \right| dt \ .$$

The integral just above can be rewritten in the following form

$$|J| \leq \frac{1}{k} \sum_{j=0}^{n} \left| \left[ \frac{g(t)}{f'(t)} - \frac{g(0)}{\sqrt{2f''(0)\ [f(t)-f(0)]}} \right]_{t_j}^{t_{j+1}} \right|$$

where $t_o = 0$, $t_{n+1} = \infty$, and

$$\frac{d}{dt_j}\left[ \frac{g(t_j)}{f'(t_j)} - \frac{g(0)}{\sqrt{2f''(0)\ [f(t_j)-f(0)]}} \right] = 0 \quad (j = 1, 2, \ldots, n).$$

Thus, if we can get a bound of the form

$$\left| \frac{g(t)}{f'(t)} - \frac{g(0)}{\sqrt{2f''(0)\ [f(t)-f(0)]}} \right| \leq A,$$

then we have

$$|J| \leq \frac{2(n+1)A}{k} \ .$$

b) Asymptotic Expression for the Transition Region

For $\phi = \pm (\pi - \phi_0)$ the asymptotic expression (A.17) is not applicable. For these values of $\phi$, the integrals of Equation A.28 are of the form:

$$I(\delta, 2\phi_0) = -\frac{1}{4\phi_0} \sin\frac{\pi\delta}{2\phi_0} \int_0^\infty \frac{H_0^{(1)}(kR)\, dx}{\cosh\frac{\pi x}{2\phi_0} - \cos\frac{\pi\delta}{2\phi_0}} \tag{A.41}$$

where $\delta$ has the values:

$$\delta_1 = \pi + \phi - \phi_0 ; \delta_2 = \pi - \phi + \phi_0; \delta_3 = \pi - \phi - \phi_0; \delta_4 = \pi + \phi + \phi_0 .$$

Using the method of the preceding section, these integrals are given by:

$$2I(\delta, 2\phi_0) \approx -\frac{e^{ik(a+r)\cot\frac{\pi\delta}{4\phi_0}}}{2\phi_0 k\sqrt{ar}} \tag{A.42}$$

For $\delta_2$ and $\delta_4$ there are no singularities. For $\delta_1$ and $\delta_3$, there are singularities at $\phi = \pm (\pi - \phi_0)$. For such integrals, Oberhettinger (Ref. 16) obtained a series representation of which the first term is used here. Oberhettinger's integrand numerator was $e^{-ika\cosh x}$; for this reason i was changed into -i and the factor $\sqrt{\frac{2}{\pi kr}}\, e^{ikr - i\pi/4}$ was added to Oberhettinger's results in order to obtain the integration of the asymptotic form of Equation A.41.

Then

$$\psi \simeq \frac{V_0 k}{2}\sqrt{\frac{2}{\pi kr}}\, e^{ikr - \frac{\pi i}{4}} \left\{ e^{-ika\cos(\phi - \phi_0)}\, U(\pi + \phi - \phi_0) \right.$$

$$- e^{-ika\cos(\phi + \phi_0)}\, U(\pi - \phi - \phi_0)$$

$$+ I^*(\delta_1, 2\phi_0) + I(\delta_2, 2\phi_0) \qquad \text{(A.43)}$$

$$\left. - I^*(\delta_3, 2\phi_0) - I(\delta_4, 2\phi_0) \right\}$$

where the I terms are given by Equation A.42 and $I^*$ by

$$I^*(\delta, 2\phi_0) \approx -\sqrt{\frac{2}{\pi kr}}\, e^{ikr - \frac{i\pi}{4}} \left\{ \frac{1}{\sqrt{\pi}}\, e^{ika\cos\delta - \frac{i\pi}{4}} S^*\left(\sqrt{2ka}\left|\sin\frac{\delta}{2}\right|\right) \operatorname{sgn}\delta \,. \right.$$

$$\left. + \sqrt{\frac{\pi}{ka}}\, e^{ika - \frac{\pi i}{4}} \left[ A_0(\delta, 2\phi_0) - A_0(\delta, 2\pi) - A_0(2\pi - \delta, 2\pi) \right] \right\} \qquad \text{(A.44)}$$

where

$$S^*(z) = \int_z^\infty e^{it^2}\, dt \quad \text{and} \quad A_0(\delta, 2\phi_0) = \frac{1}{4\phi_0\sqrt{2}} \cot\frac{\pi\delta}{4\phi_0}$$

This leads to an expression which is bounded for $\phi = \pm(\pi - \phi_0)$, and which for $\phi \neq \pm(\pi - \phi_0)$ and ka large, gives a field $E_\phi$ which reduces to Equation A.17.

Method 3: Asymptotic Expansions by Means of Continued Fractions.

A different asymptotic form of Equation A.28 may be obtained by expressing integrals of the type of Equation A.29 in the form of asymptotic series, and then converting them into continued fractions. Consider

$$I(\delta, 2\phi_o) = -\frac{\sin\frac{\pi\delta}{2\phi_o}}{4\phi_o}\int_o^\infty \frac{e^{-ika\cosh x}}{\cosh\frac{\pi x}{2\phi_o} - \cos\frac{\pi\delta}{2\phi_o}}\,dx \qquad (A.45)$$

These integrals are of the type of Equation A.29 for $r >> a$ if $i \to -i$ and the factor

$\sqrt{\frac{2}{\pi kr}}\, e^{ikr - i\pi/4}$ is added.

The asymptotic form of A-45 is:

$$I(\delta, 2\phi_o) \simeq \frac{e^{-i(ka + \frac{\pi}{4})}}{\sqrt{ka}} \sum_{n=o}^{\infty} \frac{A_n(\delta, 2\phi_o)\Gamma(n + \frac{1}{2})}{(ika)^n} \qquad (A.46)$$

where

$$\frac{\sin\frac{\pi\delta}{2\phi_o}}{2(2\phi_o)\sqrt{t+2}\left\{\cosh(\frac{\pi}{\alpha}\cosh^{-1}(1+t) - \cos\frac{\pi\delta}{\alpha}\right\}} = \sum_{n=o}^{\infty} A_n(\delta, 2\phi_o)\, t^n \quad (|t| < |\delta|)$$

This asymptotic series may be converted into a continued fraction (Ref.17)

$$I(\delta, 2\phi_o) = \frac{\frac{\cot \frac{\pi\delta}{4\phi_o}}{4\phi_o} \sqrt{\frac{\pi ka}{2}}\, e^{-i(ka + \frac{3\pi}{4})}}{\frac{1}{8}\left\{1 + \frac{2\pi^2}{4\phi_o^2}\left(\sin\frac{\pi\delta}{4\phi_o}\right)^{-2}\right\} + ika + \cdots} \qquad (A.47)$$

There are indications that the continued fraction may converge and represent $I(\delta, 2\phi_o)$, and further that the continued fraction, when cut off at a point corresponding to that at which the asymptotic series is cut off, will always give a better answer than the asymptotic series. The fields obtained from this method were calculated and compared with those obtained from the exact solution; this method was found to give a better approximation than Equation A.17.

A-1.3 Geometric Optics Solution

By adapting the field of a slot in an infinite perfectly conducting plane to an infinite perfectly conducting wedge, one obtains, for the case of short wavelengths, a first approximation to the radiation problem: this is a geometric optics approximation.

The field of a slot of length L and width W on an infinite perfectly conducting plane (see Fig. A-5) is derived as follows. Let $L \ll \lambda$ and $W \ll \lambda$. The tangential component of the electric field must be zero outside the slot and equal to $V_o/W$ across the slot. Such a field may be produced by a magnetic dipole placed in the plane of the slot along the slot: its magnetic moment is derived below. The field of a magnetic dipole at $x=0$, $y=0$ oriented along the x-axis is $\vec{E} = K \frac{e^{ikr}}{r}\left(1 - \frac{1}{ikr}\right) \hat{r} \times \hat{i}$ where K must be determined.

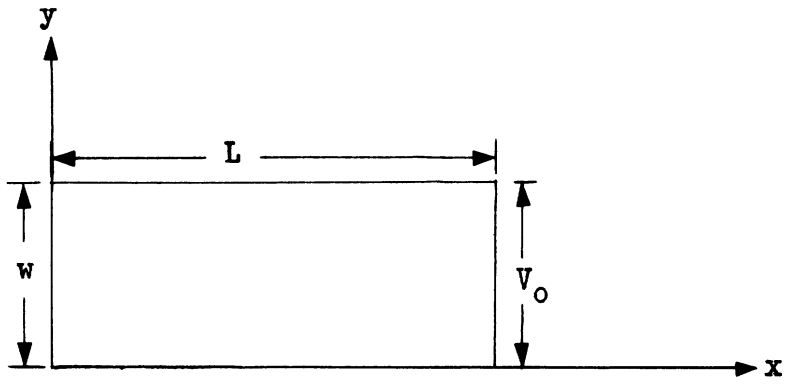


FIG A-5 SLOT CONFIGURATION

At a distance $\Delta$ above the slot, for $kr << 1$:

$$\vec{E} \simeq \frac{iK(x\hat{i} + y\hat{j} + \Delta\hat{k})x\hat{i}}{k(x^2 + y^2 + \Delta^2)^{3/2}} = \frac{iK(\Delta\hat{j} - y\hat{k})}{k(x^2 + y^2 + \Delta^2)^{3/2}} \quad . \tag{A.48}$$

As $\Delta \to 0$, the $\hat{j}$ component should vanish except at $x = y = 0$. In order to evaluate K, the tangential component is integrated over x and y. For the slot the integral has the value $-L\,V_o\,\hat{j}$, where the direction of the field has been taken to be given by the right hand rule.

Then

$$-L\,V_o = \lim_{\Delta \to 0} \frac{ik\Delta}{k} \int_{-\infty}^{\infty} \int_{-\infty}^{\infty} \frac{dx\,dy}{(x^2 + y^2 + \Delta^2)^{3/2}} = \frac{2\pi iK}{k} \tag{A.49}$$

and

$$\vec{E} = \frac{ikV_oL}{2\pi} \frac{e^{ikr}}{r} \left(1 - \frac{1}{ikr}\right) \hat{r} \times \hat{i} = \frac{V_oL}{2\pi} \nabla \times \left( \hat{i} \frac{e^{ikr}}{r} \right). \tag{A.50}$$

This gives the exact field in the case of an infinite plane. When Equation A.50 is used for an arbitrary body, integration takes place over the portion of the slot visible from the field point (Fig. A-6).

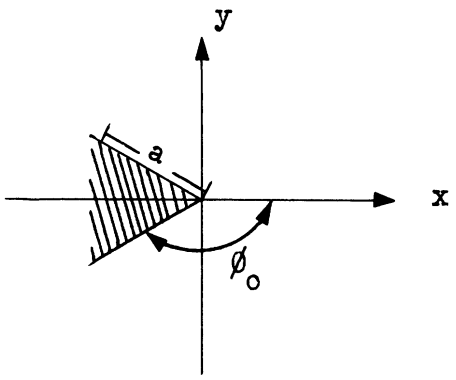


FIG A-6

For a slot parallel to and placed at a distance a from the edge of a wedge

$$\vec{E} \sim \frac{V_o}{2\pi} \nabla \times \int_{-\infty}^{\infty} \hat{k} \frac{e^{ik\sqrt{r^2 - 2ar\cos(\phi-\phi_o) + a^2 + z^2}}}{\sqrt{r^2 - 2ar\cos(\phi-\phi_o) + a^2 + z^2}} dz\, u(\pi+\phi-\phi_o)$$

which becomes

$$\vec{E} \simeq V_o \sqrt{\frac{k}{2\pi r}}\, \hat{\phi}\, e^{ik\left[r - a\cos(\phi-\phi_o)\right] - \frac{\pi i}{4}}\, u(\pi+\phi-\phi_o) \text{ for } r \gg a. \qquad (A.51)$$

This is in agreement with the geometric optics portion of Equation A.17 for $\psi_{G.O.}(\phi_o)$ .

A-1.4 Comparison between the Exact and Asymptotic Solution and Calculation of the Error of the Asymptotic Expression.

Fields for $\phi = \frac{\pi}{2}$ and $\phi_o = \pi$, $\frac{5\pi}{6}$ and $\frac{3\pi}{4}$ were calculated from the exact solution (A.9), the asymptotic solution (A.17) and the asymptotic expression obtained through the use of continued fractions. The fields from Equation A.9 and Equation A.17 are plotted in Figure A-7, and the

fields from A-9 and those obtained through the use of continued fractions in Figure A-8; for the latter calculation two terms of A.48 were used. From the graphs it is apparent that the agreement is much better for the approximation obtained through continued fractions. The approximation is also best for thin wedges and deteriorates as $\phi_0$ decreases. This may be expected from the estimated error of Equation A.17: the calculation was made through the use of formulae given in Section A-1.2 Method (2a) and results show an increase in the radius of error from $\phi_0 = \pi$ to $\phi_0 = \frac{3\pi}{4}$ .

The equation for the approximate radius of error is:

$$\frac{\pi}{\phi_0} \quad \frac{1}{8ka} \sqrt{\frac{2}{\pi}} \left\{ \frac{1}{|\cos\beta|} + \frac{1}{|\cos\beta'|} \right\}$$

where

$$\beta = \frac{\pi}{2\phi_0} (\pi + \phi) \qquad \beta' = \frac{\pi}{2\phi_0} (\pi - \phi)$$

From these graphs it is apparent that the error increases from $\phi_0 = \pi$ to $\phi_0 = \frac{3\pi}{4}$ . For $\phi_0 = \frac{\pi}{2}$ the approximate solution is exact and the error will increase from $\phi_0 = \frac{\pi}{2}$ to $\phi_0 = \frac{3\pi}{4}$ .

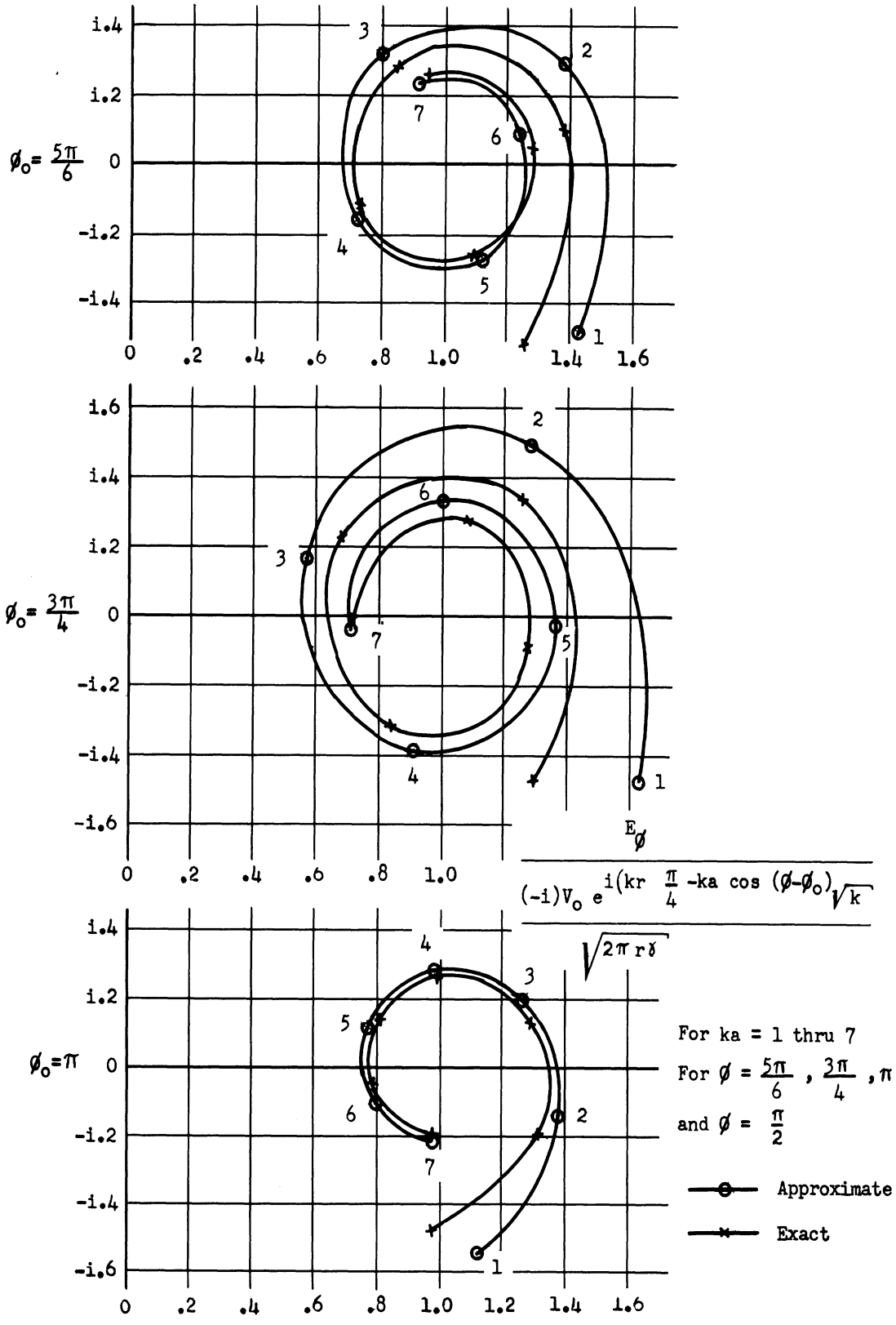


FIG. A.7 $E_\phi$ FROM EXACT SOLUTION (9) AND ASYMPTOTIC SOLUTION (17)

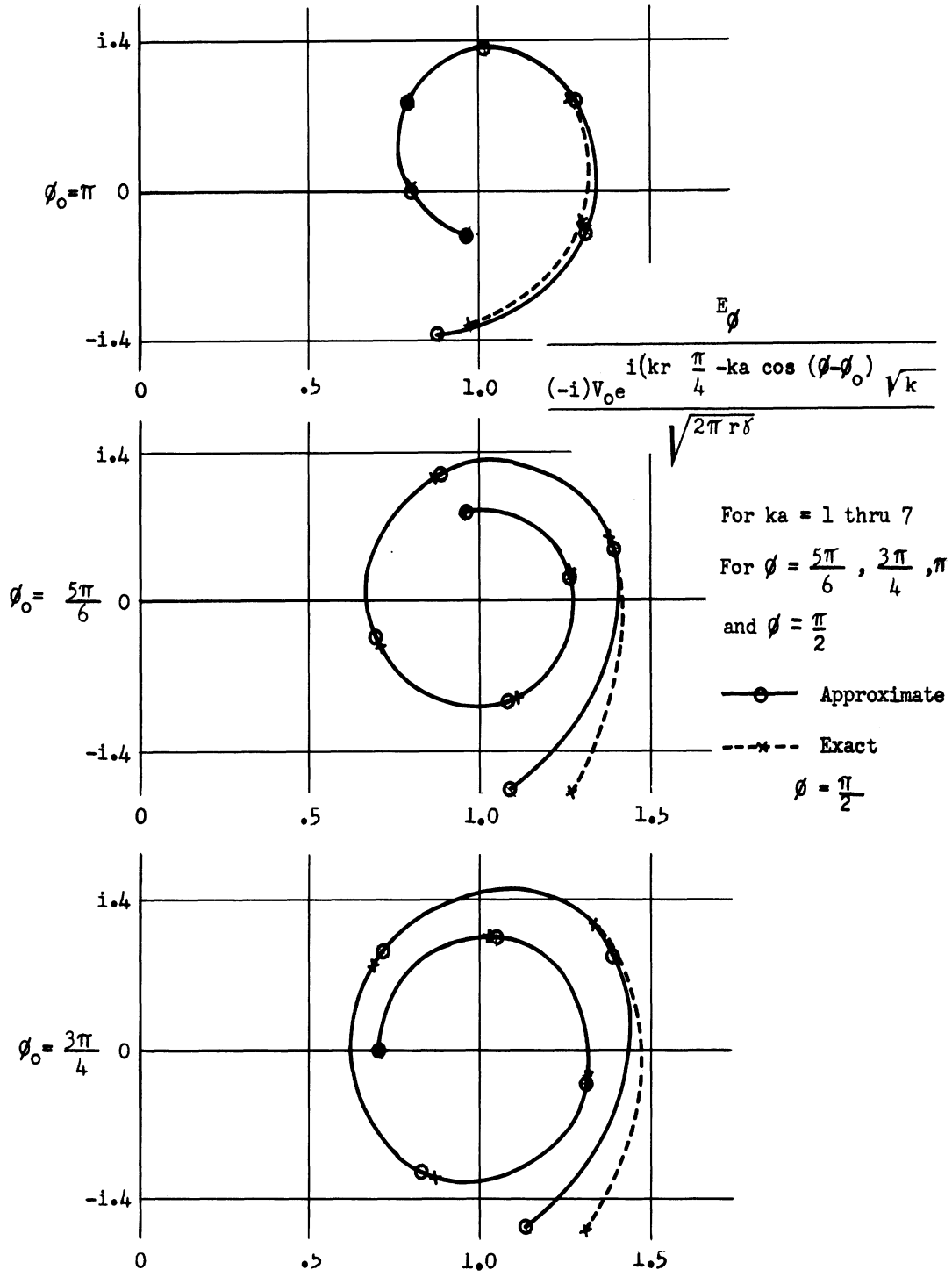


FIG. A.8 $E_\phi$ FROM EXACT SOLUTION (9) AND ASYMPTOTIC SOLUTION OBTAINED BY CONTINUED FRACTIONS

APPENDIX B.

CONE

We determine the field due to a magnetic dipole source in the presence of a perfectly conducting semi-infinite cone. With a time harmonic dependence of the form $e^{-i\omega t}$ Maxwell's equations are

$$\nabla \times \vec{E} = ik\vec{H} + \vec{M}, \quad k = \frac{\omega}{c} \tag{B.1}$$

$$\nabla \times \vec{H} = -ik\vec{E},$$

where we assume a point source $\vec{M} = \vec{m}\,\delta(\vec{r}-\vec{r}')$. Since the cone is a surface separable in spherical coordinates, we can make use of the modal representations

$$\text{E mode:} \quad \vec{E} = \nabla \times \vec{L}\Pi \tag{B.2}$$

$$\vec{H} = -ik\vec{L}\Pi$$

$$\text{H mode:} \quad \vec{\tilde{E}} = ik\vec{L}\tilde{\Pi} \tag{B.3}$$

$$\vec{\tilde{H}} = \nabla \times \vec{L}\tilde{\Pi}$$

where $\vec{L} = -i\,\vec{r} \times \nabla$ is the angular momentum operator. The scalar Hertz potentials satisfy the equation

$$(\nabla^2 + k^2)\Pi(\tilde{\Pi}) = 0 \tag{B.4}$$

away from the source.

If we eliminate the electric field from Maxwell's equations, we find that the E-mode Hertz function $\Pi$ satisfies

$$(\nabla^2 + k^2)\,\vec{L}\Pi = -\vec{M} \quad . \tag{B.5}$$

Since the operator L commutes with the Laplacian, we form

$$(\nabla^2 + k^2)\,L^2\Pi = -\vec{L}'^{*} \cdot \vec{M} \tag{B.6}$$

or

$$(\nabla^2 + k^2) = -\frac{1}{L^{2'}}\,\vec{L}'^{*} \cdot \vec{M}\,\delta(\vec{r}-\vec{r}') \tag{B.7}$$

where the primes indicate an operation with respect to the variable $(x', y', z')$. Inverting the differential operator of Equation B.6

$$\Pi = \frac{1}{L'^2}\,\vec{L}'^{*} \cdot \vec{m}\; G_D\,(\vec{r}, \vec{r}') \tag{B.8}$$

where $G_D$ is the Dirichlet Green's function for the cone.

Similarly, eliminating the magnetic field the H-mode Hertz function satisfies

$$(\nabla^2 + k^2)\,\vec{L}\tilde{\Pi} = -\frac{1}{ik}\,\nabla \times \vec{M}. \tag{B.9}$$

So by the above reasoning we find

$$(\nabla^2 + k^2)\tilde{\Pi} = -\frac{1}{ik}\frac{1}{L'^2}\,\vec{L}^{*'} \times \nabla \cdot \vec{m}\delta(\vec{r}-\vec{r}') \tag{B.10}$$

and

$$\tilde{\Pi} = \frac{1}{ik}\frac{1}{L'^2}\ \vec{L}^{*'} \times \nabla \cdot \vec{m}\, G_N(\vec{r},\vec{r}') \qquad \text{(B.11)}$$

where $G_N(\vec{r},\vec{r}')$ is the Neumann Green's function for the cone.

From the above we see that the decomposition of the exact solution into essentially a geometric optics part plus a part asymptotic in the wave number can result only from such a decomposition of the scalar Green's functions. That this is indeed the case has been shown by Felsen (see Ref. 2).

Consider a ring source of magnetic dipoles centered about the axis of a perfectly conducting semi-infinite cone of angle $\theta_0 > \frac{\pi}{2}$. Performing the operation indicated in (B.8) and (B.2) above, we have for a uniformly excited source that

$$\vec{H}(\vec{r},\vec{r}') = \hat{\phi}\,(-im)\frac{1}{2\pi}\int_C \frac{d\nu\ (2\nu+1)}{\nu(\nu+1)} \qquad \text{(B.12)}$$

$$\cdot j_\nu(kr_<)\, h_\nu^{(1)}(kr_>)\,\frac{\partial^2}{\partial\theta\,\partial\theta'}\, G_\theta(\theta,\theta',\nu)$$

where the contour includes the positive real axis in the complex plane and

$$G_\theta = -\frac{\pi}{2}\,\frac{P_\nu(\cos\theta_<)P_\nu(-\cos\theta_>)}{\sin\nu\pi}$$

$$+\frac{\pi}{2}\,\frac{1}{\sin\nu\pi}\,\frac{P_\nu(-\cos\theta_0)}{P_\nu(\cos\theta_0)}\,P_\nu(\cos\theta')\,P_\nu(\cos\theta)$$

is the decomposition of the scalar Green's function mentioned above. Provided $\theta + \theta' < 2\theta_o - \pi$, the contour can be deformed in the case of the second term to run from $-\frac{1}{2} + i\infty$ to $-\frac{1}{2} - i\infty$. This gives the diffracted term:

$$\vec{H}_{diff} = \hat{\phi} \frac{m}{\sqrt{rr'}} \frac{-ik\pi}{8} \int_{-\infty}^{\infty} dx \frac{x}{x^2 + \frac{1}{4}} \tag{B.13}$$

$$\cdot \frac{H^{(1)}_{ix}(kr)\, H^{(1)}_{ix}(kr')}{\cosh \pi x} \frac{K_x(-\cos\theta_o)}{K_x(\cos\theta_o)} \cdot K_x'(\cos\theta) K_x'(\cos\theta')$$

where $K_x^m(\cos\theta) = P^m_{-\frac{1}{2}+ix}(\cos\theta)$. For sufficiently large kr and kr' the asymptotic form of $H^{(1)}_{ix}$ may be employed in Equation B.13 to give

$$\vec{H}_{diff} \approx \hat{\phi} \frac{m}{rr'} \frac{1}{k^2} e^{ik(r+r')} \int_{-\infty}^{\infty} dx \frac{x\, e^{\pi x}}{(x^2 + \frac{1}{4})\cosh \pi x} \tag{B.14}$$

$$\cdot K_x'(\cos\theta) K_x'(\cos\theta') \cdot \frac{K_x(-\cos\theta_o)}{K_x(\cos\theta_o)} \cdot$$

For values of $\theta_o$ near $\pi$ (small cones), the employment of the asymptotic form

$$\frac{K_x(-\cos\theta_o)}{K_x(\cos\theta_o)} \approx \frac{\pi}{2\, \ell n \left(\frac{\pi - \theta_o}{2}\right)} \frac{-1}{\cosh \pi x}, \quad \theta_o \to \pi \tag{B.15}$$

in Equation B.14 permits the integration of (B.14) and yields, to the first order, for a small cone approximation

$$\vec{H}_{diff} = \hat{\phi} \frac{m}{4k^2} \frac{e^{ik(r+r')}}{rr'} \frac{2\pi}{2\ln\left(\frac{\pi - \theta_o}{2}\right)} \frac{1}{\pi} \frac{\tan\frac{\theta}{2} \tan\frac{\theta'}{2}}{\cos\theta + \cos\theta'} \tag{B.16}$$

If the source is permitted to go to the surface of the cone, the same form for $\vec{H}_{diff}$ of Equation B.16 results; hence, an evaluation is obtained for the higher order terms in the case of a circumferential slot on a small cone.

If the ring source is on the surface of the cone, the decomposition, as was pointed out by Felsen, depends upon breaking up the Legendre functions into positive and negative exponentials. That is, let

$$\overset{(1)}{\underset{(2)}{D_\nu}}(\theta) = \pm \frac{P_\nu(-\cos\theta) - e^{\mp i\nu\pi} P_\nu(\cos\theta)}{2i \sin\nu\pi} \tag{B.17}$$

so that

$$\overset{(1)}{\underset{(2)}{D_\nu}}(\theta) \approx \frac{\exp\left[\mp i\left\{(\nu+\frac{1}{2})\theta - \frac{\pi}{4}\right\}\right]}{\sqrt{2\pi\nu\sin\theta}}$$

for $\nu \sin\theta >> 1$. Substitution of Equation B.17 in Equation B.12 yields integrals of the form

$$\int_{C_1} d\nu \, \frac{\nu+\frac{1}{2}}{\nu(\nu+1)} \, j_\nu(kr') \, e^{-i(\nu+\frac{1}{2})\frac{\pi}{2}} \, \frac{P_\nu^1(\cos\theta)}{D_\nu^{(1)}(\theta_0)}$$

$$-\int_{C_1} d\nu \, \frac{\nu+\frac{1}{2}}{\nu(\nu+1)} \, j_\nu(kr') \, e^{-i(\nu+\frac{1}{2})\frac{\pi}{2}} \, \frac{P_\nu^2(\cos\theta) \, D_\nu^{(2)}(\theta_0)}{D_\nu^{(1)}(\theta) \, P_\nu(\cos\theta_0)}$$

$$+\int_{C_2'} d\nu \, \frac{\nu+\frac{1}{2}}{\nu(\nu+1)} \, j_\nu(kr') \, e^{-i(\nu+\frac{1}{2})} - \frac{P_\nu^1(\cos\theta)}{D_\nu^{(1)}(\theta_0)}$$

$$-\int_{C_2'} d\nu \, \frac{\nu+\frac{1}{2}}{\nu(\nu+1)} \, j_\nu(kr') \, e^{-i(\nu+\frac{1}{2})\frac{\pi}{2}} \, \frac{P_\nu^1(\cos\theta) \, D_\nu^{(2)}(\theta_0)}{D_\nu^{(1)}(\theta_0) \, P_\nu(\cos\theta_0)} \, ,$$

where the contours are indicated below:

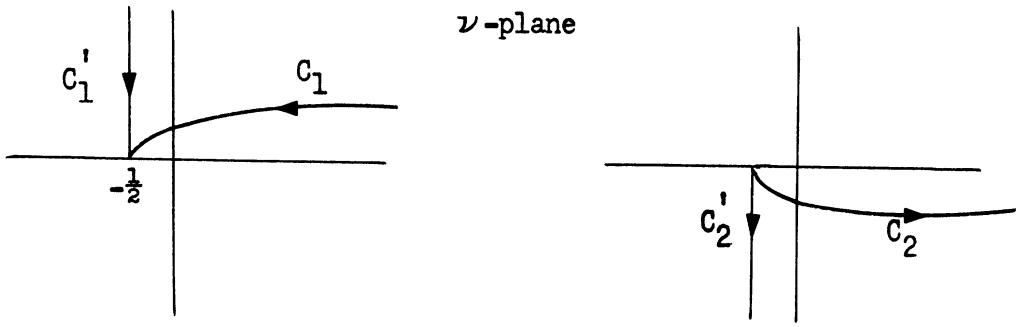


The integrals over $C_1'$ and $C_2'$ can then be evaluated, using the asymptotic form of $j_\nu$ for large $kr'$. These lead to the diffracted term, while a saddle point evaluation of the integral over $C_1$ leads to the geometric optics term.

## APPENDIX C.

## GRAPHICAL PRESENTATIONS

The expression (3.2) of Chapter 3 has been employed to obtain radiation patterns in the region $0 < \theta < \pi - \theta_o$ for the following values of the parameters ka, $\theta_o$, and n:

$$ka = 50\pi, 75\pi \ ;$$

$$\theta_o = 160^o, 165^o, 170^o \ ;$$

$$n = 1, 2, 3.$$

These patterns are shown in Figures C-1 through C-18.

The expression actually calculated is

$$\left|\vec{BE}_n\right| = \frac{\sin\theta_o}{\pi}\sqrt{\frac{ka}{2\pi}}\sqrt{\left|S'_n\right|^2 + \left|T'_n\right|^2\cos^2\theta}$$

where B is given by Equation 3.5 and $S'_n$ and $T'_n$ are given by Equation 3.3.

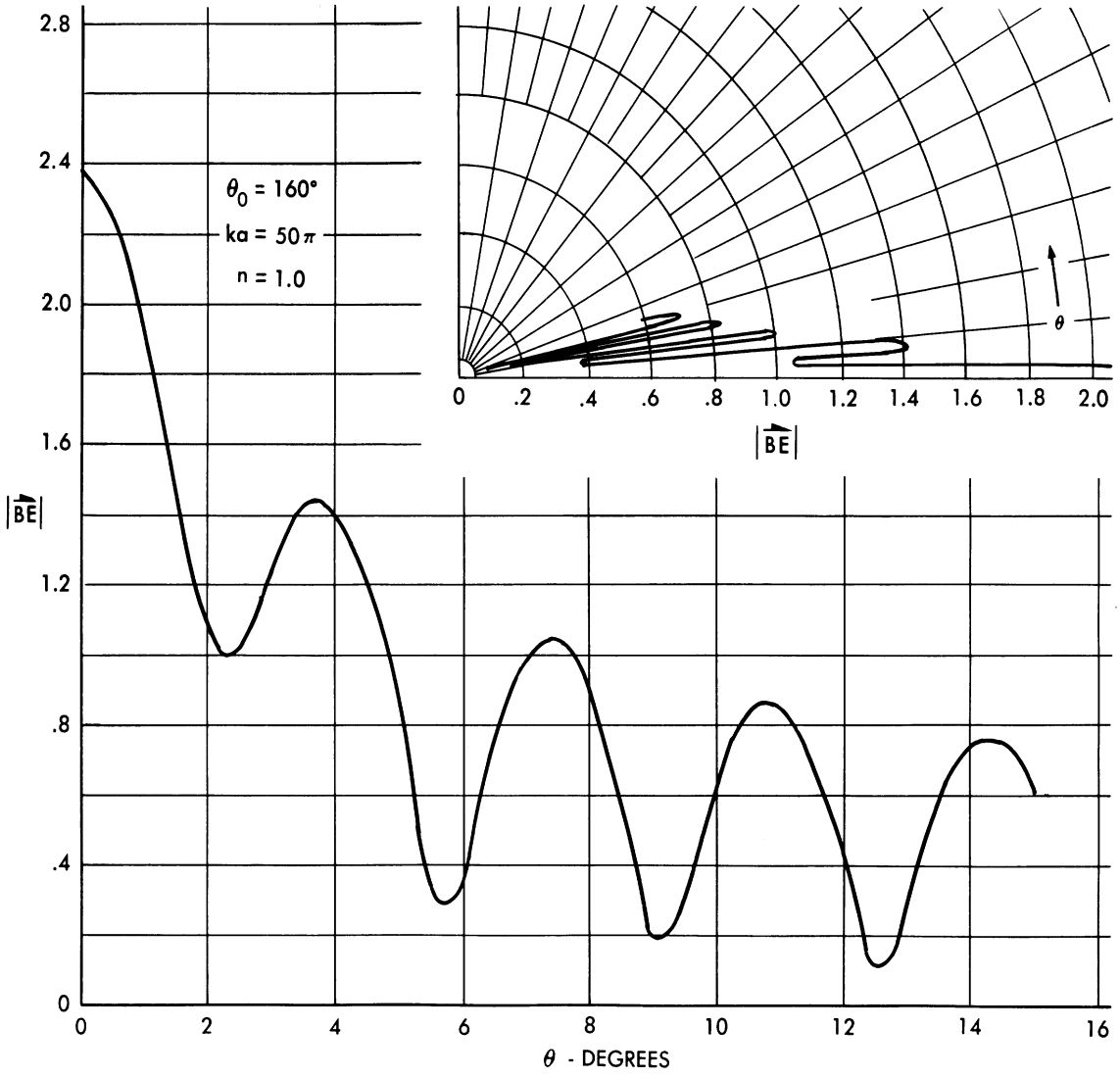


FIG. C.1 40° CONE WITH $e^{i\phi}$ EXCITED CIRCUMFERENTIAL SLOT 25 WAVELENGTHS FROM TIP

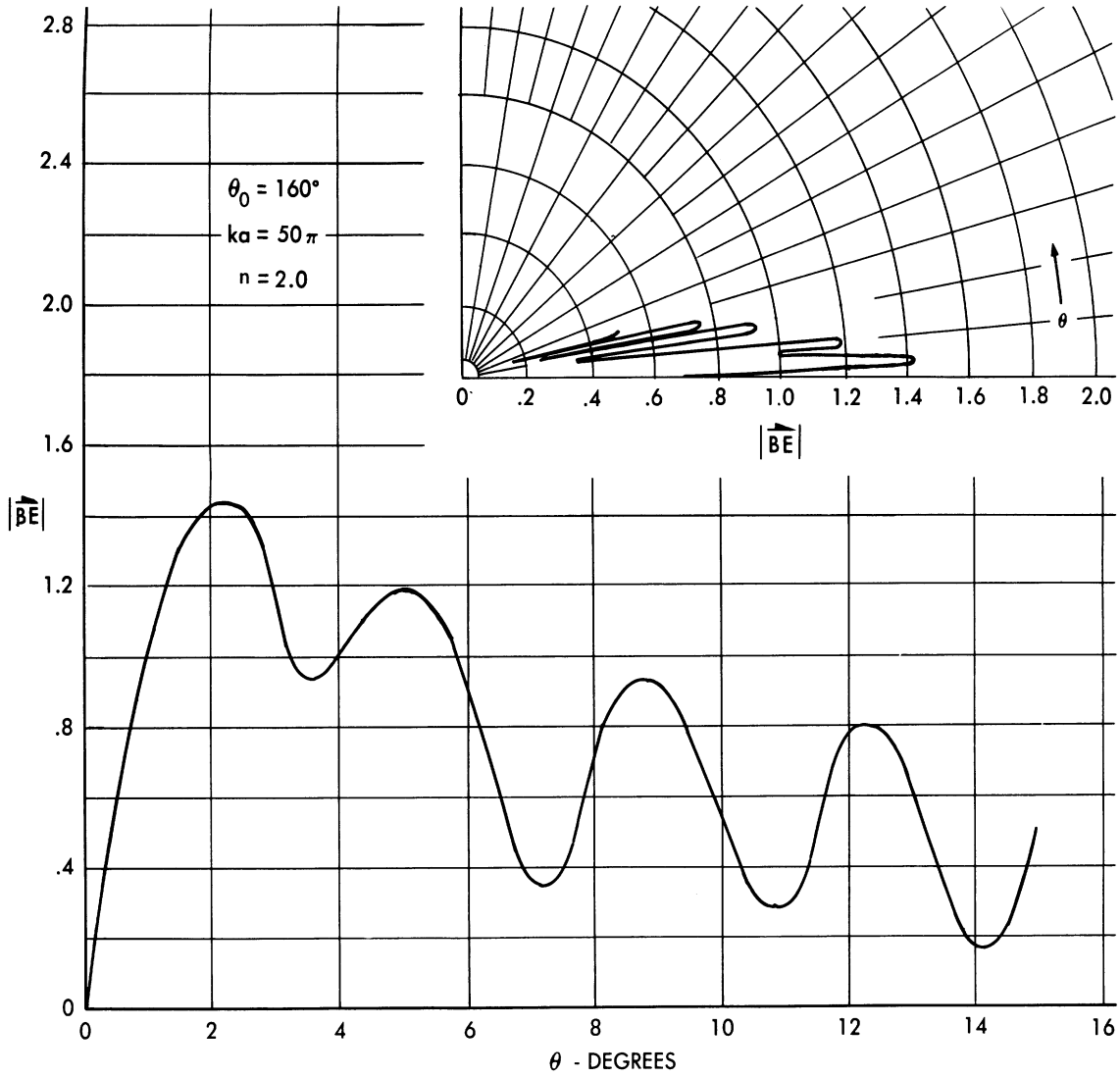


FIG. C.2 40° CONE WITH $e^{2i\phi}$ EXCITED CIRCUMFERENTIAL SLOT 25 WAVELENGTHS FROM TIP

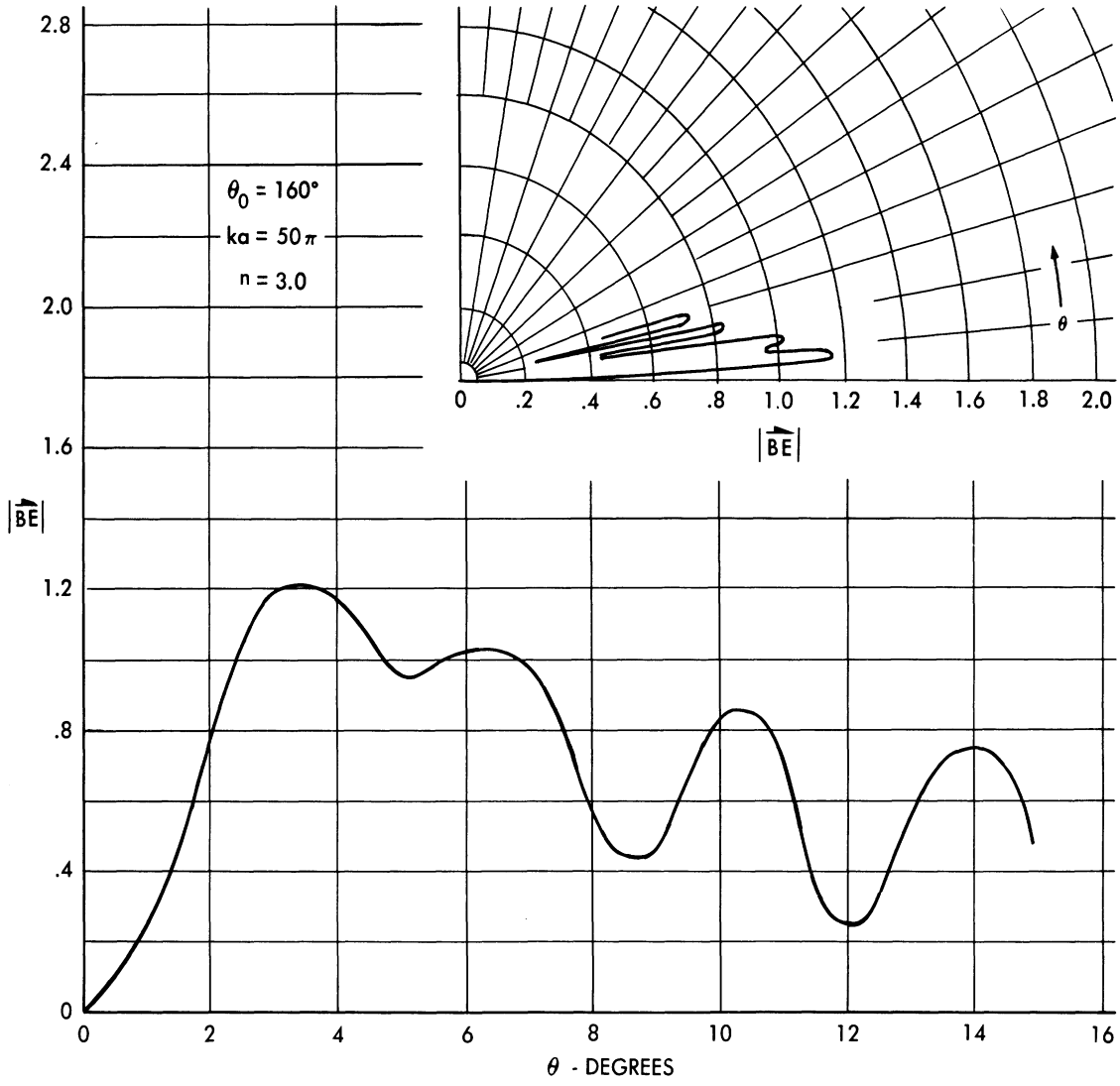


FIG C.3 40° CONE WITH $e^{3i\phi}$ EXCITED CIRCUMFERENTIAL SLOT 25 WAVELENGTHS FROM TIP

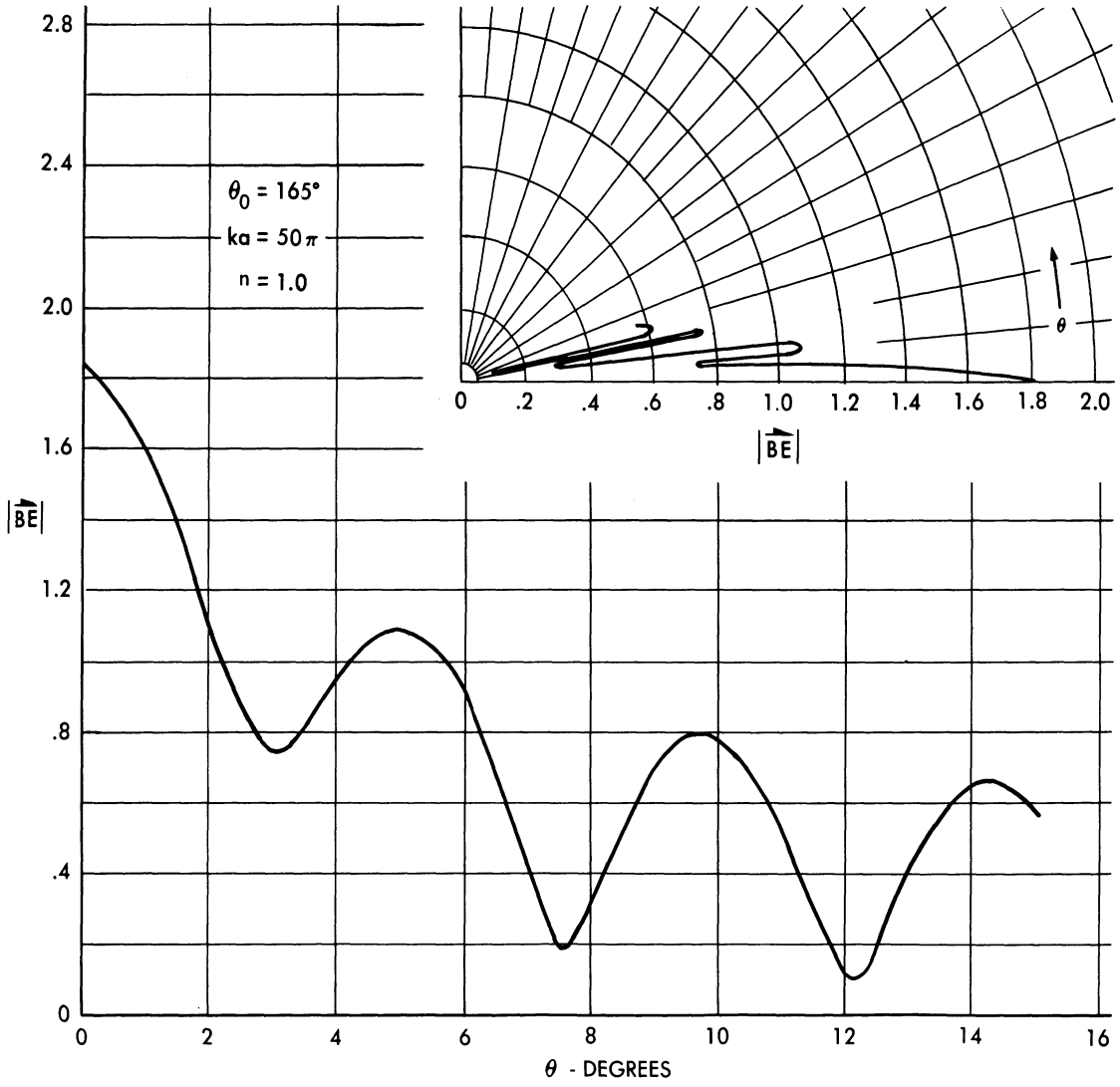


FIG. C.4 30° CONE WITH $e^{i\phi}$ EXCITED CIRCUMFERENTIAL SLOT 25 WAVELENGTHS FROM TIP

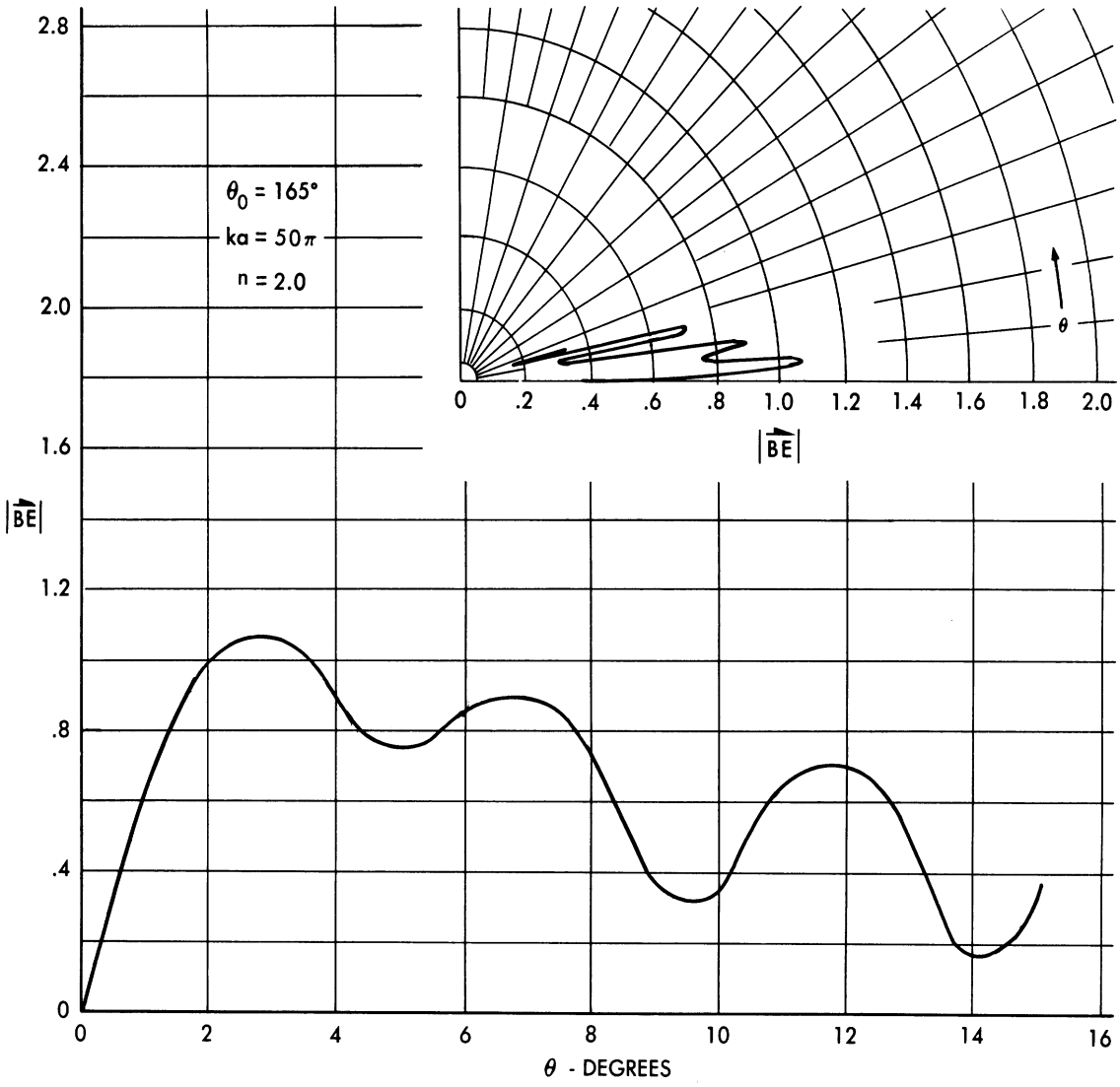


FIG. C.5 30° CONE WITH $e^{2i\phi}$ EXCITED CIRCUMFERENTIAL SLOT 25 WAVELENGTHS FROM TIP

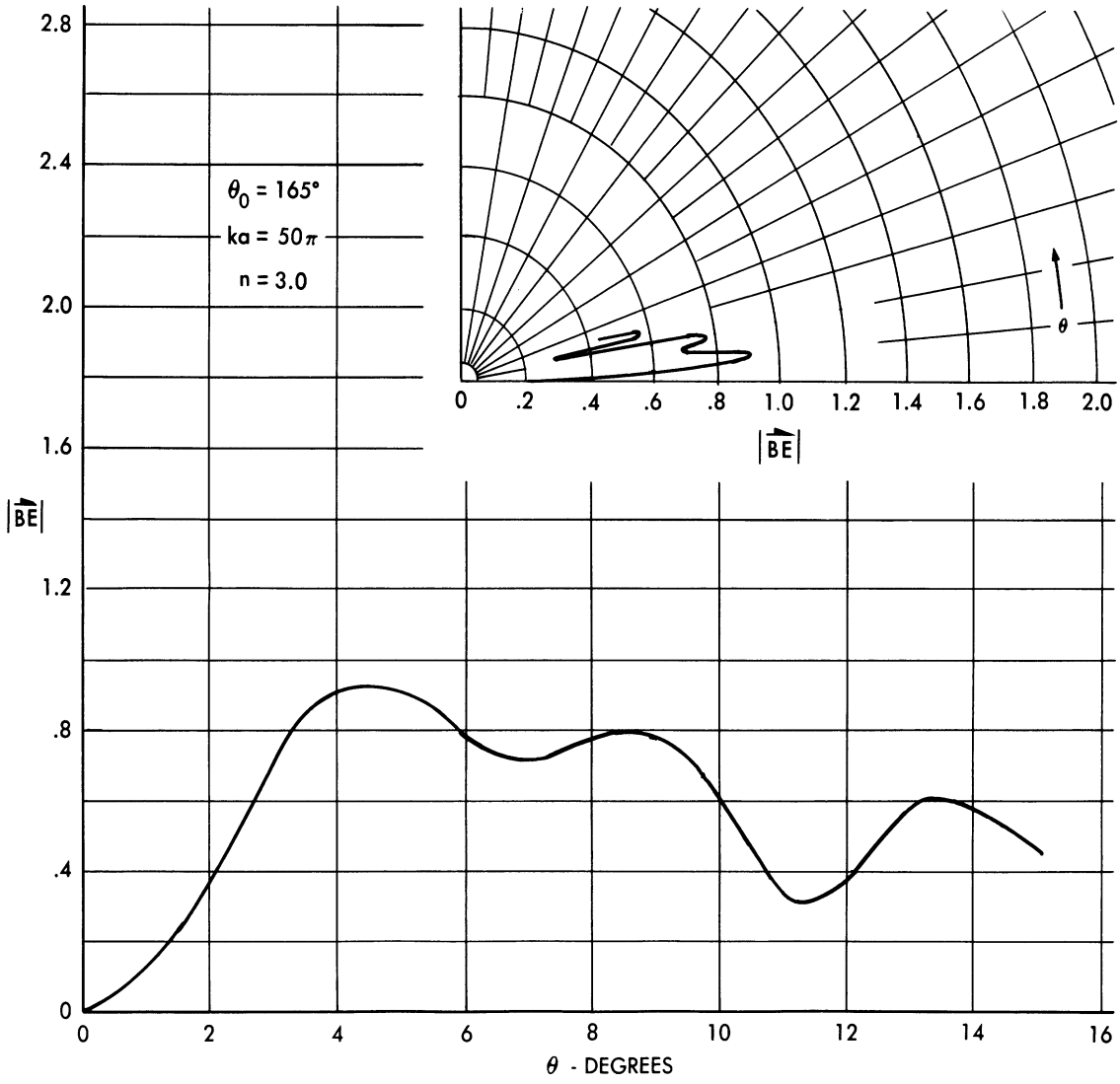


FIG C.6 30° CONE WITH $e^{3i\phi}$ EXCITED CIRCUMFERENTIAL SLOT 25 WAVELENGTHS FROM TIP

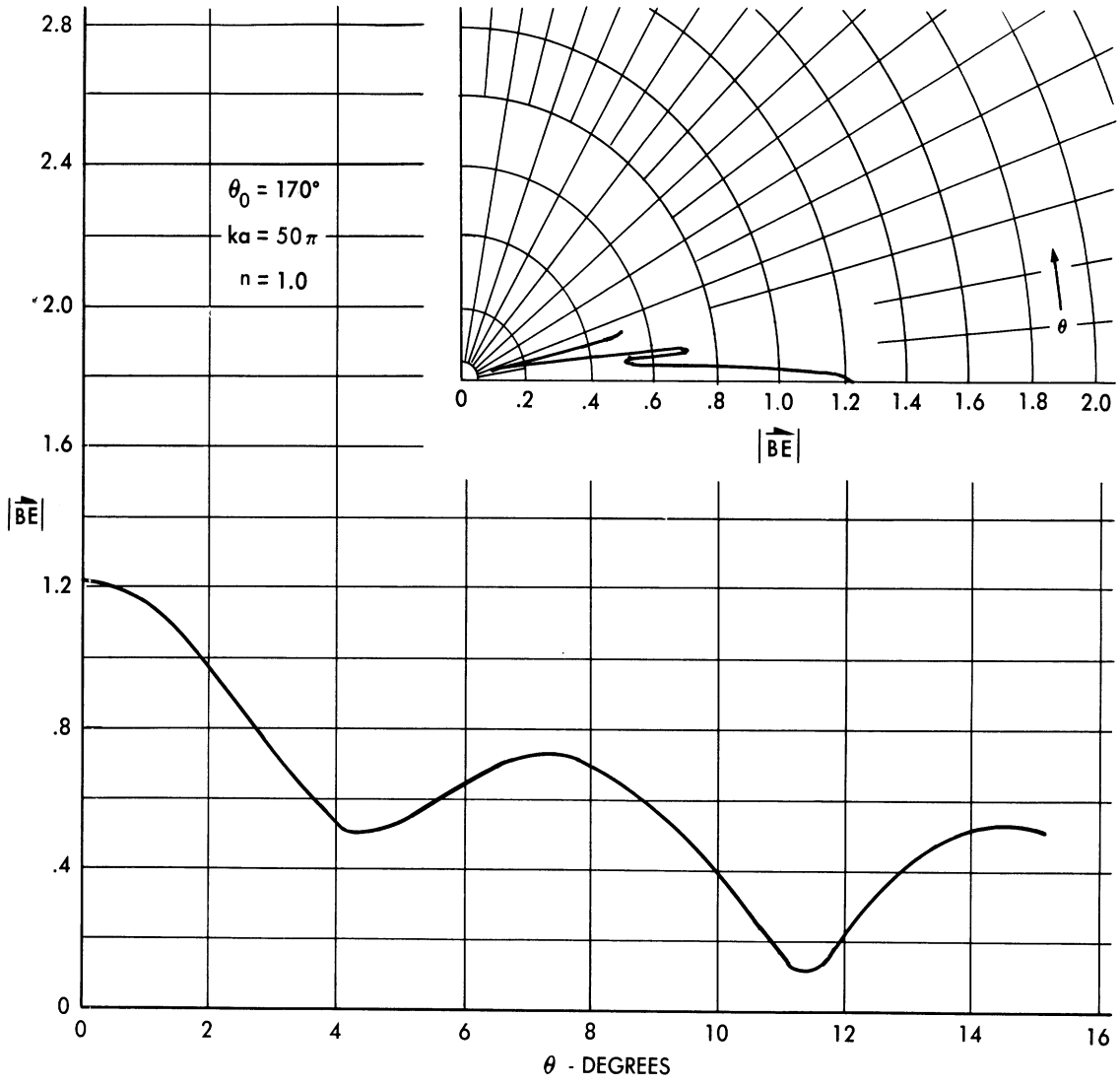


FIG. C.7 20° CONE WITH $e^{i\phi}$ EXCITED CIRCUMFERENTIAL SLOT 25 WAVELENGTHS FROM TIP

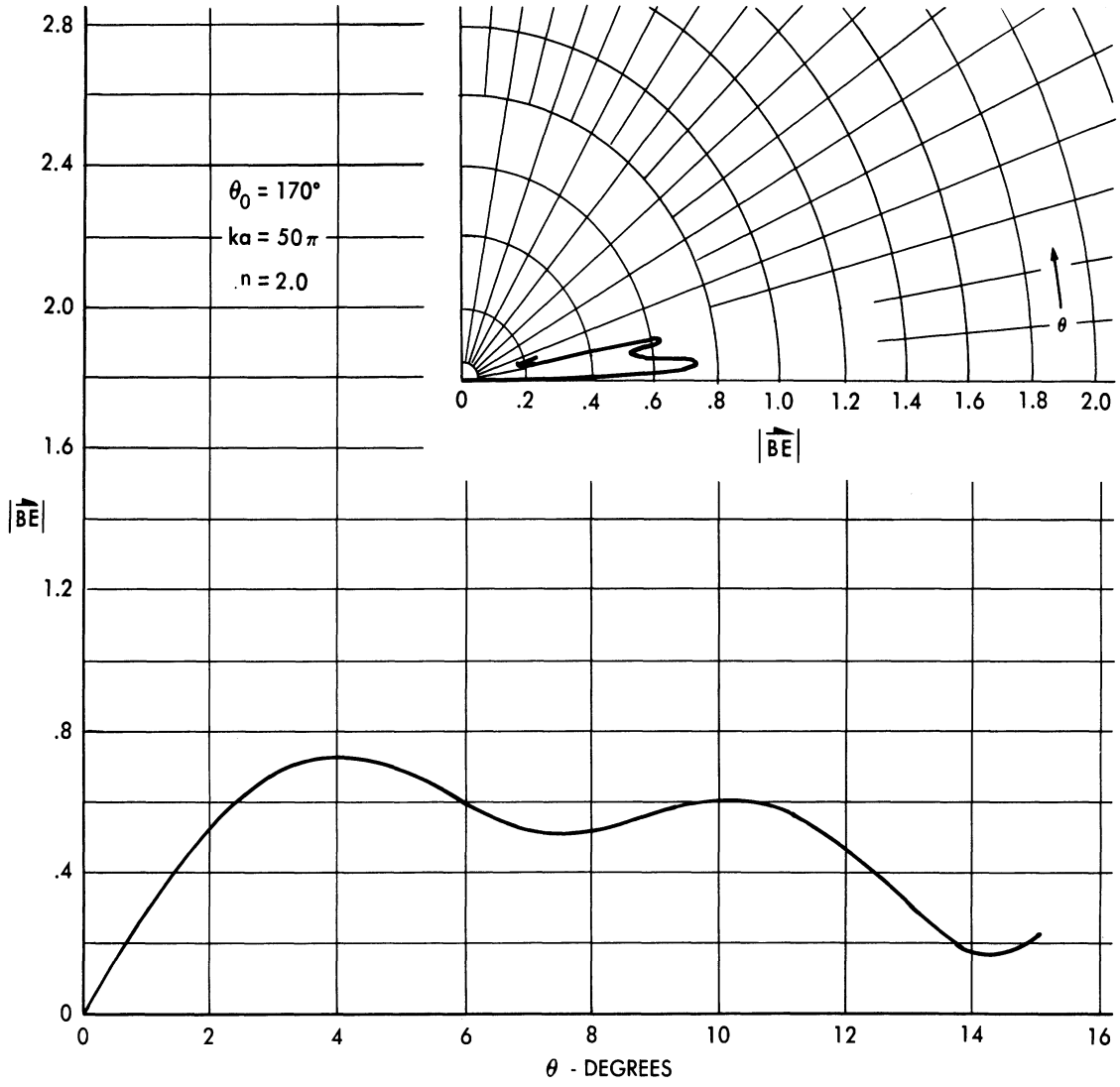


FIG. C.8 20° CONE WITH $e^{2i\phi}$ EXCITED CIRCUMFERENTIAL SLOT 25 WAVELENGTHS FROM TIP

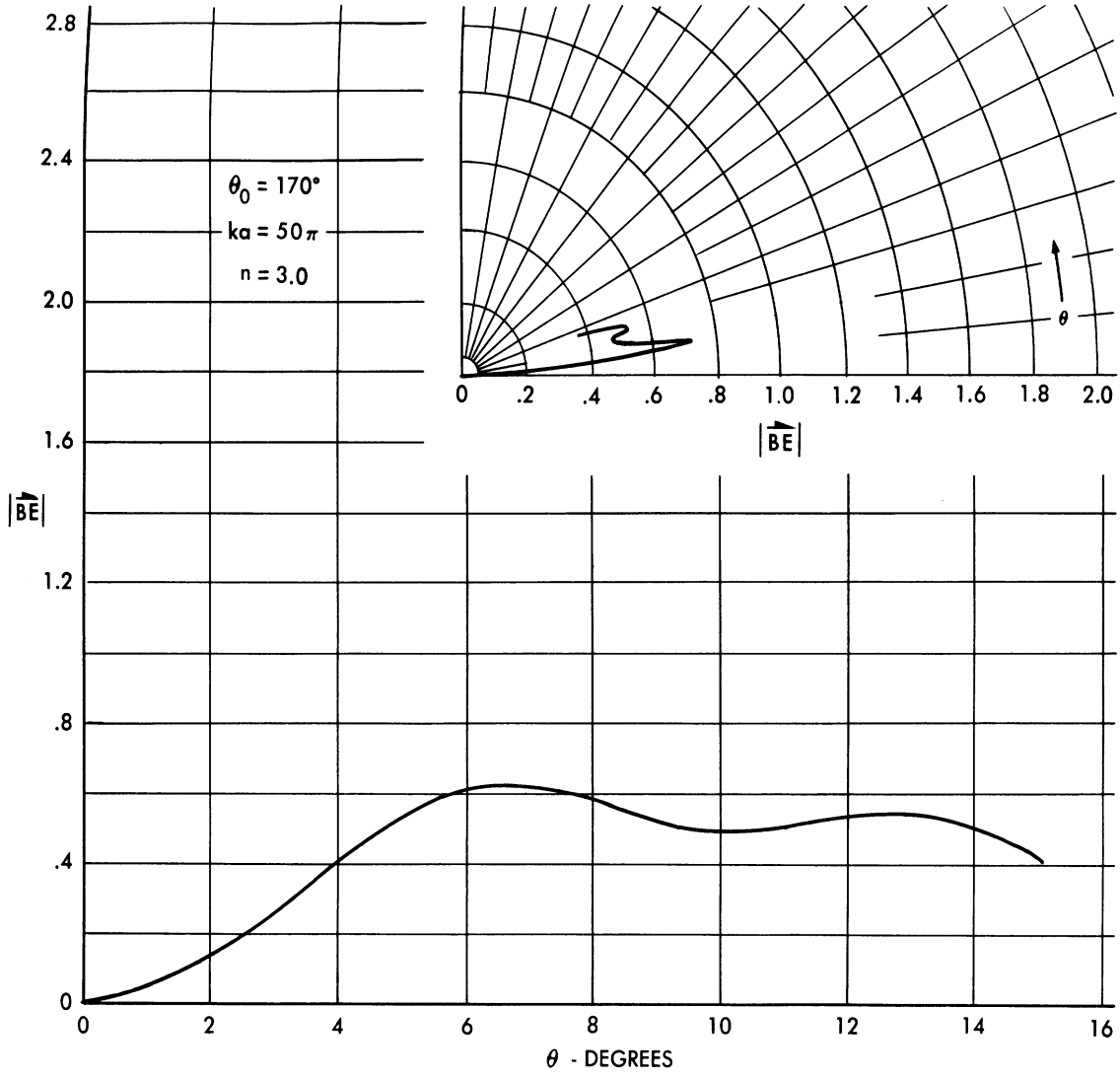


FIG. C.9 20° CONE WITH $e^{3i\phi}$ EXCITED CIRCUMFERENTIAL SLOT 25 WAVELENGTHS FROM TIP

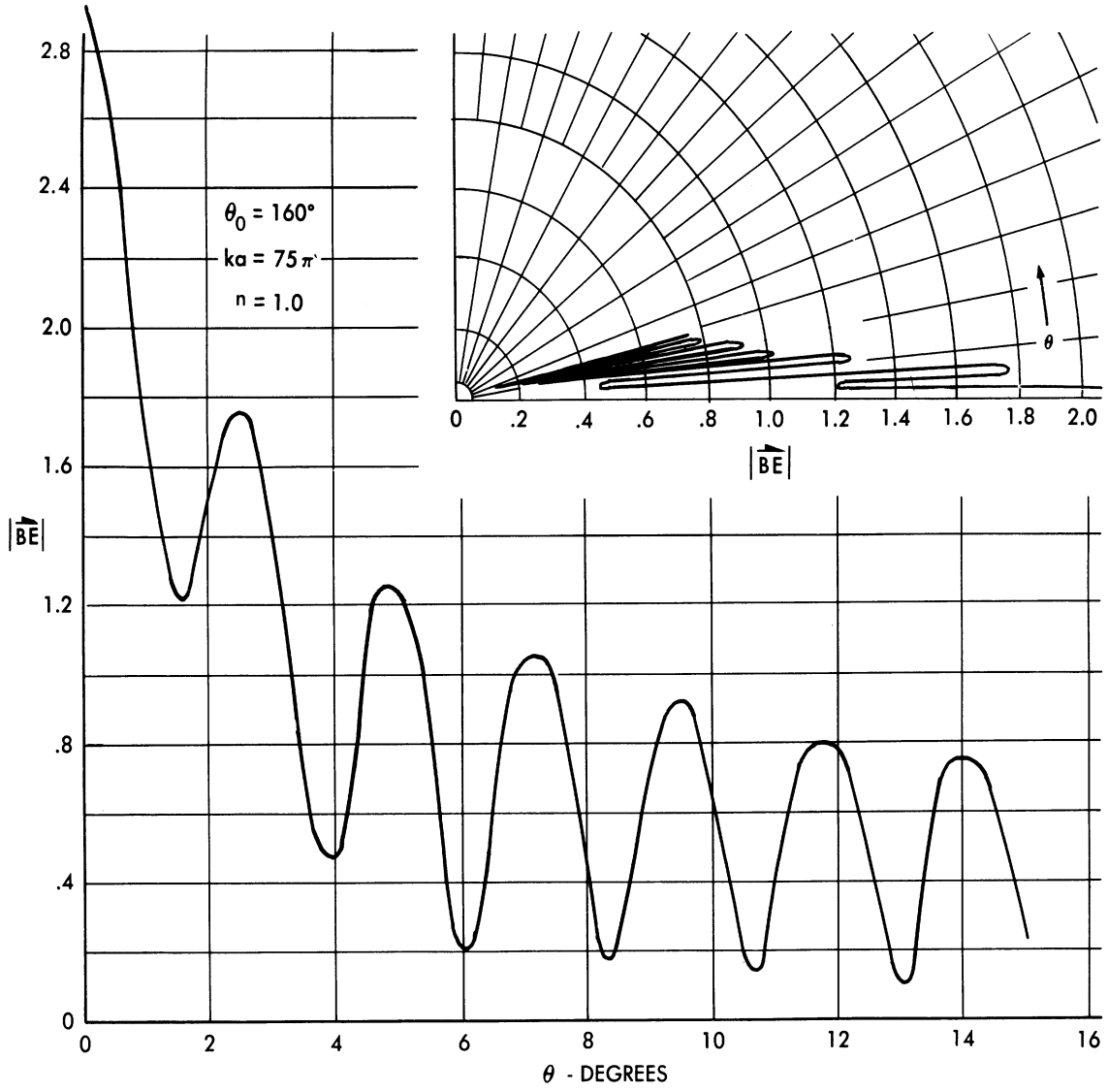


FIG C.10 40° CONE WITH $e^{i\phi}$ EXCITED CIRCUMFERENTIAL SLOT 37.5 WAVELENGTHS FROM TIP

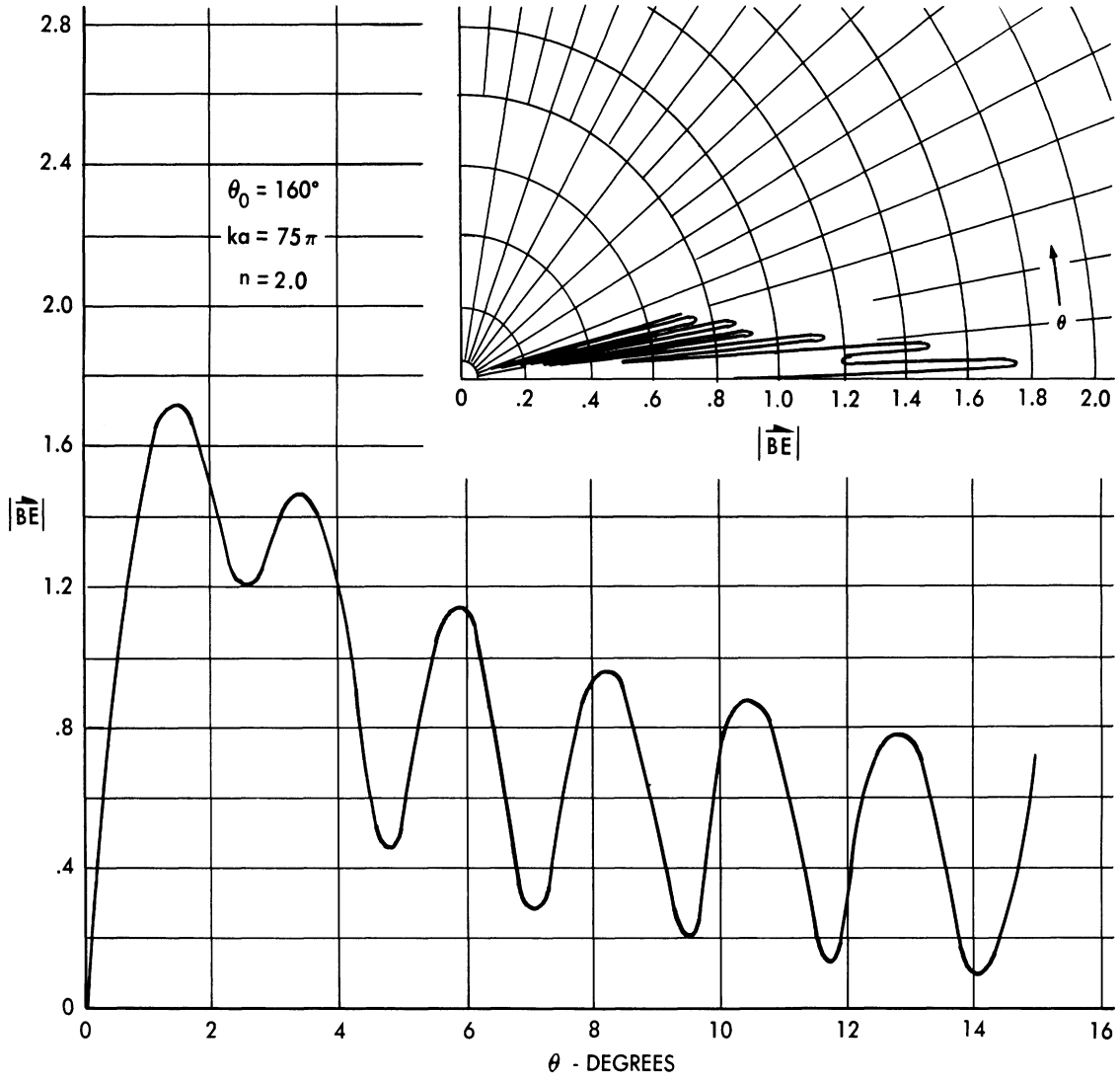


FIG. C.11 40° CONE WITH $e^{2i\phi}$ EXCITED CIRCUMFERENTIAL SLOT 37.5 WAVELENGTHS FROM TIP

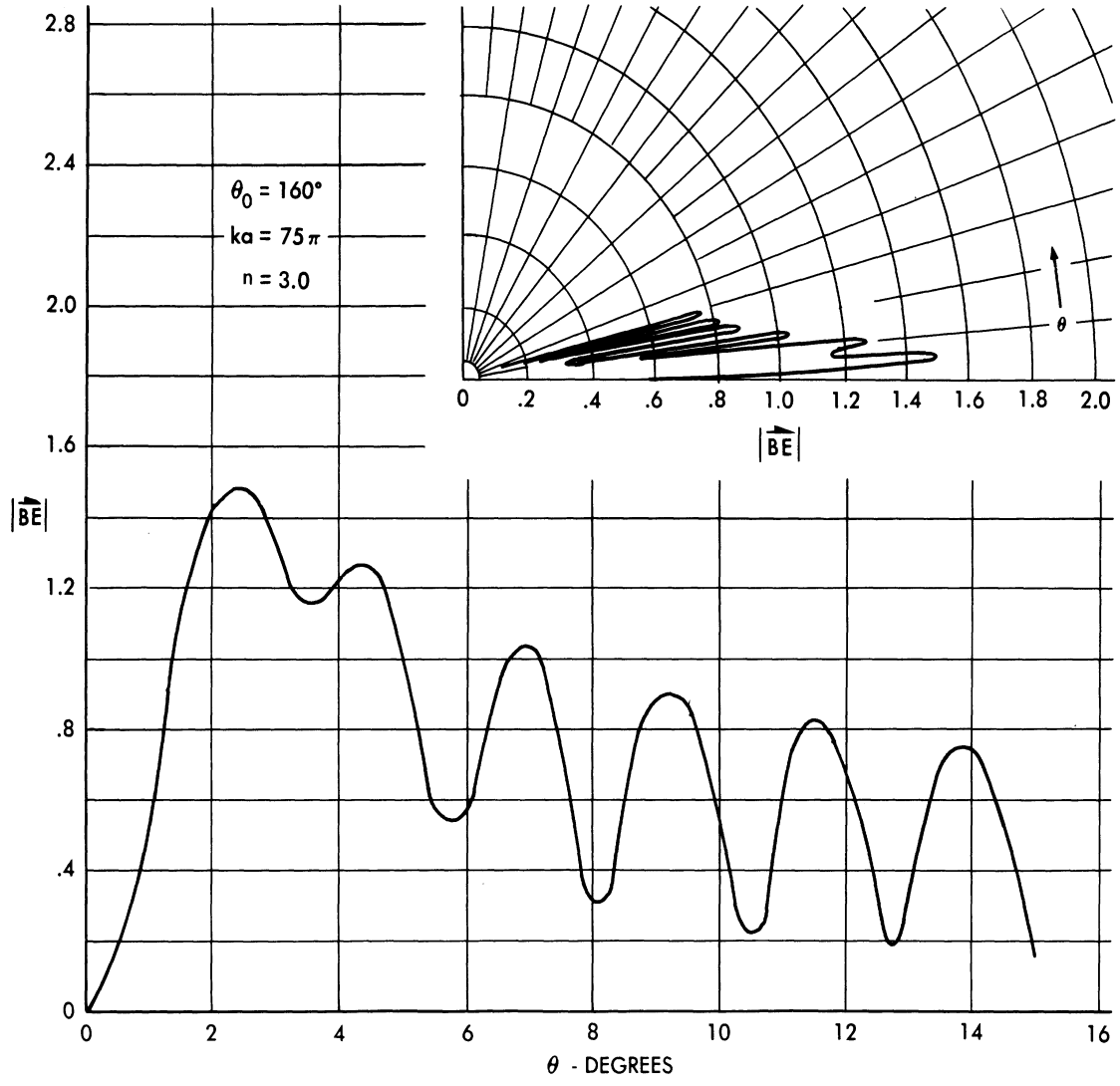


FIG. C.12 40° CONE WITH $e^{3i\phi}$ EXCITED CIRCUMFERENTIAL SLOT 37.5 WAVELENGTHS FROM TIP

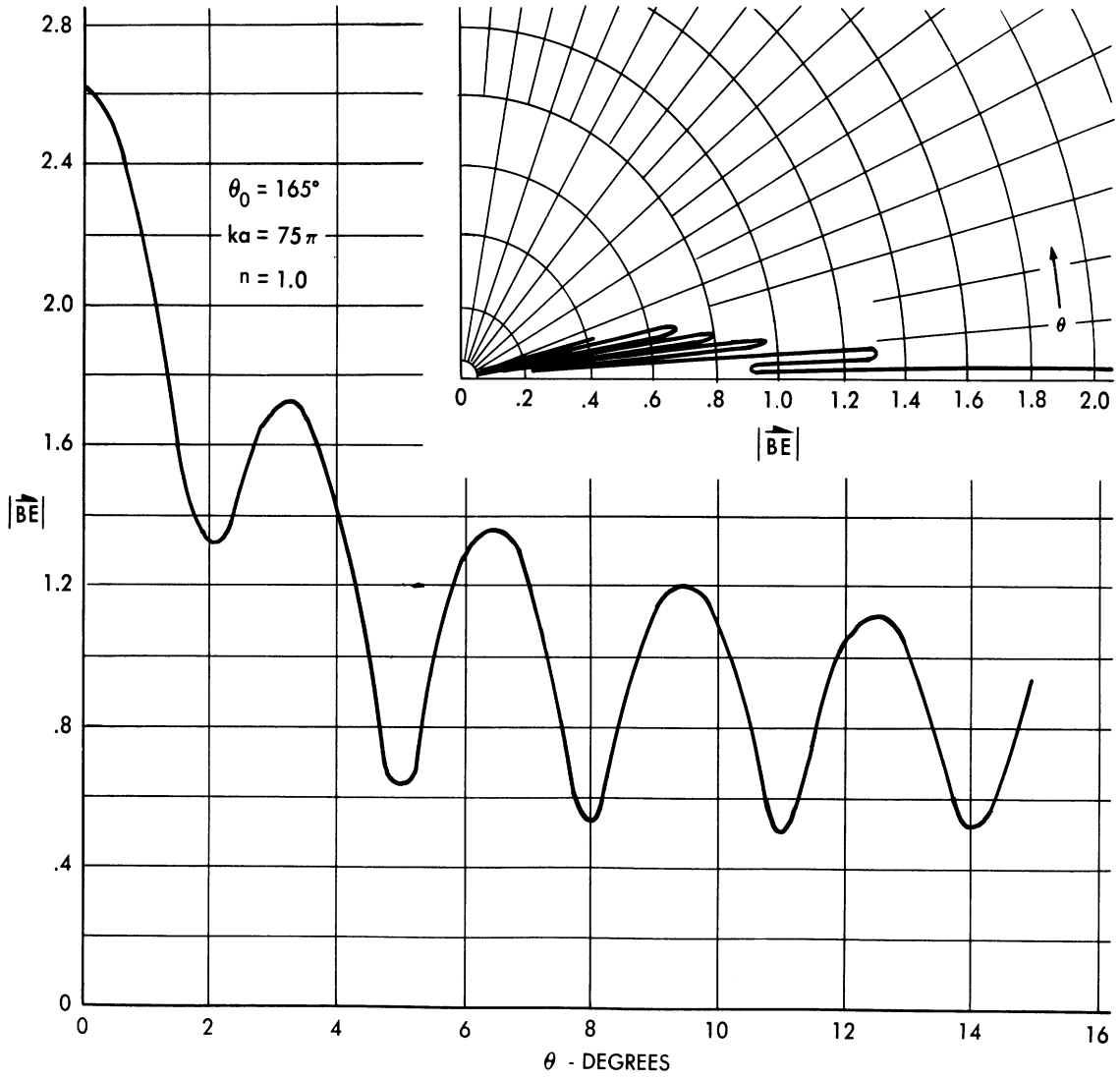


FIG. C.13 30° CONE WITH $e^{i\phi}$ EXCITED CIRCUMFERENTIAL SLOT 37.5 WAVELENGTHS FROM TIP

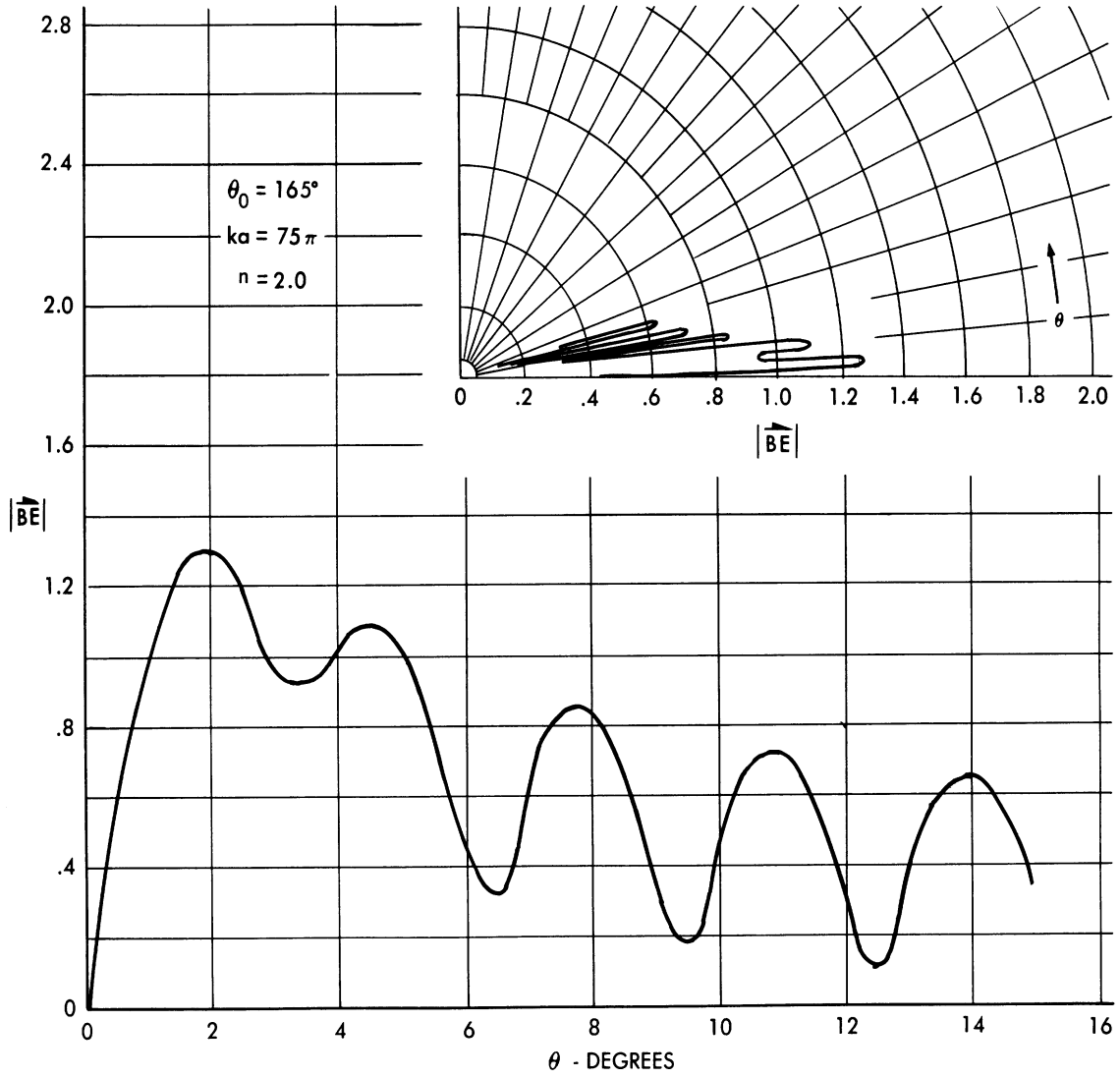


FIG. C.14 $30^\circ$ CONE WITH $e^{2i\phi}$ EXCITED CIRCUMFERENTIAL SLOT 37.5 WAVELENGTHS FROM TIP

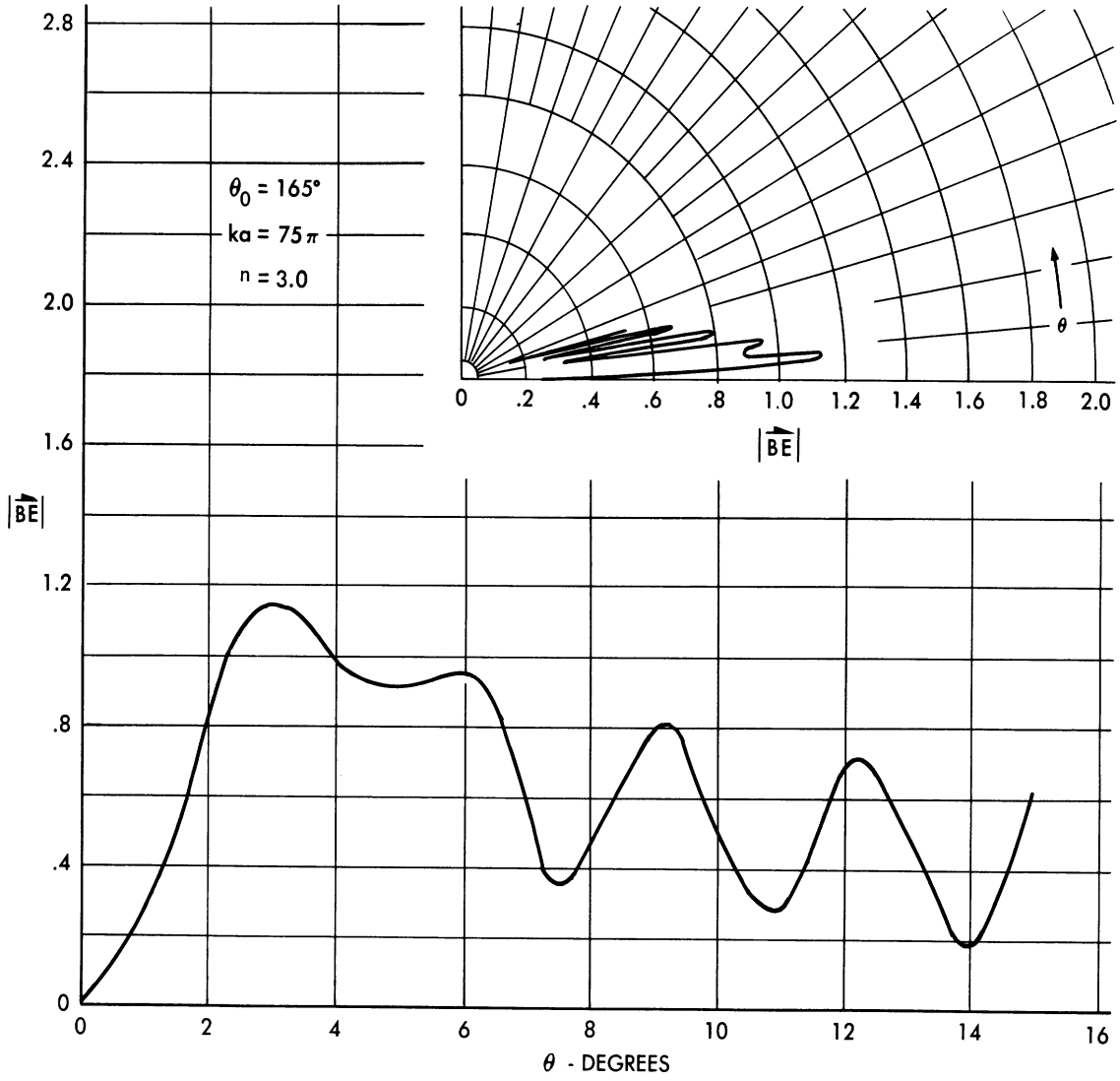


FIG. C.15 30° CONE WITH $e^{3i\phi}$ EXCITED CIRCUMFERENTIAL SLOT 37.5 WAVELENGTHS FROM TIP

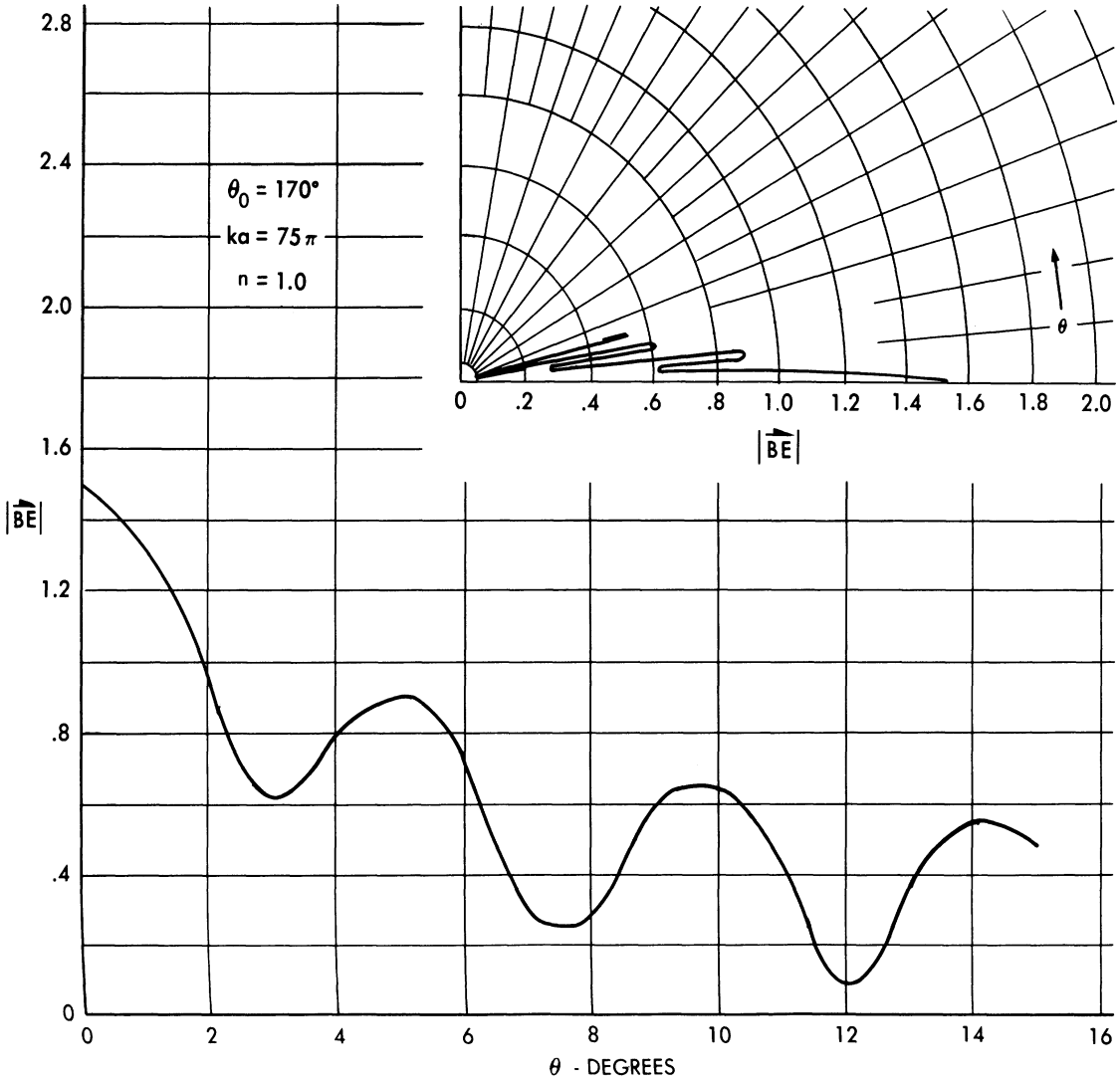


FIG. C.16 20° CONE WITH $e^{i\phi}$ EXCITED CIRCUMFERENTIAL SLOT 37.5 WAVELENGTHS FROM TIP

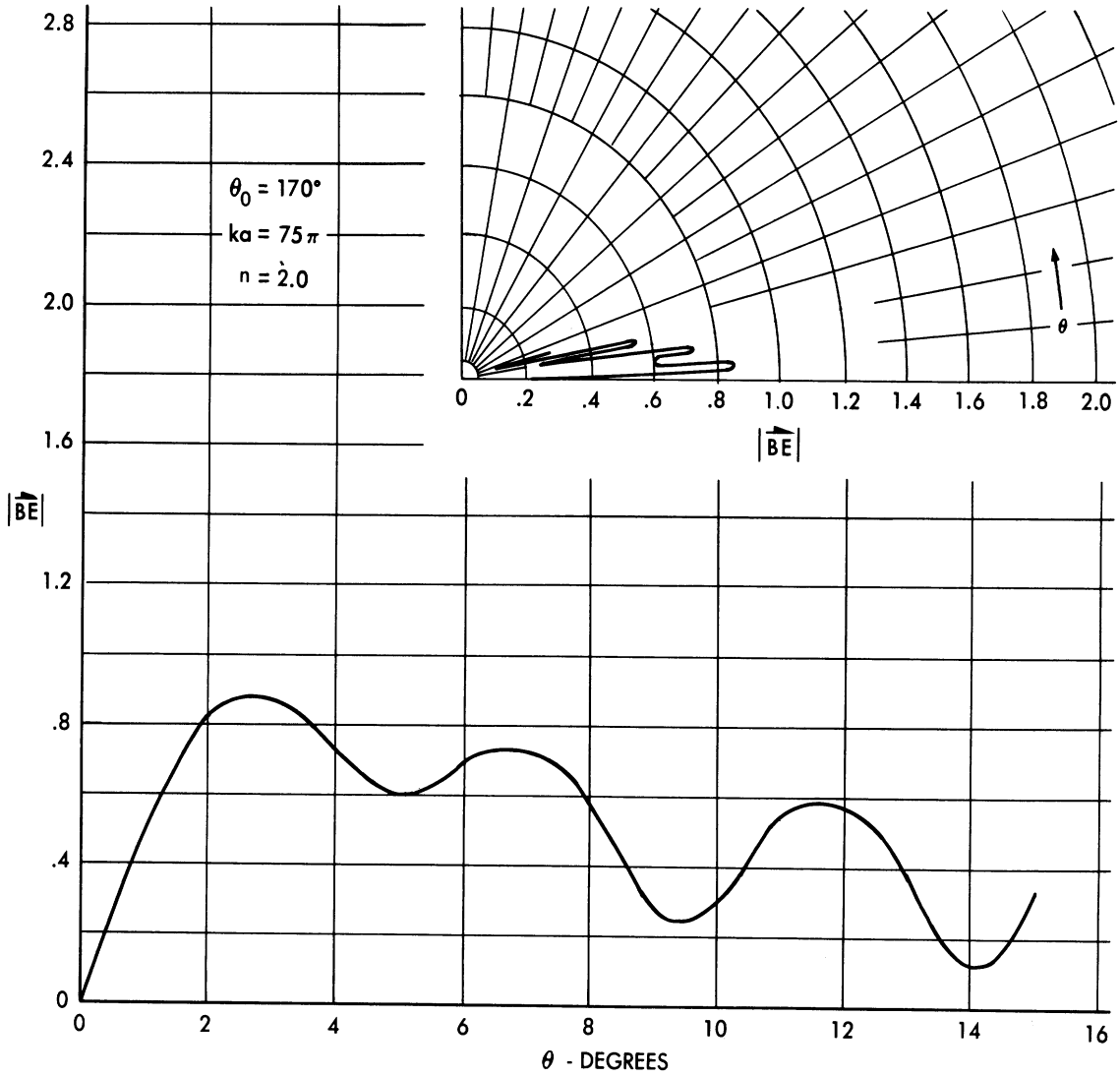


FIG. C.17 $20^{\circ}$ CONE WITH $e^{2i\phi}$ EXCITED CIRCUMFERENTIAL SLOT 37.5 WAVELENGTHS FROM TIP

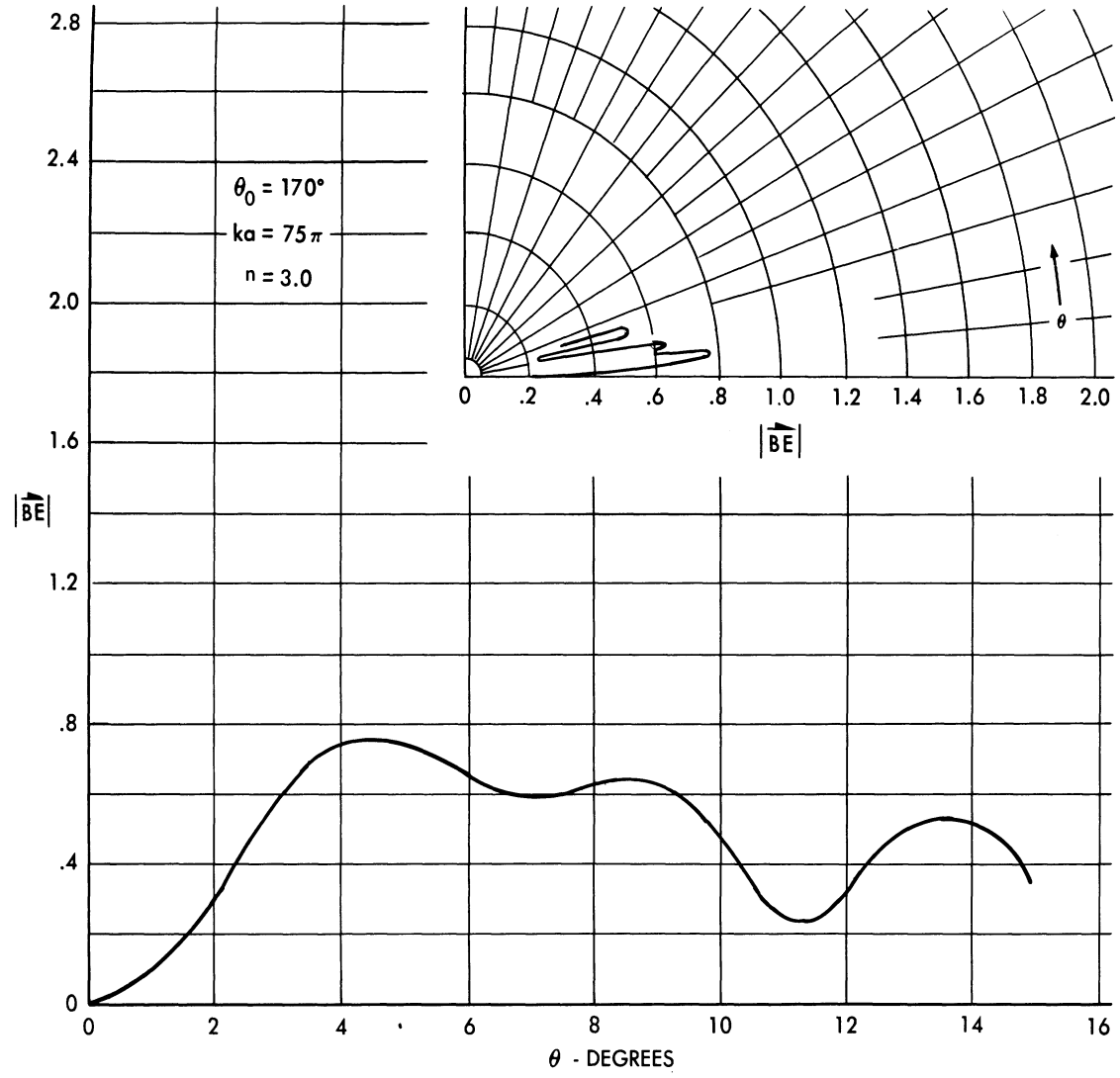


FIG. C.18 $20^\circ$ CONE WITH $e^{3i\phi}$ EXCITED CIRCUMFERENTIAL SLOT 37.5 WAVELENGTHS FROM TIP

REFERENCES

1. C. E. Schensted, "Electromagnetic and Acoustic Scattering by a Semi-Infinite Body of Revolution", Jour. Appl. Phys., 26, No. 3, 306-309 (1955).

2. L. B. Felsen, Private communications to the authors.

3. V. A. Fock, Journal of Physics X, 399 (1946).

4. L. L. Bailin, "Field Produced by a Slot in a Large Circular Cylinder", IRE Trans. Antennas and Propagation, AP-3, No. 3, 128-138 (1955).

5. W. Franz and K. Depperman, Ann. Phys. 10, 361 (1952).
I. Imai, Z. Phys. 137, 31 (1954)
W. Franz, Z. fur Naturforshung 9a, 705 (1954).

6. L. B. Felsen, "Back Scattering from Wide-Angle and Narrow-Angle Cones", J. A. P. 26, 138-151 (1955).

7. L. L. Bailin and S. Silver, "Exterior Electromagnetic Boundary Value Problems for Spheres and Cones", IRE Trans. Antennas and Propagation, AP-4, No. 1, 5-16 (1956).

8. Daniel Ray, "On Spectra of Second-Order Differential Operators", NBS Report No. 2075.

9. R. H. Cameron and W. T. Martin, "An Expression for the Solution of a Class of Non-Linear Integral Equations", American J. Math., 66, 281-298 (1944).

10. R. H. Cameron, "A 'Simpson's Rule' for the Numerical Evaluation of Wiener' Wiener's Integrals in Function Space." Duke Math. Journ. 18, 111-130 (1951).

11. L. B. Felsen, "Radiation from Slots on a Perfectly Conducting Wedge", R-492-56 Memorandum No. 13, PIB-422, Polytechnic Institute of Brooklyn.

12. F. Oberhettinger, "Diffraction of Waves by a Wedge." Communications on Pure and Applied Mathematics 7, 551-563, (1954).

13. W. Hansen and L. I. Schiff, "Theoretical Study of Electromagnetic Waves Scattered from Shaped Metal Surfaces." Microwave Laboratory, Stanford University, Quarterly Report (Feb. 1948).

14. J. Keller and A. Blank, "Diffraction and Reflection of Pulses by Wedges and Corners, N.Y.U. Symposium on the Theory of Electromagnetic Waves (1950).

15. J. Franklin and B. Friedman, "A Convergent Asymptotic Representation for Integrals", New York University, Institute of Mathematical Sciences, Division of Electromagnetic Research, Research Report No. BR-9.

16. F. Oberhettinger, "On Asymptotic Series for Functions Occurring in the Theory of Diffraction of Waves by Wedges", Journal of Mathematics and Physics 34, No. 4, January 1956. See Eq. 32.

17. H. S. Wall, "Continued Fractions", D.Van Nostrand Company Inc., (1948)

18. N. Logan, Private communication to the authors.